In memory of a pharmacy student in 1972
whose discernment of the indispensable nature of the human social condition
veered her path towards the practice and science of child welfare.

Acknowledgements

The work presented in this thesis was carried out at the Department of Pharmaceutical Chemistry, School of Pharmacy, University of Oslo, between August 2011 and October 2015, under the supervision of Professor Trond Vidar Hansen. Associate Professor Anders Vik, from the Department of Pharmaceutical Chemistry, and Professors Hege Thoresen and Arild Rustan, from the Department of Pharmaceutical Biosciences, School of Pharmacy, University of Oslo, functioned as co-supervisors. The School of Pharmacy is gratefully acknowledged for its financial support during the project period.

I would like to extend my sincerest gratitude to my supervisor Trond Vidar Hansen, for giving me the opportunity to work in the LIPCHEM group and in the PPAR project at this exciting time of change in the field. His guidance has represented a highly constructive mixture of a demand for scientific rigor and a freedom to pursue new directions. I have also appreciated his lessons in the art of presenting scientific results and I am thankful for his attentious evaluation of my scientific production in the LIPCHEM group, including this thesis.

To my co-supervisors, I would like to convey my gratitude for their advice and feedback throughout this project. Associate Professor Anders Vik has been a valuable discussion partner for topics related to, but not limited to, the day-to-day work in the organic synthesis laboratory, as well as a source of moral support. I am also grateful for his comments on my work throughout the years and for his proofreading of my thesis. I thank Professor Hege Thoresen and Professor Arild Rustan for their contributions to my appreciation of the complexity of the signaling networks in human cells. Their group meetings have been a source of inspiration and a reminder of all the things I have yet to learn about how to work with and think about living cells.

Dr. Eili Tranheim Kase deserves a special thanks for her contributions. During our collaboration on the protein-based assays, it has been an honor to learn from her skills in the laboratory and professionalism as a researcher. Her patience and unwaivering enthusiasm for the tasks at hand, have kept my spirits high and allowed me to view the results from new angles.

I would like to thank M.Sc. Cecilie Xuan Trang Vo and M.Sc. Marthe Amundsen for their synthetic efforts during their respective Master's projects, as well as for their enthusiasm and interest in the greater story of the PPARβ/δ antagonists. I am also grateful to our other collaborators Associate Professor Trine G. Halvorsen, Siri Hildonen and Magnus Mortén for their contributions, both in terms of their openness towards participating in this project, as well as for sharing generously of their time, resources and knowledge. I would also like to thank Professor Léon Reubsaet for mediating the first contact with the bioanalytical group at the Department of Pharmaceutical Chemistry.

Dr. Tuomo Laitinen and Professor Antti Poso deserve thanks for welcoming me into their computational chemistry group at the School of Pharmacy, University of Eastern Finland, for

showing me the intricacies and pitfalls of their field of research, and for many fruitful discussions on the computational approaches to the PPARγ project. Dr. Jademilson Celestino dos Santos, a former member of the The Molecular Biotechnology Group (headed by Prof. Igor Polikarpov), Institute of Physics in São Carlos (IFSC), São Paulo, Brasil, is gratefully acknowledged for his cocrystallization attempts and the differential scanning fluorimetry-based assay with the PPARβ/δ antagonists.

I also wish to thank former and current colleagues at the Department of Pharmaceutical Chemistry; Øyvind A., Yasser, Martin G., Eirik, Jens, Renate, Karoline, Marius, Jørn, Alexander and Elvar, for good times, both in the lab and in the lunch room. A special thanks to Dr. Jørn Eivind Tungen, with whom I have shared a lab, for teaching me that my crude synthetic materials are only ever as dirty as my chromatography skills. I would also like to thank my former and current colleagues and friends at the Department of Chemistry; Tor Erik, Øyvind, Kim and Martin H. for our scientific and social exchanges. A special thanks to Martin H. for bringing me into the life sciences in the first place and for being one of few colleagues to comprehend my positions from perspectives beyond the scientific.

At this point, I would like to salute my friends and loved ones, the names and nationalities of which would fill pages, for their love and loyalty, and for patiently accepting any work-related (and unrelated) reasons for my being late to our meetings. I look forward to seeing you all more in the time to come.

Finally, I am ever grateful to my brothers, my mother and my father for being the solid foundation from which I parted and to which I can always return. Your support and belief in me are invaluable. I would never have come this far without you.

Oslo, March 2016

Åsmund Kaupang

Contents

Acknowledgements . . . III
Contents . . . V
List of Papers . . . VII
Abstract . . . IX
Graphical Abstracts . . . XI
Abbreviations and Acronyms . . . XIII

I Introduction 1

1 General Introduction 3
1.1 Aim of Study . . . 4

2 PPAR Structure 5
2.1 The Modular Structure of the PPARs . . . 5
2.2 The PPAR Ligand Binding Domain . . . 6
2.2.1 Helix Numbering and Graphical Representations . . . 6
2.2.2 Overview of the LBD Structures and the PPAR Ligand Binding Pockets 7
2.2.3 Structural Aspects of PPAR Activation - the Role of Helix 12 . . . 9
2.3 Heterodimerization with RXR - Formation of Permissive Heterodimers . . . 12

3 PPAR Physiology 15
3.1 Regulation of PPAR Expression by Alternative Splicing . . . 15
3.2 Tissue Distribution Patterns and Key Physiological Roles . . . 15
3.3 Endogenous Ligands of the PPARs . . . 16

4 PPAR Transcriptional Regulation 19
4.1 General Mechanism of Transcription of Eukaryotic Genes . . . 19
4.2 Mechanisms of Transcriptional Regulation by the PPARs . . . 20

5 The PPARs as Biological Targets 23
5.1 Ligand Classification and Terminology . . . 23
5.2 PPAR Classical Agonists as Drugs to Treat Metabolic Diseases . . . 25
5.2.1 PPARα Agonists - the Fibrates . . . 25
5.2.2 PPARγ Agonists - the Glitazones . . . 25
5.2.3 PPARα/γ Dual Agonists and pan-PPAR Agonists . . . 27
5.2.4 PPARβ/δ agonists . . . 29
5.3 Emerging Therapeutic Potential for PPAR Modulators . . . 30
5.3.1 Alternative Binding Modes of PPARγ Partial Agonists . . . 30
5.3.2 Ligand-regulated Phosphorylation of PPARγ . . . 35
5.3.3 Allosteric Stabilization of the AF-2 by PPARγ Partial Agonists . . . 36
5.3.4 Clinical Trials with a PPARγ Partial Agonist . . . 37
5.3.5 Phosphorylation of the PPARα and PPARβ/δ LBDs and Ligands with Alternative Binding Modes . . . 38
5.4 PPAR Antagonistic Ligands . . . 42
5.4.1 Inverse Agonists - the AF-2-pocket Revisited . . . 42
5.4.2 Clinical Outlooks for PPARγ Inverse Agonists . . . 42
5.5 Covalent Reactivity of the PPARs . . . 44

5.5.1 Covalent Ligands of PPARα . . . 44
5.5.2 Covalent Ligands of PPARγ . . . 44
5.5.3 Covalent Ligands of PPARβ/δ . . . 46
5.6 Motivations and Backgrounds of Study . . . 47

II Results & Discussion 49

6 Papers I and II: Synthesis and Biological Evaluations of PPARβ/δ Antagonists 51
6.1 Syntheses of Key Intermediates . . . 51
6.2 Design and Synthesis of CC618 and 5-H-CC618 . . . 51
6.3 Biological Evaluations of CC618 . . . 52
6.4 New 5-trifluoromethyl-2-sulfonylpyridine PPARβ/δ Antagonists . . . 56
6.5 Synthesis of New PPARβ/δ Antagonists . . . 56
6.6 Introduction to TR-FRET . . . 59
6.7 Results from the TR-FRET-based Ligand Displacement Assays . . . 60
6.7.1 TR-FRET Assays with PPARβ/δ . . . 61
6.7.2 Determination of IC_{50}-values . . . 63
6.7.3 TR-FRET Assays with PPARα and PPARγ . . . 63
6.8 Conclusions . . . 66

7 Paper III: Investigations on the Mode of Action of PPARβ/δ Antagonistic Ligands 69
7.1 Structural Evaluation of PPARβ/δ Antagonistic Ligands . . . 69
7.1.1 Sulindac sulfide, Indomethacin and FH535 . . . 69
7.1.2 GSK0660 and its Recent Analogues . . . 71
7.1.3 A Virtual Screening Hit and Carboxylic Acids . . . 72
7.1.4 GSK3787, CC618 and DG172 . . . 73
7.2 Chemical and Biological Assays . . . 73
7.3 Results and Ligand Classification . . . 76
7.3.1 Irreversibly Binding Antagonists . . . 76
7.3.2 Reversibly Binding Inverse Agonists . . . 79
7.4 Conclusions . . . 80

8 Paper IV: Principal Component Analyses of PPARγ Structural Data 83
8.1 Principal Component Analysis of Biological Structural Data . . . 83
8.2 Structural Aspects of PTM Inhibition and Allosteric Stabilization of Helix 12 . 84
8.3 Data Selection and Analysis Software . . . 85
8.4 Results from the PCA Analyses . . . 86
8.5 Conclusions . . . 88

9 Conclusions and Future Work 89

References 91

Appendix A 109

Appendix B 113

List of Publications

I. *Synthesis, biological evaluation and molecular modeling studies of the PPARβ/δ antagonist CC618*

Åsmund Kaupang, Steinar Martin Paulsen, Calin C. Steindal, Aina W. Ravna, Ingebrigt Sylte, Trine G. Halvorsen, G. Hege Thoresen, Trond Vidar Hansen

European Journal of Medicinal Chemistry, **2015**, *94*, 229 - 236.

II. *Synthesis of 5-trifluoromethyl-2-sulfonylpyridine PPARβ/δ antagonists: Effects on the affinity and selectivity towards PPARβ/δ*

Åsmund Kaupang, Eili T. Kase, Cecilie Xuan Trang Vo, Marthe Amundsen, Anders Vik, Trond Vidar Hansen

Bioorganic & Medicinal Chemistry, **2016**, *24*, 247 - 260.

III. *Involvement of covalent interactions in the mode of action of PPARβ/δ antagonists*

Åsmund Kaupang, Siri Hildonen, Trine G. Halvorsen, Magnus Mortén, Anders Vik, Trond Vidar Hansen

RSC Advances, **2015**, *5*, 76483 - 76490.

IV. *Structural review of PPARγ in complex with ligands: Cartesian and dihedral principal component analysis of x-ray crystallographic data*

Åsmund Kaupang, Tuomo Laitinen, Antti Poso, Trond Vidar Hansen

Manuscript

Abstract

The peroxisome proliferator-activated receptors (PPARα, PPARβ/δ and PPARγ) are nuclear receptors whose target genes have fundamental roles in human health and disease. The PPAR-regulated expression of these genes influences a range of physiological processes, including cell differentiation and proliferation, inflammation and lipid metabolism. Thus, the ligand-dependent modulation of PPAR activity is a potential point of pharmacological intervention in e.g. metabolic-, neurodegenerative- and dermatologic diseases. Recent reports on the involvement of PPARβ/δ in the pathophysiologies of breast cancer and psoriasis, highlight this PPAR subtype as a target of particular interest.

The effects of agonistic ligands on PPAR target gene expression have been studied for nearly two decades and a structurally diverse collection of agonists has been reported. In contrast, fewer PPAR antagonists have been reported and the knowlegde about their various modes of action is less developed than that of agonists. In this thesis, the development of new members of a class of covalent PPARβ/δ antagonists is presented. Our studies demonstrate that the selectivity of the new antagonists for PPARβ/δ could be increased through subtle modifications of the structure of a previously reported antagonist, without affecting its mode of action.

In extension of these studies, an investigation into the modes of action of the reported antagonistic ligands of PPARβ/δ was undertaken. In this study, an emphasis was put on the possible involvement of covalent bond formation between PPARβ/δ and the antagonistic ligands. Through a series of chemical and biological assays, it could be demonstrated that the reported antagonistic ligands differ markedly in their modes of action. Our results thus contribute to a more nuanced classification of the studied PPARβ/δ ligands.

Finally, the recent dicovery of a novel post-translational modification of PPARγ, has impacted on the understanding of the beneficial effects of PPARγ agonists as drugs to treat metabolic diseases. The nature of the ligand-dependent inhibition of this undesired regulatory event, has shifted the focus of PPARγ ligand development away from full agonists, towards the development of partial- and non-agonists. The large body of structural data from x-ray crystallography on PPARγ in complex with ligands displaying a diverse set of binding modes, permitted a collective analysis of these data, aiming to identify structural trends in the influences of the ligands on PPARγ. Our study employed principal component analyses of the atomic coordinates and dihedral angles of PPARγ. The results of this investigation demonstrate a separation of the PPARγ structures, corresponding to a varying degree of stabilization of a region of the protein, known to be important for the undesired biological effects of full agonists. Thus, our analysis provides a mapping of the PPARγ structures with potential utility in the development of new partial- and non-agonistic PPARγ ligands.

Graphical Abstracts

Paper 1: Synthesis, biological evaluation and molecular modeling studies of the PPARβ/δ antagonist CC618

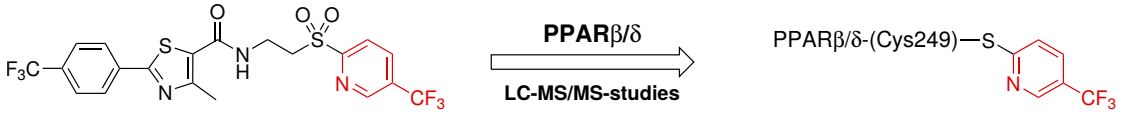

Paper 2: Synthesis of 5-trifluoromethyl-2-sulfonylpyridine PPARβ/δ antagonists: Effects on the affinity and selectivity towards PPARβ/δ

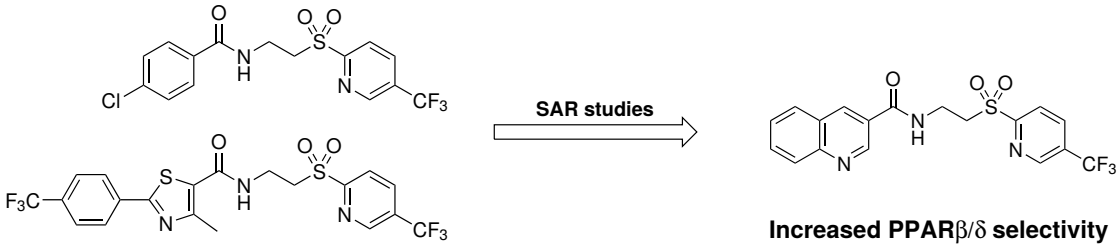

Paper 3: Involvement of covalent interactions in the mode of action of PPARβ/δ antagonists

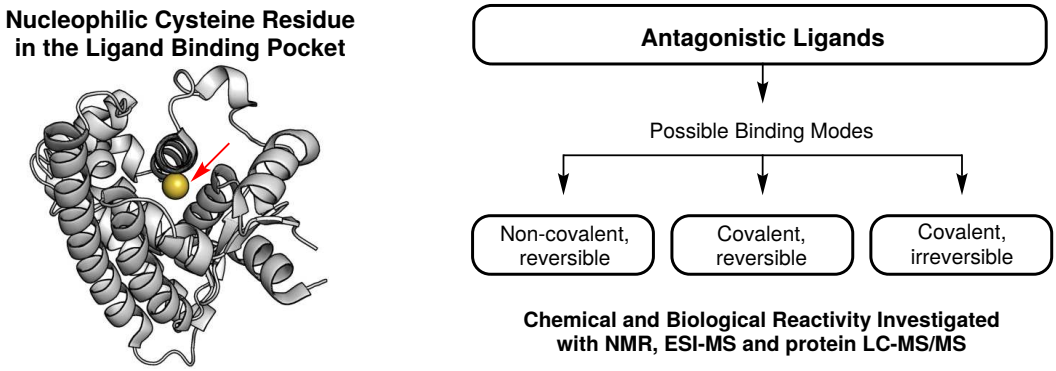

Paper 4: Structural review of PPARγ in complex with ligands: Cartesian and dihedral principal component analysis of x-ray crystallographic data

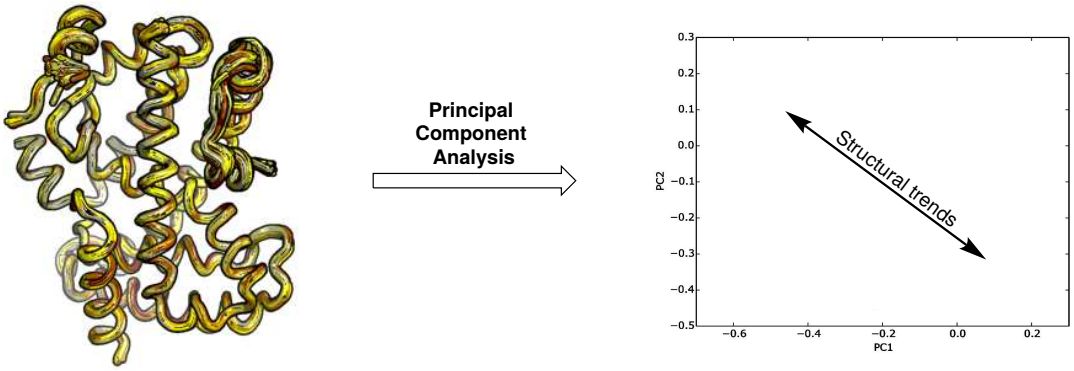

Abbreviations

2-ME	2-Mercaptoethanol
Boc	*tert*-Butyloxycarbonyl
CHARMM	Chemistry at Harvard Molecular Mechanics
DBD	DNA-binding domain
DCC	*N*,*N*'-dicyclohexylcarbodiimide
DCGI	Drug Controller General of India
DHA	(4*Z*,7*Z*,10*Z*,13*Z*,16*Z*,19*Z*)-Docosahexaenoic acid
DMF	Dimethylformamide
DMSO	Dimethylsulfoxide
DNA	Deoxyribonucleic acid
DSF	Differential scanning fluorimetry
EMA	European Medicines Agency
EPA	(5*Z*,8*Z*,11*Z*,14*Z*,17*Z*)-Eicosapentaenoic acid
ESI	Electrospray ionization
ETE	(8*Z*,11*Z*,14*Z*,17*Z*)-Eicosatetraenoic acid
FA	Fatty acid
FABP	Fatty acid-binding protein
FDA	United States Food and Drug Administration
FRET	Fluorescence resonance energy transfer
HAT	Histone acetyltransferase
HBTU	*O*-(Benzotriazol-1-yl)-*N*,*N*,*N*',*N*'-tetramethyluronium hexafluorophosphate
HDAC	Histone deacetylase
HDHA	Hydroxydocosahexaenoic acid
HDL	High-density lipoprotein
HDX-MS	Hydrogen-deuterium exchange coupled to mass spectrometry
HEPA	Hydroxyeicosapentaenoic acid
HETE	Hydroxyeicosatrienoic acid
HOBt	Hydroxybenzotriazol
HODE	Hydroxyoctadecadienoic acid
HPLC	High-performance liquid chromatography
LA	Linoleic acid
LBD	Ligand-binding domain
LBP	Ligand-binding pocket
LC	Liquid chromatography
L-FABP	Liver-type Fatty Acid-binding Protein
LPS	Lipopolysaccharide
m-CPBA	3-Chloroperbenzoic acid
MD	Molecular dynamics
MS	Mass spectrometry

MUFA	Monounsaturated fatty acid
NAFLD	Non-alcoholic fatty liver disease
NaHMDS	Sodium *bis*(trimethylsilyl)amide
NASH	Non-alcoholic steatohepatitis
NMR	Nuclear magnetic resonance
NSAID	Non-steroidal anti-inflammatory drug
OA	Oleic acid
OTE	(6*Z*,9*Z*,12*Z*)-Octadecatrienoic acid
PBC	Primary biliary cirrhosis
PCA	Principal component analysis
PGC-1α	Peroxisome proliferator-activated receptor γ coactivator 1-α
PKC	Protein kinase C
PPAR	Peroxisome proliferator-activated receptor
PPRE	Peroxisome proliferator response element
PTM	Post-translational modification
RCSB-PDB	Research Collaboratory for Structural Bioinformatics - Protein Data Bank
RET	Resonance energy transfer
RMSD	Root-mean-square deviation
RNA	Ribonucleic acid
RNAPII	RNA polymerase II
RRMS	Relapsing-remitting multiple sclerosis
RXR	Retinoid X-receptor
SAR	Structure-activity relationship
SHARP	SMRT and histone deacetylase-associated repressor protein
SHTG	Severe hypertriglyceridemia
SMRT	Silencing mediator for retinoid and thyroid hormone receptors
SRC	Steroid receptor coactivator
TBAI	Tetra-*n*-butylammonium iodide
TBP	TATA-binding protein
THA	(6*Z*,9*Z*,12*Z*,15*Z*,18*Z*,21*Z*)-Tetracosahexaenoic acid
TR-FRET	Time-resolved fluorescence resonance energy transfer
TFA	Trifluoroacetic acid
THF	Tetrahydrofuran
TLC	Thin-layer chromatography
TZD	Thiazolidinedione
UNIPROT	Universal Protein Resource
UV	Ultraviolet
WADA	World Anti-Doping Agency
WHO	World Health Organization
WPMY-1	A myofibroblast stromal cell line

Part I

Introduction

1 General Introduction

The modulation of genetic expression frequency by ligand-binding transcription factors, also called nuclear receptors, constitutes a decisive element in the ability of an organism to respond adaptively to its environment.[1] As nuclear receptors influence transcription at multiple gene loci and in turn, the expression levels of multiple proteins, a pharmacological intervention in their function, e.g. by the provision of a synthetic ligand, may be expected to have significant, and possibly negative, physiological ramifications for the organism under study. Nonetheless, such an intervention would allow for an influence over a complex and finely tuned system of protein expression - one that is used and controlled by the organism itself. Given the demonstrated involvement of a dysregulation of the expression of multiple genes in the pathophysiologies of several human diseases,[2] a reequilibration of the upstream signalling in control of the aberrant gene expression patterns, by the administration of nuclear receptor ligands, could prove instrumental in the treatment of such diseases.

The potentially pleiotropic functional impact of the modulation of the activity of nuclear receptors also highlights a distinctive feature of this intervention strategy, setting it apart from strategies in which proteins or enzymes with more peripheral functions, are targeted. As pharmaceutical targets, nuclear receptors represent fundamental and powerful points of intervention in the homeostasis, and consequently, the discovery of compounds with the ability to modulate their activity has been amply pursued in the history of pharmaceutical research. Guided by the discoveries of endogenously produced ligands and natural products to which the nuclear receptors respond, this pursuit has yielded ligands displaying an astonishing diversity of physiological effects - from anabolic steroids, through anti-inflammatory glucocorticoids to contraceptive estradiols.[3]

The path towards safe and efficient pharmacotherapeutics targeting nuclear receptors, is however rid with obstacles, as nuclear receptors and their function are themselves tightly regulated in terms of chromatin morphology, receptor expression patterns and post-translational modifications.[4] Furthermore, as the theoretical framework of nuclear receptor signalling has transformed away from an understanding of the nuclear receptors as simple on-off switches for transcription, the effects produced by exogenous nuclear receptor ligands are now understood to be inextricably entwined with those of an organism's endogenous ligands. In the case of nuclear receptors with large ligand-binding pockets, such as the peroxisome proliferator-activated receptors, this challenge comprises not only the effects of a competition between ligands for the receptor, but the composite effects of multiple ligands binding to the receptor simultanously.

1.1 Aim of Study

- A primary aim of this work was the development of new antagonists of the peroxisome proliferator-activated receptor β/δ (PPARβ/δ).
- Furthermore, we sought to study the role of a reactive cysteine residue in the binding modes of the PPARβ/δ antagonists and inverse agonists reported to date.
- Finally, the recent discovery of a novel post-translational modification (PTM) of PPARγ has provided an opportunity to classify PPARγ ligands with more nuance, as some ligands inhibit this PTM without causing a classical activation of transcription. We thus sought to analyze PPARγ structural data from x-ray crystallography in order to shed light on ligand-dependent changes in the PPARγ structure.

A more in-depth description of the motivations and applications of the studies performed in the context of this thesis, can be found in Section 5.6 at the end of Part I.

2 PPAR Structure

The following chapter introduces the PPARs from a structural perspective and serves to give the reader an overview of the PPAR structure, along with a current consensus regarding the function of some key regions. The examples given in this chapter are mainly based on the available structural data from x-ray crystallographic studies, which are referenced by their ID codes in the RCSB Protein Data Bank.[5] Additional insights from in-solution dynamics studies of the PPARs, from techniques such as nuclear magnetic resonance (NMR) spectroscopy are presented where applicable.

2.1 The Modular Structure of the PPARs

The structure of the three known subtypes of the PPAR family, PPARα, PPARβ/δ and PPARγ (NR1C1-3), consists of four major domains: the A/B-, C-, D- and E/F-domains. Respectively, these comprise an N-terminal activation function (AF-1), a DNA-binding domain (DBD), a linker region and a C-terminal ligand-binding domain (LBD) (see Figure 2.1). This modular suprastructure is analogous to that of many transcription factors. Furthermore, the PPAR structure closely corresponds to those of the other non-steroidal nuclear receptors, such as the thyroid hormone receptors (TRs, NR1A1 - 2), retinoic acid receptors (RARs, NR1B1 - 3), Reverse Erbs (REV-ERBs, NR1D1 - 2), retinoid-related orphan receptors (RORs, NR1F1 - 3), liver X receptors (LXRs, NR1H2 - 3), farnesoid X receptors (FXRs, NR1H4 - 5), the vitamin D receptor (VDR, NR1I1), the pregnane X receptor (PXR, NR1I2) and the constitutive androstane receptor (CAR, NR1I3). These NRs bind to DNA as heterodimers with the retinoic X receptors (RXRα, RXRβ and RXRγ),[6–8] whereas NRs such as the estrogen receptors (ERs, NR3A1 - 2), the glucocorticoid receptor (GR, NR3C1), mineralocorticoid receptor (MR, NR3C2), progesterone receptor (PR, NR3C3) and the androgen receptor (AR, NR3C4) usually bind as homodimers.

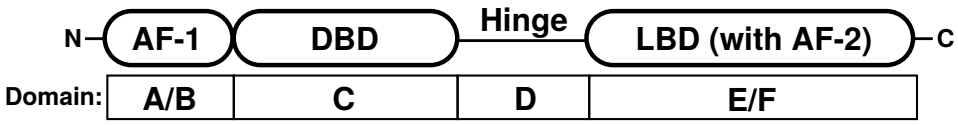

Figure 2.1. A schematic overview of the structure of the PPARs.

The N-terminal A/B-domain is a poorly structured region, the sequence of which is highly variable between the PPAR subtypes. The A/B domain houses the AF-1, which influences aspects of PPAR function such as their ligand-independent (constitutive) transcriptional activities and interactions with coregulator proteins. Given its intrinsically mobile nature, a lack of available data on its three-dimensional structure(s) has made the elucidation of structure-function relationships of the AF-1 challenging. However, the region has been shown to be

subject to a number of post-translational modifications (PTMs) e.g. phosphorylation.[9,i] The AF-1 is also a site of sequence variation between the different known isoforms of each PPAR subtype, produced by alternative splicing of their respective transcripts (see Section 3.1).

While the lengths and sequences of the A/B- and D-domains (the linker region) are variable, the C- and E/F-domains display higher degrees of homology between the PPARs, both in terms of sequence and structure. Thus, while the sequence identity of the DNA-binding C-domains of the three PPARs is 77%, that of the E/F-domains (hereafter referred to as their LBDs) is 55% (see pairwise comparisons in Figure 2.2).[10]

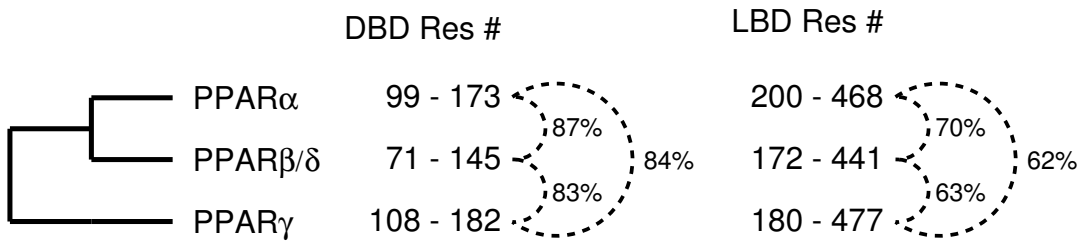

Figure 2.2. A phylogenetic tree showing the sequence relationship of the PPAR DBDs and LBDs, with residue intervals and pairwise homologies indicated.

2.2 The PPAR Ligand Binding Domain

2.2.1 Helix Numbering and Graphical Representations

The numbering of the PPAR LBD helices, used throughout this text, is shown in Figure 2.3.[11] This numbering scheme may be applied to similar nuclear receptors and is based on that of RXRα (see Figure 2.3a).[12]

The graphical representations of the structure of the PPAR LBDs shown in this thesis employ three viewing angles that are used as consistently as possible throughout the text. These generally locate the N-terminal downwards or deepest into the page plane. Viewing angle 1 displays the protein with helix 3 parallel to the plane, the β-sheets to the left and helix 12 to the right (see Figure 2.3b or Figure 2.4, top row). Viewing angle 2 is reached by a 90° forward rotation of viewing angle 1, placing helix 3 orthogonally to the plane, while maintaining the opposite lateral positions of the β-sheets and helix 12 (see Figure 2.3c or Figure 2.4, bottom row). Viewing angle 3 represents an approximately 45° forward rotation from viewing angle 1, combined with an expansion of the LBP region. In this viewing angle, helix 2, the Ω-loop and the N-terminal half of helix 3 are hidden to improve the visibility of the LBP and bound ligands (see Figure 5.9 in Chapter 5). While these viewing angles are reversed (by a 180° in-plane rotation) in relation to the ones commonly shown in the literature, it is the opinion of this author that the presented viewing angles more efficiently present the most dynamic regions of the LBD and provide a more detailed view of the LBP.

[i] Phosphorylation of the AF-1 has, however, not been demonstrated in PPARβ/δ.

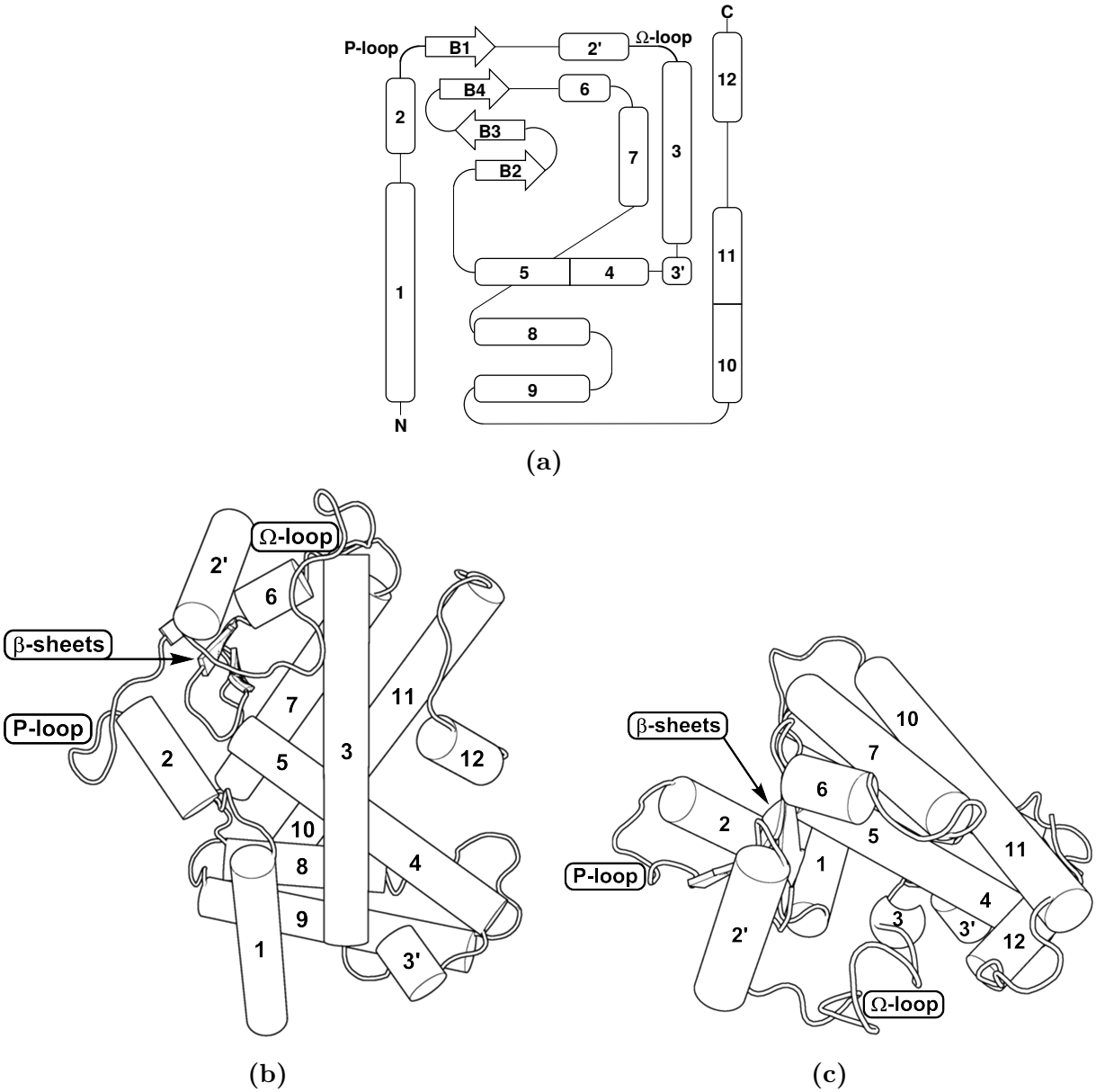

Figure 2.3. Helix numbering for the PPARs, displayed schematically (a) and on the structure of apo-PPARγ, seen from viewing angle 1 (b) and viewing angle 2 (c) (PDB ID: 2ZK0, chain A). The schematic representation was adapted from Uppenberg et al. (1998).[11] The structures were visualized with PyMOL.[13]

2.2.2 Overview of the LBD Structures and the PPAR Ligand Binding Pockets

The similarity of the overall folds of the PPAR LBDs renders the subtypes practically indistinguishable, in a representation of their secondary and tertiary structures (see Figure 2.4). Each LBD comprises a non-parallel, multihelical sandwich that forms a large ligand binding pocket (LBP) around a central helix (helix 3). The PPAR LBPs are roughly Y-shaped, with two arms stretching upwards and downwards along helix 3. The third arm reaches past helix 3, towards helices 11 and 12. The two first arms comprise a large pocket between helix 3 and the β-sheets, which in this thesis will be referred to as the Ω-pocket,[14] in reference to the Ω-loop covering its entrance. On the far side of helix 3, the third arm leads to a subpocket between helices 3, 11 and 12, which will be referred to as the AF-2-pocket.[14]

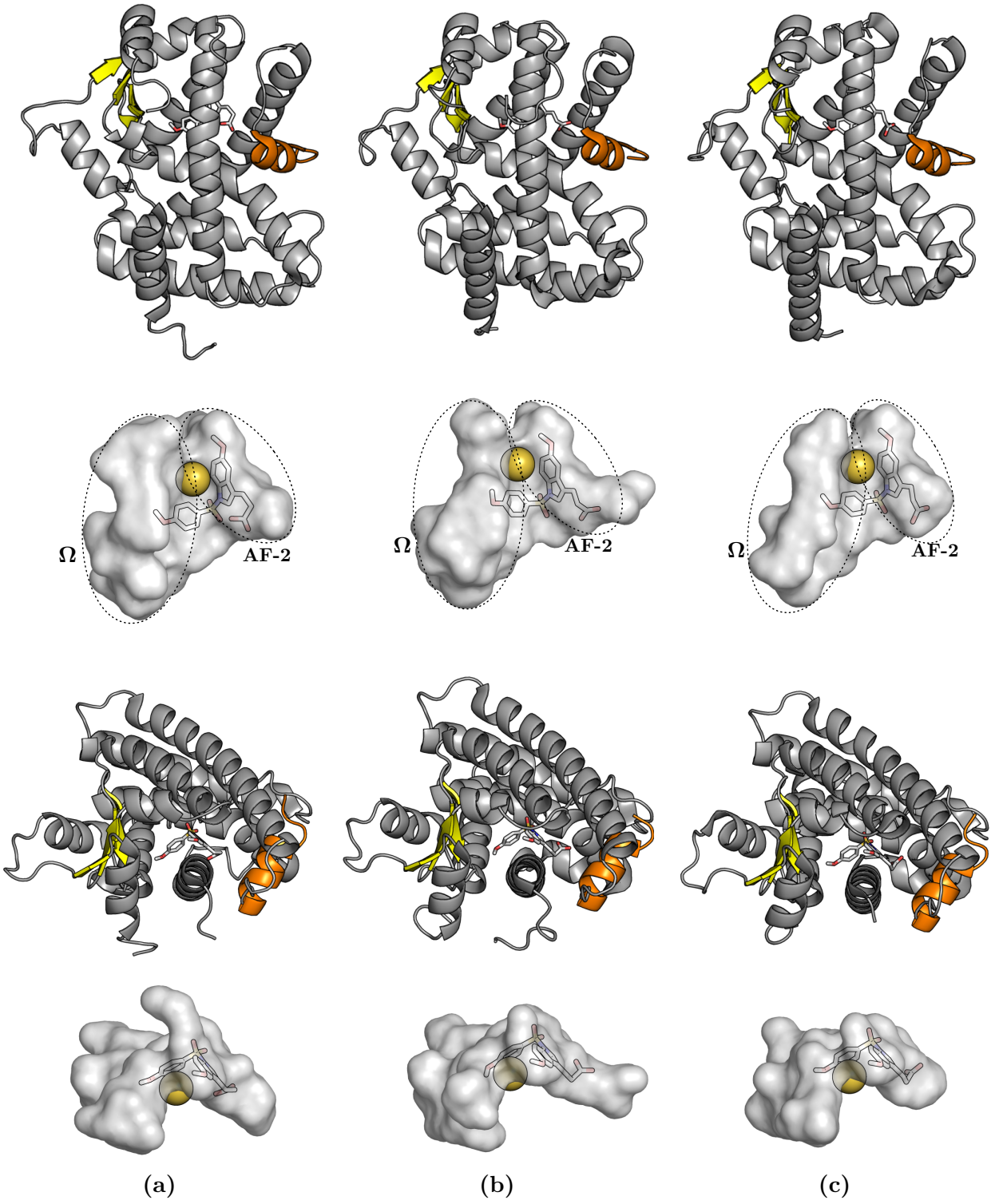

Figure 2.4. The structures of the LBDs and shapes of the binding pockets of PPARα (a), PPARβ/δ (b) and PPARγ (c) in complex with the pan-PPAR agonist indeglitazar (**1**), shown with gray carbons (see chemical structure in Figure 5.3 in Chapter 5). The β-sheets are shown in yellow and helix 12 in orange. The sulfur atom of the conserved nucleophilic cysteine residue is shown as a sphere (see Section 5.5 in Chapter 5). The Ω-pocket and the AF-2-pocket are circled in the frontal view of the LBPs. In order to display the LBPs in greater detail, their surfaces are shown at larger scale than the LBD structures. The PPARα, PPARβ/δ and PPARγ structures were taken from PDB IDs: 3ET1, 3ET2 and 3ET3,[15] respectively. The structures were visualized with PyMOL.[13] and the LBP surfaces were generated with HOLLOW.[16]

In general, the residues lining the PPAR LBPs are mostly hydrophobic in nature. The AF-2 pocket, however, houses more polar residues. These include a near completely conserved cluster of histidines and tyrosines on helices 5, 11 and 12,[ii] that are capable of forming a hydrogen bonding network with e.g. the carboxylate head groups of fatty acid ligands. These interactions, in particular those with the conserved tyrosine residue, provides a functionally important stabilization of the position of helix 12 (*vide infra*). Despite these similar traits, the clearly different shapes of the PPAR LBPs are indicative of their distinct substrate specificities (see Figure 2.4 and details about their endogenous ligands in Section 3.3).

The LBP of each PPAR also houses a nucleophilic cysteine residue, located on helix 3 (Cys276, Cys249 and Cys285, in PPARα, PPARβ/δ and PPARγ, respectively) (see Figure 2.4). The reactions of these cysteine residues with ligands will be treated in Section 5.5 in Chapter 5.

2.2.3 Structural Aspects of PPAR Activation - the Role of Helix 12

Since the first determinations of the structures of nuclear receptors (NRs) in their apo-forms and bound to agonists, the folding state and position of helix 12 has been recognized as central for their ligand-induced activation. In the human apo-RXRα (PDB ID: 1LBD), helix 12 was observed to extend away from the core of the LBD as a continuation of helix 11, while in human RARγ (PDB ID: 2LBD) and rat TRα,[17,iii] bound to their respective endogenous agonists, helix 12 was positioned orthogonally to helices 3 and 11. The same repositioning of helix 12 was later observed in RXRα bound to its endogenous (agonistic), ligand 9-*cis*-retinoic acid (**2**, see Figure 2.5) (PDB ID: 1FBY).

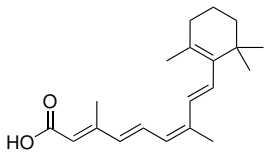

9-*cis*-retinoic acid (**2**)

Figure 2.5. The structure of the endogenous RXR ligand 9-*cis*-retinoic acid (2*E*,4*E*,6*Z*,8*E*-retinoic acid).

Taken together, these observations supported the formulation of a "mouse trap" model, in which the binding of a ligand (an agonist) would "spring the mouse trap", inducing a conformational change in the LBD, leading to the repositioning of helix 12.[18,19] While the necessity of helix 12 for transcriptional activation was known from studies with recombinant receptors missing helix 12,[20] further evidence for the role of its conformation relative to the LBD, in the mechanism of transcriptional activation by NRs, came from structural data of e.g. PPARγ cocrystallized with an agonist and an oligopeptide derived from the NR-interaction moieties of the steroid receptor coactivator 1 (SRC-1).[21] These findings reinforced the previ-

[ii] The residue position on helix 5 of His287 in PPARβ/δ and His323 in PPARγ, holds Tyr314 in PPARα. The second histidine on helix 11 and the tyrosine on helix 12 are fully conserved.

[iii] These structural data do not appear to have been deposited in the RCSB Protein Data Bank.[5]

ously proposed hypothesis from studies of the ER,[22,23] that the agonist-induced conformation of helix 12 was important for the binding of NRs to coactivator proteins, which play a critical role in the events taking place prior to the initiation of transcription (see Section 4.1 for more details on the mechanism of transcription and 4.2 for the role of coregulator proteins).

On the other hand, a crystallographic elucidation of the position(s) of helix 12 in the PPARs in the *absence* of ligands, has been complicated by the demonstration that recombinant PPAR LBDs, produced in bacterial expression systems, are often occupied by bacterial fatty acids.[24,25,iv] Nevertheless, structures of apo-PPARγ have been published that, judging by their electron density maps,[28] do not contain ligands in their LBPs.[21,29] In these homodimeric structures, helix 12 is observed in two distinct positions. One of the monomers display helix 12 in the canonical active position (type A chain), while in the other monomer, helix 12 assumes an alternative position (type B chain) (see Figure 2.6a and Figure 2.6c, respectively).

In the large body of x-ray crystallographic data on PPARγ, the observation of two types of chains, differing mainly in their position of helix 12, are common and has provided insight into the dynamics of this helix. The position assumed by helix 12 in the type A chains, is in overall correspondence with its position in PPARγ complexes that include coactivator proteins (see e.g. Figure 2.7). Consequently, this position is referred to as the "active" position. In the type B chains, on the other hand, helix 12 is found in a retracted position, which has tentatively been referred to as "inactive". The alternative position of helix 12 observed in the PPARγ type B chains, has not been observed in structures of PPARα or PPARβ/δ determined by x-ray crystallography.[v] On the other hand, in-solution NMR-studies of apo-PPARγ have demonstrated that the observed ensemble of LBD conformations populate several minima, attesting to the high mobility of the PPARγ LBD in the absence of a ligand. As noted by Johnson et al., this may indicate that the two distinct positions of helix 12, observed in crystallographic studies, stem from conformations that are selectively stabilized by the crystal packing.[30] Furthermore, a representative model[vi] of an ensemble of PPARγ structures from another NMR-study (PDB ID: 2QMV),[32,33] shows helix 12 in a position that is approximately intermediate between the positions observed with x-ray crystallography (see Figure 2.6b).

In the crystallographic data on the structure of the PPARs in general, there are other notable examples of alternative positions of helix 12. In one of these, PPARβ/δ was cocrystallized with a partial agonist, the binding mode of which appeared to destabilize helix 12.[34] The resulting structure showed a partially resolved helix 12, in an extended conformation (see Figure 2.6d) reminiscent its conformation in a PPARα complex with an antagonist (see Figure 2.6e). The latter complex also included an oligopeptide derived from the transcriptional corepressor protein silencing mediator for retinoid and thyroid hormone receptors (SMRT). The affinity of the PPARα structure with an extended helix 12 for this peptide supported a general hypothesis, based on findings from other NRs, that helix 12 would need to assume

[iv] A revision of the electron density maps from a reported apo-PPARβ/δ structure (PDB ID: 2GWX)[26] revealed the presence of a molecule of *cis*-vaccenic acid (11*Z*-octadecenoic acid, see chemical structure in Appendix A) in the LBP.[27]
[v] Based on a survey of the PPARα and PPARβ/δ structures available in the RCSB Protein Data Bank,[5] January 2016
[vi] Determined by the online service OLDERADO.[31]

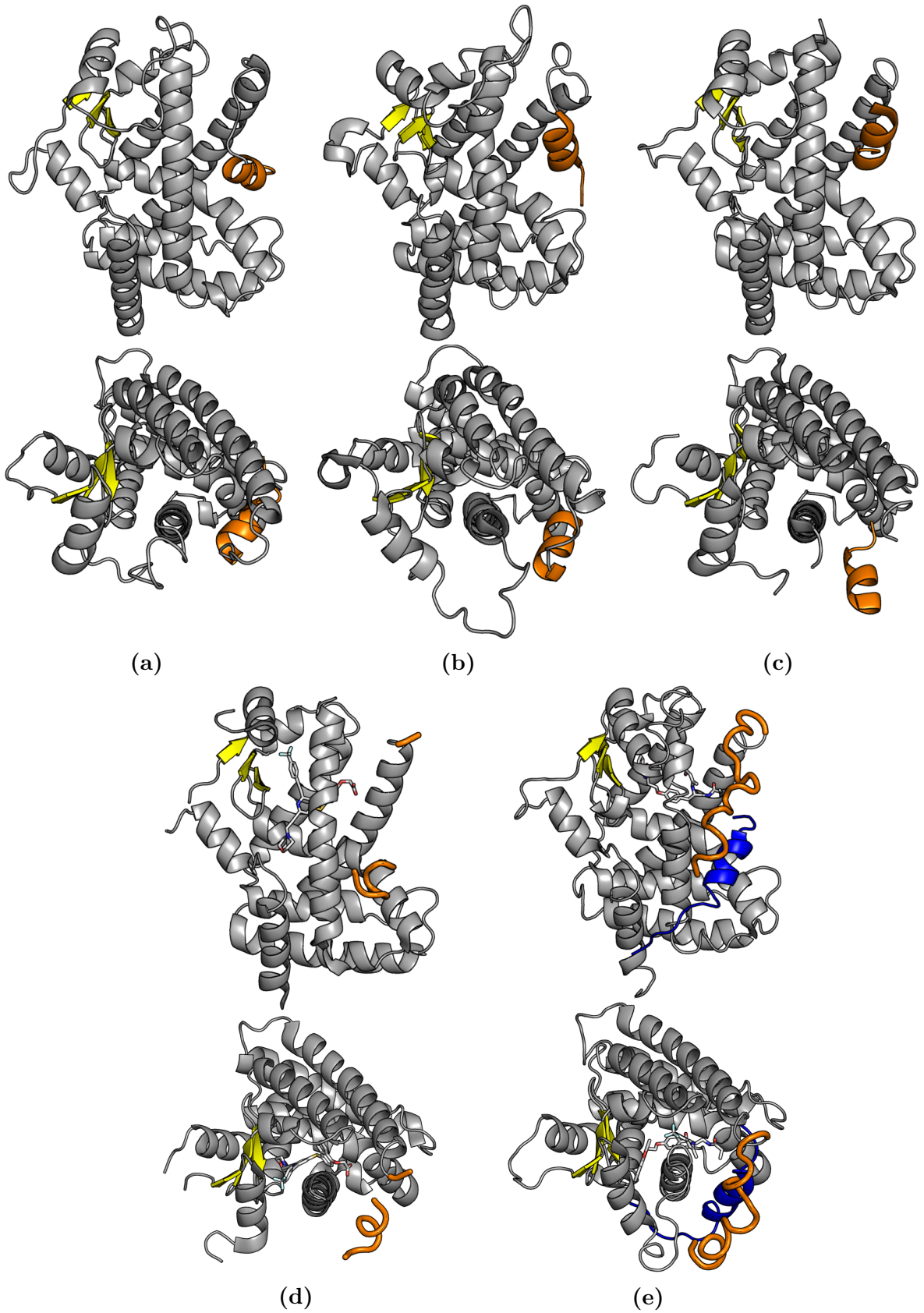

Figure 2.6. Observed positions of helix 12 in the crystal phase and by NMR. (a and c) Apo-PPARγ as seen by crystallography (PDB ID: 2ZK0, chains A and B)[29] and (b) by NMR spectroscopy (PDB ID: 2QMV, state 1).[33] (d) PPARβ/δ in complex with a partial agonist (PDB ID: 2Q5G).[34] (e) PPARα in complex with an antagonist and an SMRT-derived peptide (shown in blue) (PDB ID:1KKQ).[35] The β-sheets are coloured yellow and helix 12 is coloured orange. In the PPARβ/δ and PPARα structures helix 12 is disordered and thus shown in a tube representation for increased visibility. The structures were visualized with PyMOL.[13]

an alternative conformation from the one observed in the type A chains (or in complexes with agonists in general), in order to accomodate the NR-binding moiety of the corepressor protein[35] (see further details in Section 4.2). Whether the change in the conformation of helix 12, required for binding to corepressor proteins, must correspond to a nearly unfolded state as observed in PPARα (Figure 2.6e) or PPARβ/δ (Figure 2.6d), or simply to a repositioning of helix 12, as observed in the PPARγ type B chains (Figure 2.6c), is not entirely clear. On the other hand, a ligand-induced destabilization of helix 12, which possibly results in structures of the type seen in Figure 2.6c, d and e, has been employed as a strategy to design PPAR antagonistic ligands (see Section 5.4.1).

2.3 Heterodimerization with RXR - Formation of Permissive Heterodimers

The PPARs form obligate heterodimers with the RXRs, through an interface predominantly made up of helices 7, 10 and 11 (see Figure 2.3c).[36,37] The RXRs are prone to multimerization and are found as dimers and tetramers when not engaged in the binding of their nuclear receptor partners. The heterodimerization with the RXRs is important for the binding of the PPAR:RXR heterodimer to peroxisome proliferator response elements (PPREs) in DNA and contributes to the selectivity of the PPAR subtypes for different promoter structures.[38] The heterodimer formed between PPAR and RXR is characterized as permissive, which is meant to indicate that ligands for both nuclear receptors affect the transcriptional regulation by the heterodimer. In the case of PPAR:RXR, however, PPAR ligands seem to exert a dominant effect.[36,39,40]

The crystallization and structure determination of the near full-length PPARγ:RXRα heterodimer (missing the A/B-domains), bound to a partial PPRE, was achieved by Chandra et al. in 2008. The structure in Figure 2.7 shows the heterodimer in complex with the agonists 9-*cis*-retinoic acid (**2**) rosiglitazone (**3**, see Section 5.2.2) in the RXRα- and PPARγ LBPs, respectively. This structure provided important insights regarding the interaction surfaces of the heterodimer, and those of the heterodimer and the DNA strand. Figure 2.7 (top right) shows the highly symmetrical heterodimer interface, attesting to the structural auto-complimentarity of the conserved nuclear receptor fold. Also evident in Figure 2.7, is the proximity of the PPARγ P-loop (see Figure 2.3) to the RXRα DBD. The proximity of these structural elements has been implicated in the modulatory effects a post-translational modification (PTM) in this region has on PPAR:RXR transcriptional regulation (discussed in the context of PPAR ligands in Sections 5.3.2 and 5.3.5). However, more recent in-solution structure determinations of the full-length PPAR:RXR heterodimer and DNA, have shown the complex to be extended, with the LBDs at a distance from the DBDs. While both the observed structures may be functionally relevant, these results underline the difficulty in observing the dynamic nature of multidomain protein complexes by x-ray crystallography.[23]

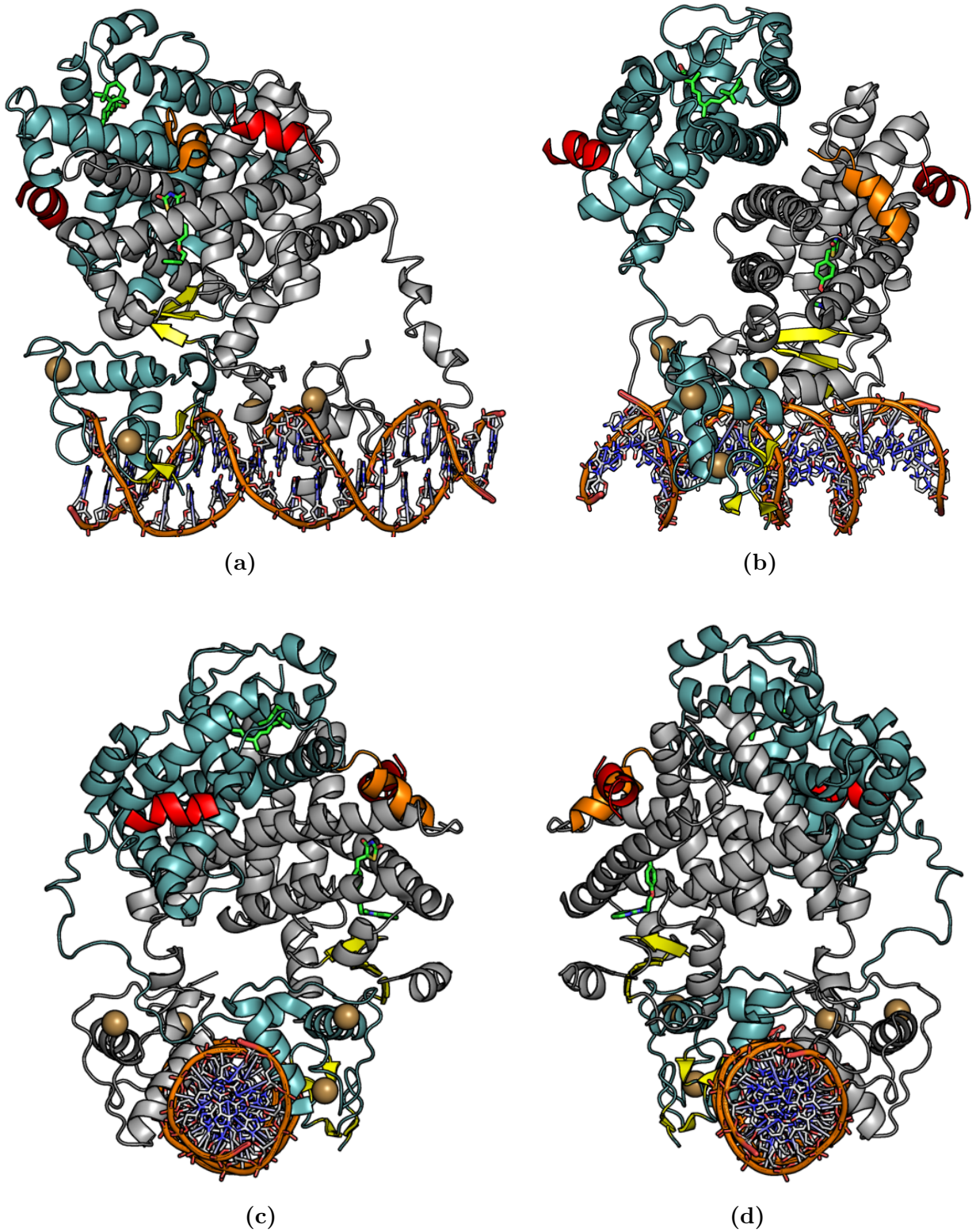

Figure 2.7. PPARγ:RXRα (in grey and teal, respectively) bound to a direct repeat 1 (DR1) element - a partial peroxisome proliferator response element (PPRE) (see Section 4.2). The structure includes domains C, D and E/F, but not the N-terminal A/B domain. The PPARγ and RXRα ligands rosiglitazone (see Section 5.2.2) and 9-*cis*-retinoic acid are shown with green carbons. Oligopeptides derived from the nuclear receptor binding motifs of coactivator protein SRC-1 are coloured red (see Section 4.2). β-sheets are coloured yellow and helix 12 of PPARγ is coloured orange. The four zinc atoms are coloured light brown. The structural data were taken from PDB ID: 3DZY[41] and visualized with PyMOL.[13]

3 PPAR Physiology

The PPARs are widely expressed in the human body and their activity impacts on several processes including lipid and glucose metabolism, cellular differentiation and inflammation. In the first part of this chapter, a brief introduction to the expression patterns and known roles of the PPARs in human physiology will be given, followed by an overview of the known endogenous PPAR ligands. The second part of the chapter looks at the roles of the PPARs in the regulation of transcription, through their interaction with DNA and transcriptional coregulator proteins.

3.1 Regulation of PPAR Expression by Alternative Splicing

As introduced in the previous chapter, three PPAR subtypes are known. However, each PPAR subtype also presents several sequence variants, which in this thesis are referred to as PPAR isoforms. According to the UNIPROT database, two PPARα isoforms, four PPARβ/δ isoforms and three PPARγ isoforms have been identified thus far in humans.[10] The distinct transcripts produced by alternative splicing show varying translational efficiency,[42,43] which in turn affects the resulting expression level of each PPAR subtype. Some of the transcripts also code for non-functional[44] or dominantly repressive receptors.[42,43] A study of PPARγ that identified three additional isoforms in macrophages (PPARγ4, -5 and -7), also demonstrated that the expression of the individual isoforms may be modulable through the treatment of PPARγ with different ligands[45] (*PPARG* is a target gene of PPARγ).[46] This further supports the notion of a regulatory role for the alternative splicing observed in the PPARs.

Notwithstanding this diversity of isoforms, the treatment of PPARα and PPARβ/δ in this thesis will refer to their primary isoforms, PPARα1 and PPARβ/δ1. For human PPARγ, two isoforms, PPARγ1 and PPARγ2, are well-studied and differ by PPARγ2 having 28 residues added to the N-terminal A/B domain. In this chapter, PPARγ1 and PPARγ2 will be described separately to highlight their tissue-specific distribution patterns. In the rest of this thesis, in which their identical LBDs are discussed, they will be described collectively as PPARγ.

3.2 Tissue Distribution Patterns and Key Physiological Roles

PPARα is highly expressed in tissues involved in fatty acid catabolism, such as the heart, the liver and skeletal muscle.[47] In the liver, PPARα activation by fasting or by administration of synthetic agonists, increases mitochondrial and peroxisomal β-oxidation. PPARα also upregulates the hepatic glucose production during fasting.[48] In relation to inflammation, activation of PPARα inhibits the expression of proinflammatory cytokines such as IL-6.[49]

PPARβ/δ is expressed throughout the body, with relatively higher levels found in the brain, the gastrointestinal tract, in skeletal muscle and in skin.[47,50] In the context of metabolism, PPARβ/δ is a key regulator of energy expenditure in skeletal muscle, in response to fasting

and physical exercise. In this tissue, PPARβ/δ activation leads to a preferential utilization of lipids, while limiting the carbohydrate metabolism. It is also involved in the remodeling of muscle fibers towards type I oxidative fibers and treatment with synthetic PPARβ/δ agonists is capable of mimicking responses to endurance exercise.[51] PPARβ/δ activation is also linked to an anti-inflammatory effect. In the absence of a ligand, PPARβ/δ has been shown to interact with the transcriptional repressor protein B-cell lymphoma 6 (BCL6). Ligand activation of PPARβ/δ releases BCL6, enabling it to repress pro-inflammatory target genes in macrophages.[52]

PPARγ displays a somewhat more selective distribution pattern than the other PPARs. The isoform PPARγ2 is exclusively expressed in adipose tissue, where it is the most abundant of the PPARs. PPARγ1, on the other hand, is found in high levels in the gastrointestinal tract, the lungs and the heart.[47] PPARγ is a master regulator of adipogenesis and is necessary for the formation of adipose tissue. PPARγ is also involved in the regulation of the glucose homeostasis and its target genes influence insulin sensitivity.[53]

3.3 Endogenous Ligands of the PPARs

The identification of *bona fide* endogenous PPAR ligands in humans has presented certain challenges. The PPARs may be construed to function as lipid sensors, as they promiscuously bind to a host of endogenously occurring fatty acids, fatty acid conjugates and metabolites (summarized in Table 3.1, see chemical structures in Appendix A). However, most of the lipid-derived ligands shown to bind to the PPARs display affinities in the micromolar range[26] and many fail to meet the criterium of displaying affinities for the their respective PPAR LBPs that match their observed concentrations in a given cell type or tissue.[54,55] While serum concentrations of long-chain fatty acids do reach the micromolar range,[56] less is known about their intracellullar concentrations, which in turn may depend on the presence and the substrate selectivity of fatty acid transporters.[51] In the case of PPARγ, the hypothesis that the receptor functions as lipid sensor is both supported and complicated by the observation that the PPARγ LBP is capable of housing more than one ligand simultaneously, suggesting that the transcriptional regulation by PPARγ may be a function of the composite effects of multiple bound ligands.[24,57] This phenomenon has been observed in x-ray crystallographic studies of PPARγ in complex with 2 - 3 molecules of nonanoic acid (PDB ID: 3SZ1, 4EMA), 2 molecules of 9*S*-HODE (PDB ID: 2VSR), or with 15-oxo-ETE and 5-methoxyindole acetate (PDB ID: 3ADW). Thus far, the binding of multiple molecules of endogenous origin has not been observed crystallographically in PPARα and PPARβ/δ.[i]

[i] Based on a survey of the PPARα and PPARβ/δ structures available in the RCSB Protein Data Bank,[5] January 2016

Table 3.1. Summary of selected endogenously occurring fatty acids and fatty acid-derived molecules binding to the PPARs. The table summarizes several entries from the literature.[24,26,29,58–68] A ● indicates a reported high affinity for a PPAR, while a vacant position indicates that a compound does not bind or binds with very low affinity. The symbols ○, ○○ and ○○○ indicate $IC_{50} > 30$, > 5 and $< 5\,\mu M$, respectively, for the displacement of ^{3}H-labelled synthetic agonists, measured in scintillation proximity assays.[26] The table is not meant to represent a comprehensive list of endogenous PPAR ligands. The chemical structures of the compounds in the table can be found in Figure 9.1 and Figure 9.2 in Appendix A.

Group	Name	PPARα	PPARβ/δ	PPARγ
FAs	Nonanoic acid (C9:0)[a]			●
	Decanoic acid (C10:0)			●
	Lauric acid (C12:0)	●		
	Myristic acid (C14:0)	○○	○	○
	Palmitic acid (C16:0)	○○○	○○	
	Stearic acid (C18:0)	○○○	○○	
MUFAs	*cis*-Vaccenic acid ($C18:1_{n-7}$)		●	
	Oleic acid ($C18:1_{n-9}$)	○○○	○○	○○○
PUFAs[b]	Linoleic acid ($C18:2_{n-6}$)	○○○	○○	○○
	γ-Linolenic acid ($C18:3_{n-6}$)	●	●	●
	α-linolenic acid ($C18:3_{n-3}$)	○○○	○○	○○
	Dihomo-γ-linolenic acid ($C20:3_{n-6}$)	○○○	○○○	○○○
	Arachidonic acid ($C20:4_{n-6}$)	○○○	○○○	○○○
	EPA ($C20:5_{n-3}$)	○○○	○○○	○○○
	DHA ($C22:6_{n-3}$)	●		●
OH-PUFAs[b]	8(S)-HETE	●		
	15(R)-HETE/15(S)-HETE		●	
	9(S)-HODE			●
	13(S)-HODE		●	●
	4-HDHA			●
FA-CoAs[b]		Pristanoyl-CoA Phytanoyl-CoA Arachidonoyl-CoA DHA-CoA		
Nitro-FAs[b]				9- and 10-NO_2-OA 10- and 12-NO_2-LA
Oxo-PUFAs[b]				6-oxo-OTE 5-oxo-ETE 8-oxo-ETE 15-oxo-ETE 5-oxo-EPA 4-oxo-DHA 6-oxo-THA
Eicosanoids		Leukotriene B_4	Prostacyclin (PGI_2) Prostaglandin A_1 Prostaglandin A_2	15d-PGJ_2

[a] By x-ray crystallography, 2 - 3 molecules have been observed in the LBP simultaneously (PDB ID: 4EM9, 3SZ1).
[b] EPA; eicosapentaenoic acid, DHA; docosahexaenoic acid, HETE; hydroxyeicosatetraenoic acid, HODE; hydroxyoctadecadienoic acid, HDHA; hydroxydocosahexaenoic acid, CoA; Coenzyme A, OTE; octadecatrienoic acid, ETE; eicosatetraenoic acid, THA; tetracosahexaenoic acid, OA; oleic acid, LA; linoleic acid

4 PPAR Transcriptional Regulation

In order to regulate the expression of proteins, nuclear receptors influence the process of gene transcription. Transcription involves the complimentary duplication of stretches of polynucleotides from one strand of DNA to produce a single strand of RNA. Following RNA processing, the product mRNA may in turn be translated by ribosomes into a polypeptide. Subsequent folding of the polypeptide chain, assembly with other protein subunits and eventual post-translational modifications (PTMs) yield a functional protein. PTMs can also occur at a later stage in the lifetime of a protein and may cause a change in its function or localization. Thus, by affecting the frequency with which genes are transcribed, nuclear receptors can change the constitution of the RNA pool available for ribosomal translation and consequently the constitution of the cell's proteome.

4.1 General Mechanism of Transcription of Eukaryotic Genes

The molecular events involved in the initiation of transcription are both structurally and functionally complex. In short, the transcription of eukaryotic genes coding for proteins is dependent on the assembly of a multiprotein complex of general transcription factors, including the RNA polymerase II (RNAP II), immediately upstream of the transcription start site. Since DNA is highly compacted within the condensed chromatin structure, it must be uncoiled from its nucleosome scaffold to expose the transcription start site of the gene to be transcribed.[69] The opening of the chromatin structure is part of a dynamic behaviour, known as chromatin remodelling, that can be brought about by covalent modification of histone N-terminal tails by nuclear enzymes. An essential modification is the *N*-acetylation of lysine residues by histone acetyltransferases (HATs). Lysine *N*-acetylation contributes to a weakening of the interactions between the DNA strand and the histone, in part caused by a change in the net charge of the histone upon acetylation. Histone deacetylases (HDACs), on the other hand, cleave *N*-acetylated lysine residues, lowering the accessibility of DNA. Other known histone modifications include mono- and poly-*N*-methylation of lysine and arginine residues,[70] *O*-phosphorylation of serine, threonine and tyrosine residues,[71] and *N*-ubiquitylation of lysine residues and N-terminal amino acids.[72]

Together referred to as the "histone code", these modifications constitute a signalling language that is integral to the regulation of transcription. Moreover, they serve purposes beyond altering the physical accessibility of the polynucleotide chain, as epigenetic markers linked to normal cell development, pathogenesis, DNA maintenance and inheritance.[73]

Being intrinsically structural in nature, the "histone code" is recognized, read and edited by complexes of auxiliary proteins including the nuclear enzymes that carry out the modifications. These *coregulator* protein complexes also interact with ligand-modulated transcription factors, such as the PPARs, in order to integrate their regulatory input (either ligand-dependent or -independent). These interactions thus create a bridge between extra- or intracellullar signals, e.g. in the form of nuclear receptor ligands, and the regulation of

transcription. Additional layers of complexity are added to the ongoing elucidation of these regulatory circuits by the more recent realization that both nuclear receptors and coregulator complexes themselves are subject to covalent modifications and PTMs, such as phosphorylation, sumoylation, methylation, acetylation and ubiquitylation.[4,74]

4.2 Mechanisms of Transcriptional Regulation by the PPARs

The PPARs affect transcription, mainly through the binding of the PPAR:RXR heterodimer (see also Section 2.3) to DNA sequences, known as peroxisome proliferator response elements (PPREs), located in the promoter regions of target genes. In the absence of ligands, the binding of the apo-PPAR:RXR heterodimer to PPREs commonly represses the transcription of target genes. Transcriptional repression involves the recruitment of coregulator proteins known as corepressor proteins, such as nuclear receptor corepressor (NCoR), silencing mediator for retinoid and thyroid hormone receptors (SMRT) or SMRT and histone deacetylase-associated repressor protein (SHARP). These proteins associate with HDACs and their recruitment thus contributes to the repression of transcription (see Figure 4.1a).[75–77]

In the presence of agonistic ligands, the PPARs loose their affinity for corepressor proteins and instead recruit coactivator proteins, including the PGC-1α, the SRC family, CBP and the mediator complex (TRAP220/DRIP205). The coactivator proteins may in turn recruit HATs, which facilitate transcription (see Figure 4.1b).[78,79] A major structural determinant of this change in the affinity of the PPAR LBD for the different coreregulator protein classes, is the position of helix 12 relative to the LBD (see Section 2.2.3). The PPAR-binding motif of corepressor proteins is a leucine-rich, three turn α-helix with consensus sequence: L/I-XX-I/V-IL-XXX-I/L-XXX-L,[i] while that of coactivator proteins, is a shorter two turn α-helix with consensus sequence: L-XX-LL.[20,i] Based on the observed position of helix 12 in agonist-bound PPARs in complex with oligopeptides derived from the PPAR-binding motif of coactivator proteins (see Figure 2.7), it is hypothesized that an unfolding- or retraction of helix 12 in the apo-PPAR LBD is necessary to accomodate the longer binding motif of corepressor proteins.[35]

In contrast to this simplified view, interactions between *agonists*-bound PPARs and *corepressor* proteins such as ligand-dependent nuclear receptor corepressor (LCoR),[81] receptor-interacting protein-140 (RIP-140)[82–84] and TNFα-induced protein 3-interacting protein 1 (TNIP1),[85] have been demonstrated. In analogy to the binding mode of coactivator proteins, the interactions of these atypical corepressor proteins with the PPARs are mediated by L-XX-LL motifs. However, in similarity to other corepressor proteins, they repress transcription either through the recruitment of other coregulator proteins with HDAC-activity or HDAC-independent transcriptional repressors, such as C-terminal binding protein (CtBP) 1 or 2.[86] This indicates that the transcriptional effects of PPAR agonists may involve a concomitant induction and repression of PPAR target genes that is dependent on the expression level and availability of coregulator proteins in a given cellular context.

Another characterized mechanism of transcriptional regulation in the presence of agonists,

[i] L = leucine, I = isoleucine, V = valine and X = any amino acid.

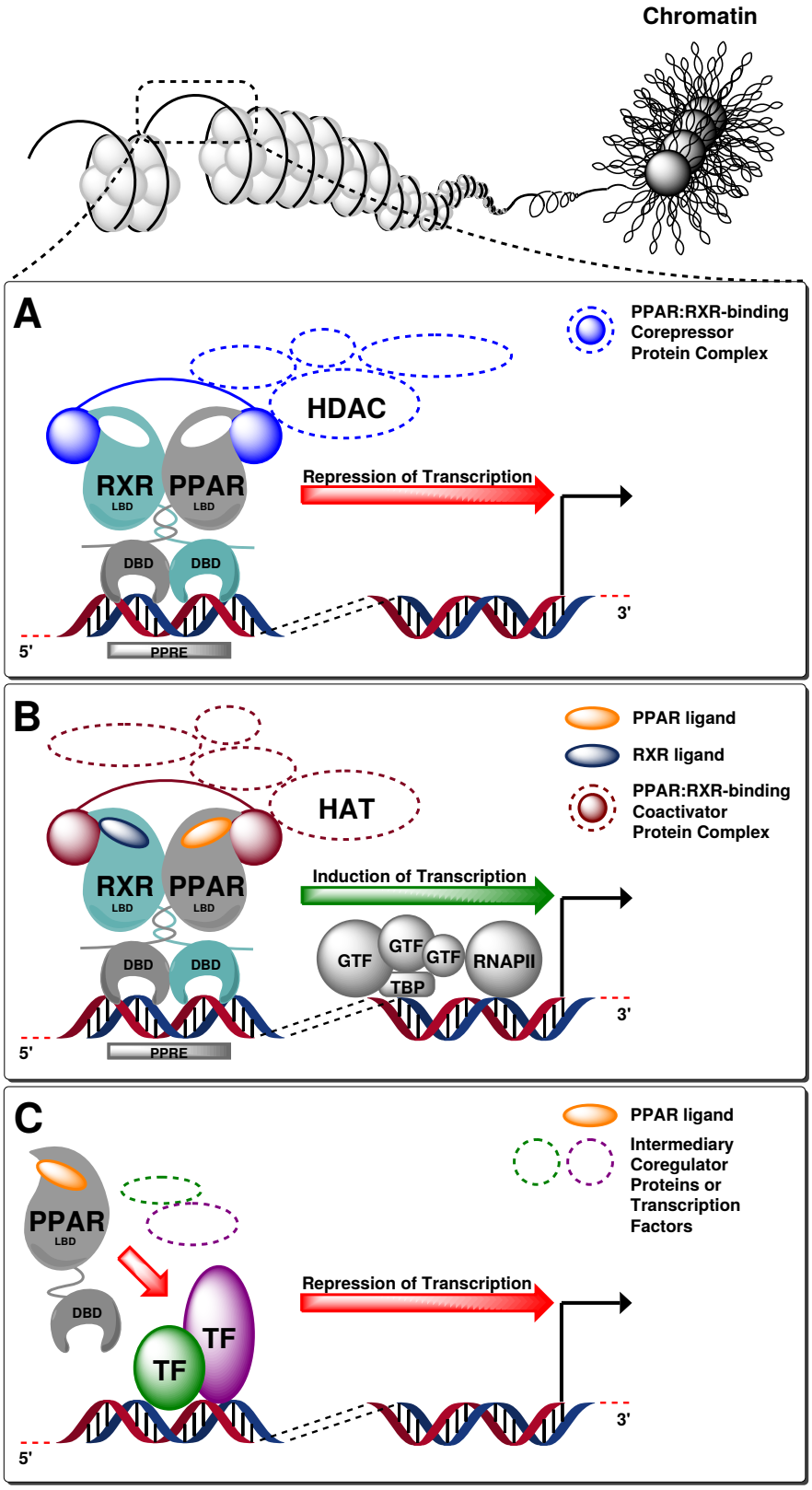

Figure 4.1. *Above*: The coiling of DNA around the nucleosomes and their packing into the condensed chromatin structure (with the scale increasing progressively from right to left). *Below*: Schematic representations of three important mechanisms of transcriptional regulation by the PPARs: (**A**) ligand-independent repression through interaction with corepressor proteins, (**B**) ligand-dependent (trans)activation through interaction with coactivator proteins, and (**C**) ligand-dependent transrepression by interactions of a monomeric PPAR with other transcription factors and/or coregulator proteins. GTF; General transcription factor TBP; TATA-binding protein. RNAPII; RNA polymerase II. The figure was adapted from Kornberg (2007),[69] and Ricote and Glass (2007).[80]

is transrepression. This mechanism does not involve the PPAR:RXR heterodimer, but rather the monomeric PPARs, which are capable of repressing other signalling pathways through interactions with their respective transcription factors and coregulator proteins. This type of mechanism has been demonstrated to be central to e.g. the anti-inflammatory effects of PPAR activation (see Figure 4.1c).[80,87]

In contrast to the above mentioned repression of target gene transcription by the apo-PPARs, the presence of *antagonistic* ligands may also cause repression of transcription. Antagonists may prevent the dissociation of corepressor proteins by blocking the access of agonists to the LBP, inducing an apo-like state, or by interacting with the LBP in a way that prevents helix 12 from assuming its active position (see Section 5.4.1).

In summary, the above described mechanisms of transcriptional regulation indicate that the binding of PPAR:RXR to PPREs may entail both repressive and inductive transcriptional consequences, depending on the presence of ligands and coregulator proteins.

5 The PPARs as Biological Targets

In the following, accounts of historically important developments in the field of PPAR research will be given. The chapter is organized to primarily focus on the different ligand classes and their roles in the elucidation of structure-function relationships in the PPARs, rather than on the actual chronology of the events.

The chemical structures of the ligands presented in this thesis are prepared two-dimensionally to resemble the three-dimensional poses in which they are observed in their respective PPAR LBPs (where structural data are available). The structure of each ligand thus corresponds to its pose as observed from viewing angle 1 of the PPAR LBDs, described in Section 2.2.1.

5.1 Ligand Classification and Terminology

To date, PPAR ligands of several functional classes have been described. Historically, the description of these ligands has based itself on the relationship of their effects to those of agonists - inducers of transcription. Thus, the effects of ligands that compete with the binding of agonists and consequently diminish their effect, have generally been characterized as antagonistic. Among these ligands, two subclasses may be distinguished, based on the transcriptional effects of the ligand in question, in the *absence* of a competing agonist. Ligands that, on their own, induce a level of transcription that is lower than that of reference agonists, have been described as partial agonists. On the other hand, ligands that on their own are transcriptionally silent, have been described as antagonists. Naturally, the use of these terminologies has varied depending on the assay systems and the cellular contexts in which a ligand has been evaluated.

The last decade has seen discoveries of divergent modes of ligand-dependent modulation of PPAR activity, which in turn are linked to the binding modes of the different ligand classes. These findings have left the typically employed ligand classifications in need of more precise definitions, in order to describe these binding modes and their effects on PPAR activity. Firstly, ligands that bind to regions of the PPAR LBPs, distant from the AF-2-pocket, may induce transcription through allosteric stabilization of helix 12. Secondly, in PPARγ, it has been elucidated that the inhibition of a post-translational modification (PTM) of the LBD, is both ligand-dependent and selectively affects the transcription of a subset of the known PPARγ target genes. More importantly, the ability of a ligand to inhibit this PTM did not correlate with its ability to induce transcription of classical PPARγ target genes.[88] Thirdly, ligands have been introduced, that display inverse agonistic effects on the expression of PPAR target genes or induce a phenotypic reversal in cells, along PPAR-regulated morphogenetic axes.[89,90] Finally, and with relevance to the effects of PPAR ligands in an *in vivo* context, the demonstrated simultaneous binding of multiple ligands to the PPAR LBPs suggests that certain ligand combinations may yield synergistic effects. These effects may stem from the binding of multiple equivalents of the same ligand or from heterogeneous ligand combinations. This property is, however, challenging to incorporate in the description of a ligand.

Thus, in the interest of conveying an association between the name of a ligand class and the binding modes and functional effects of its members, new definitions of the ligand classes referred to in this thesis, are given below. Since the examples of ligand functional diversity described above do not (yet) apply to all three PPARs, their binding modes, as observed by x-ray crystallography, NMR or hydrogen deuterium exchange coupled to mass spectrometry (HDX-MS), are taken as primary characteristics for their classification. Conversely, if the binding mode of a ligand is unknown, its classification is based on its observed effects on PPAR target gene expression. To compliment the structural and transcriptional data, a ligand may also be classified based on its effects on the affinity of the ligand:PPAR complex for peptides derived from coactivator- or corepressor proteins, as measured in time-resolved fluorescence resonance energy transfer (TR-FRET) experiments.

Finally, it should be noted that the ligand class definitions given here may prove insufficient to completely describe the functional effects of PPAR ligands, as data on the complete transcriptional profiles of their complexes with the PPARs become available.

(Classical) agonists are defined as ligands that bind to the AF-2 pocket and directly stabilize helix 12. These ligands often strongly induce the transcription of PPAR target genes, but there are also examples of weak (classical) agonists. This class also includes covalently binding (classical) agonists.

Partial agonists are defined as ligands that primarily bind to regions of the LBPs distant from helix 12 (often in the vicinity of helix 3 and in the Ω-pocket), but that do induce a measurable level of AF-2-mediated transcription, likely through an allosteric stabilization of helix 12. This class also includes covalently binding partial agonists. Finally, the few recently introduced ligands of this class, that do not induce a measurable level of AF-2 mediated transcription, are referred to as **non-agonists**.

Antagonists are defined as ligands that compete with classical agonists and to some degree partial agonists, but that by themselves do not induce a significant level of transcription. Certain members of this class interact with helix 12, but are transcriptionally silent. These ligands thus form a bridge between weak classical agonists and helix 12-interacting inverse agonists (defined below). A (silent) antagonist may also be classified as such based on the lack of recruitment of either coactivator- or corepressor proteins by the antagonist:PPAR complex in TR-FRET experiments. Furthermore, this class contains multiple examples of **covalent antagonists**.

Inverse agonists are defined as ligands that suppress the transcription of PPAR target genes below their basal expression levels and/or increase the interactions of the ligand:PPAR complex with corepressor proteins. Inclusion of the latter type of data causes this class to comprise both ligands for which an involvement of a direct destabilization of helix 12 is highly likely (as in PPARα or PPARγ) and ligands for which no data on their binding modes exist (as in PPARβ/δ).

5.2 PPAR Classical Agonists as Drugs to Treat Metabolic Diseases

The three known PPAR subtypes α, β/δ and γ (NR1C1 - 3) display both wide and tissue-specific distribution patterns in the human body. While new physiological roles of the PPARs are in the process of being elucidated, their key regulatory roles in metabolically active tissues are well established (see Section 3.2). As such, the ligand-dependent modulation of PPAR activity has been explored for its impacts on lipid and glucose metabolism in the development of pharmacotherapeutics to treat human metabolic disorders, such as type II diabetes mellitus (T2DM) and metabolic syndrome. Over the course of the last two decades, intense efforts by PPAR researchers have resulted in an array of small-molecular compounds capable of binding to each of the three PPAR subtypes with high affinity.

Following their discoveries, a number of small-molecular compounds targeting the PPARs have been subjected to clinical trials for indications related to metabolic disorders, some of which are presently active.[i] Several of these clinical candidates have, in turn, been approved by the United States Food and Drug Administration (FDA)[ii] and the European Medicines Agency (EMA)[iii] for the treatment of human metabolic disorders.

5.2.1 PPARα Agonists - the Fibrates

A notable group of PPAR-targeting pharmacotherapeutics include formulations containing PPARα agonists of the fibrate family such as clofibrate (**4**), gemfibrozil (**5**), fenofibrate (**6**), bezafibrate (**7**), ciprofibrate (**8**) or the more recently introduced, GFT505 (**9**) (see Figure 5.1).[iv] While the fibrates display beneficial effects in humans, such as decreases in serum triglycerides and increases in high density lipoprotein cholesterol (HDL-C),[91] clofibrate (**4**) was withdrawn from the U.S. market in 2002 due to hepatotoxicity[92,93] and an observed increase in the incidence of death by cancers in the treatment group, in a trial conducted by the World Health Organization (WHO).[94] Nonetheless, fibrates **5** - **8** are still considered first-line treatments in patients with severe hypertriglyceridaemia, or for cases in which statins are contraindicated.[91,95] GFT505 (**9**), on the other hand, which targets both PPARα and PPARβ/δ, is being investigated as a possible treatment for non-alcoholic fatty liver disease (NAFLD), a hepatic inflammatory condition related to insulin resistance and metabolic syndrome.[96]

5.2.2 PPARγ Agonists - the Glitazones

In clinical trials, PPARγ agonists of the thiazolidinedione (TZD) class, such as troglitazone (**10**, CS-045), rosiglitazone (**3**, BRL 49653) and pioglitazone (**11**, AD-4833) (see Figure 5.2),[v] were all efficacious in increasing insulin sensitivity and improving glycemic control in adults

[i] Public records pertaining to a number of the clinical trials referred to herein may be accessed through `http://clinicaltrials.gov/` or `http://www.clinicaltrialsregister.eu/`, by searching for the drug/compound in question.

[ii] `http://www.fda.gov/`

[iii] `http://www.ema.europa.eu/`

[iv] Sold under trade names Atromid-S (clofibrate); Gemcor, Lopid, Jezil, Gen-Fibro (gemfibrozil); Lipanthyl, Antara, Tricor, Lofibra, Fenoglide (fenofibrate); Bezalip, Cedur, Eulitop and Befizal (bezafibrate); Lipanor, Modalim (ciprofibrate).

[v] Sold under trade names Rezulin (troglitazone); Avandia, Avandamet, Avaglim, Avandaryl (rosiglitazone); Actos (pioglitazone)

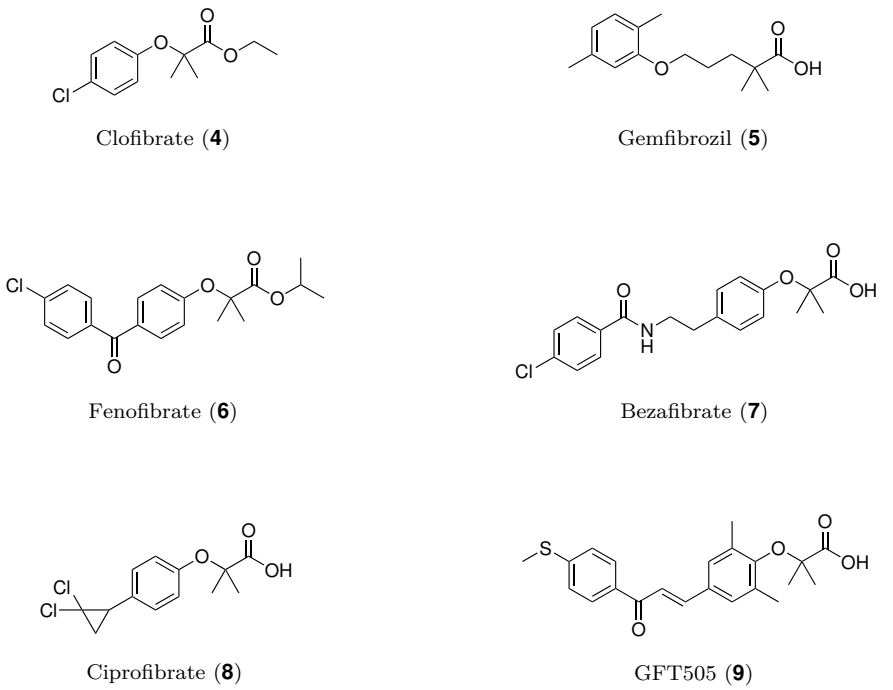

Figure 5.1. PPARα agonists previously and currently in use in clinical settings. Clofibrate (**4**) and fenofibrate (**6**) serve as prodrugs for their respective fibric acid derivatives, requiring enzymatic ester hydrolysis.

with type II diabetes.[97–99] Troglitazone (**10**, CS-045), was nevertheless withdrawn after a mere three years on the U.S. market, due to acute hepatotoxicity[100,101] and cases of pulmonary edema.[102] While rosiglitazone (**3**), reported by GlaxoSmithKline (GSK, then SmithKline Beecham Pharmaceuticals) in 1994[103,104] and approved by the FDA in 1999,[105] remains on the US market, its prescription and use were restricted by the FDA in 2011.[106] In contrast, in Europe and in India, its marketing authorization was suspended by the EMA in 2010[107] and its sale prohibited by the Drug Controller General of India (DCGI) the same year.[108] These regulatory actions reflected studies linking rosiglitazone treatment to an increased risk of myocardial infarction (heart attack).[109–111] Nevertheless, in 2013, the FDA lifted their restrictions on the utilization of **3** in response to a reevaluation of the data from the Rosiglitazone Evaluated for Cardiovascular Outcomes and Regulation of Glycemia in Diabetes (RECORD) trial.[112] The design of this GSK-funded trial and the conclusions drawn from it have been questioned by others.[113,114] A response from GSK to the latter of these critiques has also been published.[115]

Moreover, having seen widespread clinical use since its introduction, the awareness of the toxicological findings related to **3** resulted in civil and federal lawsuits against GSK in the United States of America. While most of these lawsuits were resolved prior to trial by settlements, totalling in excess of US$ 500 million, GSK agreed to plead guilty to having failed to include results from their own studies demonstrating an increased risk of congestive heart failure and myocardial infarction in their reports to the FDA, resulting in a US$ 240 million criminal fine.[116]

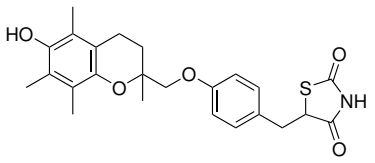

Troglitazone (**10**)

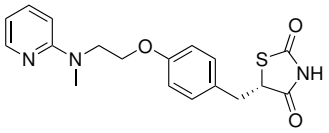

Rosiglitazone (**3**)

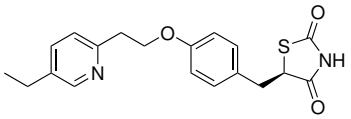

Pioglitazone (**11**)

Figure 5.2. PPARγ agonists previously and currently in use in clinical settings. Rosiglitazone (**3**) is depicted as its *S*-enantiomer, as this is the enantiomer observed in the LBP in x-ray crystallographic studies of PPARγ treated with racemic **3** (PDB ID: 2PRG, 4EMA). Similarly, pioglitazone (**11**) is shown as its *R*-enantiomer, for the same reason (PDB ID: 2XKW). Both **3** and **11** are used as racemic mixtures in drug formulations.

The TZD pioglitazone (**11**), which also displays significant affinity for PPARα, is associated with a lower risk of heart failure than rosiglitazone (**3**).[117] However, the use of **11** has been linked to the development of cancers in the bladder, the pancreas and the prostate.[118,119] While the FDA, pending an ongoing long-term safety review, has approved the continued use of pioglitazone-containing formulations with labels stating the increased risk of bladder cancer,[120] the EMA recently withdrew the marketing authorizations for pioglitazone.[121,122]

In parallel, a body of evidence has grown demonstrating additional class-wide side effects of TZDs including weight gain (through fluid retention and increased adipose tissue mass) and decreased bone density (with concomitant increased fracture risk).[123] Consequently, on account of their side effects, the use of TZDs is decreasing worldwide.[124–126] In conlusion, the story of the glitazones has spurred debates, in academia and in the general community, on the need for stricter requirements regarding the safety endpoints of clinical trials and the moral operating principles of the pharmaceutical industry.[100,127,128]

5.2.3 PPARα/γ Dual Agonists and pan-PPAR Agonists

The sligthly less severe side effects associated with pioglitazone (**11**), combined with its effects on PPARα, led to the hypothesis that the undesirable effects of the TZD class of PPARγ agonists on serum lipids, and consequently on the risk of adverse ischemic events, could be overcome by concurrent activation of PPARα. In a more general perspective, it was envisioned that the simultaneous activation of all three PPARs by *pan*-PPAR agonists would result in a "balanced" overall effect.[129–131] To this end, efforts by several pharmaceutical companies were directed at the development and evaluation of a family of dual PPARα/γ agonists called the glitazars. Notable compounds from this family include naveglitazar (**13**, LY519818) by Eli Lilly, ragaglitazar (**14**, NN622) by Dr. Reddy's Laboratories/Novo Nordisk, tesaglitazar (**15**) by AstraZeneca, muraglitazar (**16**) by Bristol-Myers Squibb, aleglitazar (**17**) by

GSK and saroglitazar (**18**) by Zydus Cadila (see Figure 5.3).

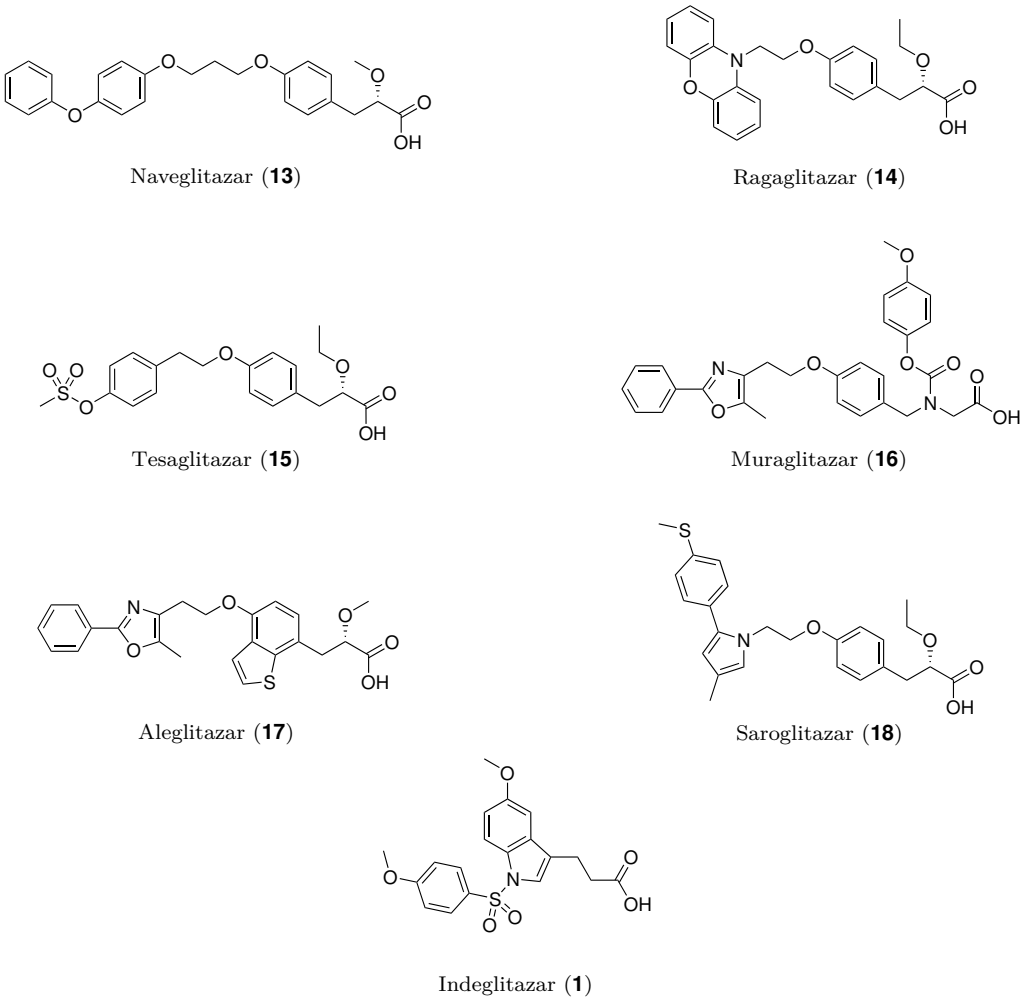

Figure 5.3. Dual PPARα/γ agonists **13** - **17** used in clinical trials, saroglitazar (**18**) which is available on the Indian market and the pan-PPAR agonist indeglitazar (**1**).

While most of these compounds displayed beneficial effects in laboratory experiments and early-stage clinical trials, only saroglitazar (**18**) reached the market. It was approved by the DCGI in 2013 for use in India in the treatment of T2DM and dyslipidemia.[132] In contrast, muraglitazar treatment was associated with an increased risk of death by adverse cardiovascular events such as congestive heart failure or myocardial infarction.[133] Among the major contributing reasons for the discontinuation of the developments of the other mentioned clinical candidates, were findings of sarcomas and urinary- and gall bladder cancers in rodents treated with the compounds.[134–137] Finally, the pan-PPAR agonist indeglitazar (**1**, PPM-204) displayed plasma glucose-lowering effects in mice and rats, as well as weight reductions in hamsters and bonnet macaques.[15] Indeglitazar was also submitted to clinical trials in human patients with type II diabetes mellitus,[vi] however the results of these trials do not appear to have been reported.

[vi] See EudraCT Numbers 2005-004227-19 and 2006-003897-87 at `http://www.clinicaltrialsregister.eu/` and identifier NCT00425919 at `http://clinicaltrials.gov/`.

5.2.4 PPARβ/δ agonists

To date, no PPARβ/δ agonist has reached the market. Both the recently introduced MBX-8025 (**19**) and the well-known PPARβ/δ agonist GW501516 (**20**)[138] (see Figure 5.4) apparently fared well in phase II trials in patients with dyslipidemia.[139–142] However, Cymabay Therapeutics has announced that they will redirect the development of **19** towards rare and orphan diseases, or conditions for which there are few treatment options, such as homozygous familial hypercholesterolemia (HoFH), severe hypertriglyceridemia (SHTG), primary biliary cirrhosis/cholangitis (PBC) and non-alcoholic steatohepatitis (NASH).[143] In the case of GW501516 (**20**), its further development by GSK was suspended, likely based on evidence from studies in rodents, demonstrating carcinogenic effects of **20** in multiple tissues.[144,145] Although the roles of PPARβ/δ in the pathophysiologies of human cancers are not fully understood,[146,147] other reports have also supported the involvement of PPARβ/δ agonism in carcinogenesis.[148–151]

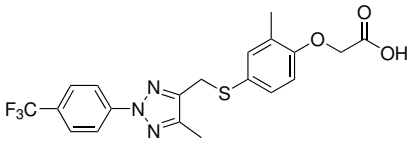

MBX-8025 (**19**)

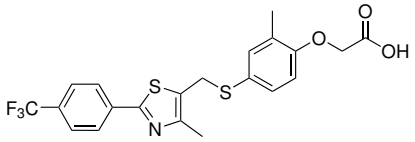

GW501516 (**20**)

Figure 5.4. PPARβ/δ agonists used in clinical trials.

While GW501516 (**20**) was never approved for use in humans, there has been a significant interest in PPARβ/δ agonists from the athletic community, particularly on the part of endurance athletes and bodybuilders. The extent of this interest, likely sparked by publications describing the increased running endurance of laboratory animals treated with **20**,[152,153] is reflected in a somewhat unusual warning issued by the World Anti-Doping Agency (WADA), in which they urge athletes seeking performance enhancement to abstain from using GW501516 (**20**), due to its demonstrated toxicity (carcinogenesis).[154] Only in 2013, however, several professional cyclists tested positive for use of **20**.[155] On the other hand, the enthusiasm concerning **20**, also known as “Endurobol” or “Cardarine” in the bodybuilding community, may be gleaned from online resources such as Youtube[vii] and forums dedicated to the topic of bodybuilding.[viii] What the long term physiological effects of these "anectdotal trials” will be for the individuals involved, remains to be seen.

[vii] Search for “GW501516” on YouTube, `http://www.youtube.com/results?search_query=GW501516`

[viii] Examples include: `http://www.elitefitness.com/forum/`, `http://www.worldclassbodybuilding.com/forums/`

5.3 Emerging Therapeutic Potential for PPAR Modulators

In the following, some emerging areas of research into the ligand-dependent modulation of the PPARs are discussed. Several of the accounts draw heavily on data from PPARγ, being the most amply studied member of the PPARs. As such, it should be noted that the regulatory mechanisms demonstrated in one of the PPARs, may not be applicable to the other members. Nonetheless, given the high degree of homology and conservation of the fold between the PPARs, in addition to the concrete examples of coinciding modes of ligand-dependent modulation and PTMs presented, the implication that similar mechanisms may exist in the other PPARs, is generally justified. In the least, such an approach will serve to highlight aspects of the structure and function of a particular PPAR subtype that appear to be understudied to date.

5.3.1 Alternative Binding Modes of PPARγ Partial Agonists

In the previously described developments of PPAR classical agonists as drugs to treat metabolic diseases (see Section 5.2), the clinical candidates spanned a narrow spectrum of molecular structures. The apparent lack of therapeutic potential attributed to ligands of other chemical classes, as judged by their absence in the clinical trials described thus far, may reflect the development of the theoretical framework of ligand-dependent PPAR modulation (*vide infra*).

Since the disclosures of the first x-ray crystallographical determinations of PPARγ (1998),[11,21] PPARβ/δ (1999)[26] and PPARα (2001)[156] in complex with ligands, structure-activity relationships (SARs) have been explored, guided by the observed interactions between key residues in the PPAR LBPs and the ligands. Notably, the binding modes observed with early PPARγ agonists were similar to those of agonists in other nuclear receptors.[21,157,158] These findings reinforced the view that a stabilization of helix 12 in the C-terminal AF-2 (see Chapter 2 for structural details) was a critical feature of the mechanism through which a ligand:PPAR complex activates transcription.

Over the course of nearly two decades of PPAR research, however, several PPARγ ligands with alternative binding modes have been discovered. These ligands include specific endogenous fatty acids and their metabolites,[29,64,66,67] serotonin metabolites (see Figure 5.5),[14] and a range of natural products (see Figure 5.6)[159] and synthetic ligands (see Figure 5.7).[160] Many of these ligands display only a moderate activation of reporter gene assays and may, as such, have been disregarded as viable clinical candidates. However, their importance as lead structures for the development of new modulators of PPARγ has become clear in light of the developments of the last five years. This shift in focus may reflect the relative failure of PPAR classical agonists (many of them full agonists) to provide therapeutical benefits that outweigh their various toxicities, but also the establishment of a new mode of ligand-dependent modulation of PPARγ activity (*vide infra*).

Studies on the structure and dynamics of PPARγ in complex with partial- and non-agonistic ligands have accumulated data that demonstrate both the structurally wide range of ligands hosted by the PPARγ LBP, as well as the distinct patterns of stabilization caused by

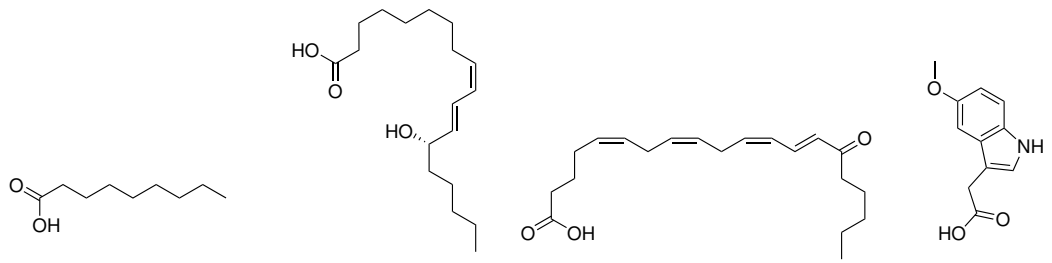

Nonanoic acid (**21**) 13(S)-HODE (**22**) 15-oxo-ETE (**23**) MIA (**24**)

Figure 5.5. Selected endogenous PPARγ partial agonists.

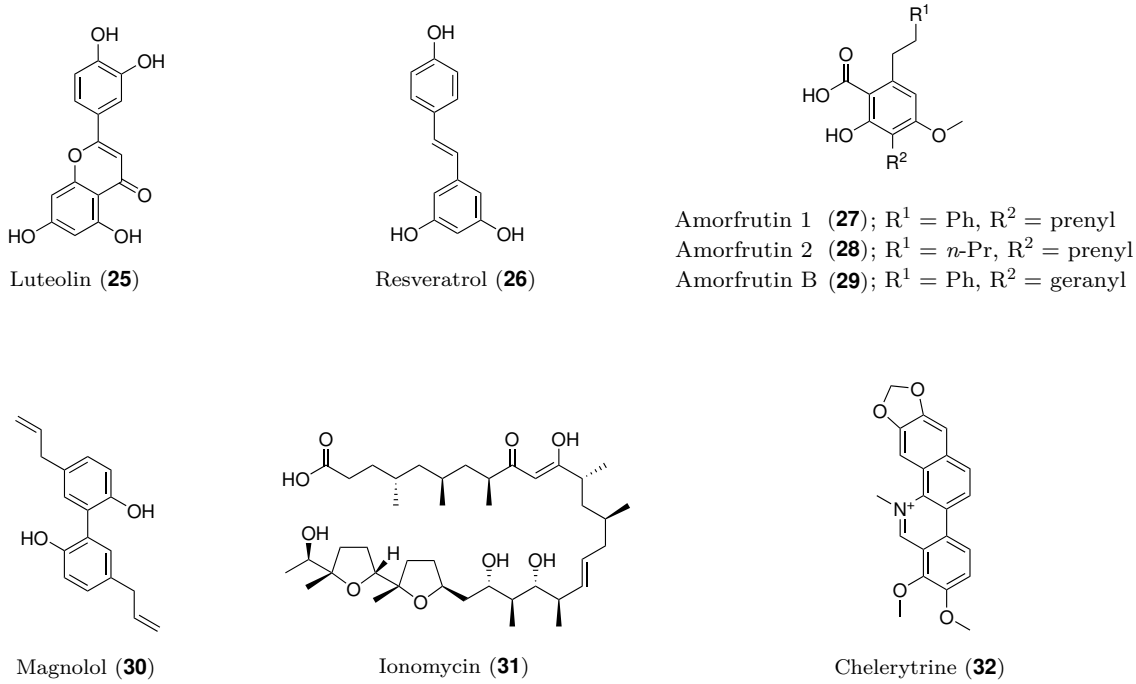

Luteolin (**25**) Resveratrol (**26**)

Amorfrutin 1 (**27**); R^1 = Ph, R^2 = prenyl
Amorfrutin 2 (**28**); R^1 = *n*-Pr, R^2 = prenyl
Amorfrutin B (**29**); R^1 = Ph, R^2 = geranyl

Magnolol (**30**) Ionomycin (**31**) Chelerytrine (**32**)

Figure 5.6. Selected natural product PPARγ partial agonists.

the binding of these ligands. Among the techniques used in these studies, x-ray crystallography, NMR spectroscopy and HDX-MS have proven instrumental in demonstrating that several of these ligands bind to a region of the LBP distant from the AF-2-pocket, and as such, do not directly stabilize helix 12 (see Figure 5.8 and Figure 5.9). More precisely, the ligands interact with helix 3, the Ω-pocket and the Ω-loop. The distinct stabilization of these regions has been observed e.g. in the B-factors from x-ray crystallographic data, in chemical shift values from NMR spectroscopy and in a differential protection against hydrogen-deuterium exchange in HDX-MS studies.[161–165] Interestingly, ligands of this type also display beneficial effects in animal models of metabolic disease and in humans, and thus show promise as ligands that may achieve the long-sought goal of separating the ligand-dependent PPARγ regulation of glucose metabolism from that of adipogenesis. Ligands displaying this ability have somewhat generally been coined selective PPARγ modulators (SPPARγMs).[160,166,167]

In this context, seminal work by Itoh et al., Waku et al. and more recently by Hughes et al.,

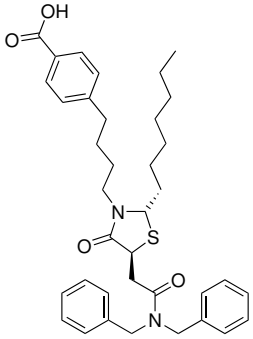

GW0072 (**33**)

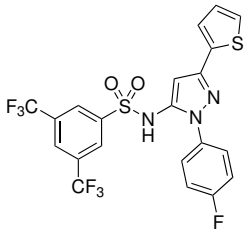

Compound 1 (**34**)

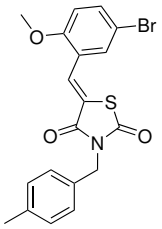

GQ-16 (**35**)

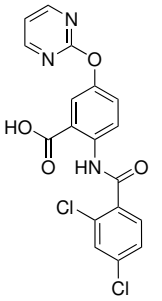

BVT.13 (**36**)

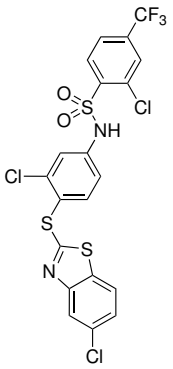

T2384 (**37**)

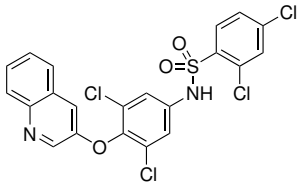

INT131 (**38**)

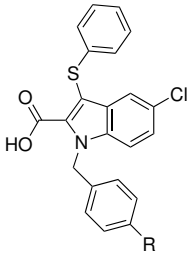

nTZDpa (**39**); R = Cl
SR145 (**40**); R = H
SF147 (**41**); R = OMe

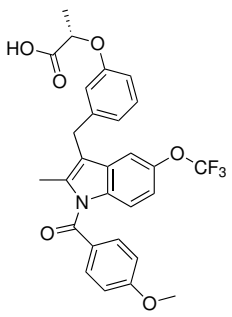

MRL24 (**42**)

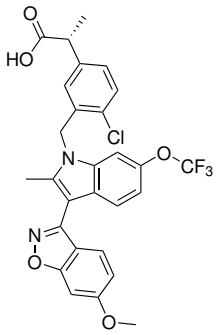

SPPARγM2 (**43**)

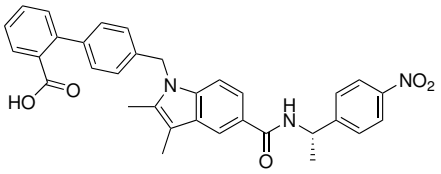

SR1664 (**44**)

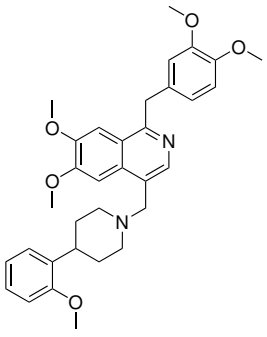

PA-082 (**45**)

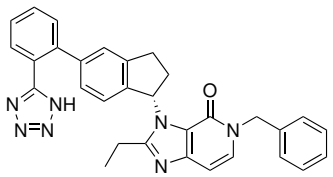

Compound 12b (**46**)

Figure 5.7. Selected synthetic PPARγ partial agonists (SPPARγMs).

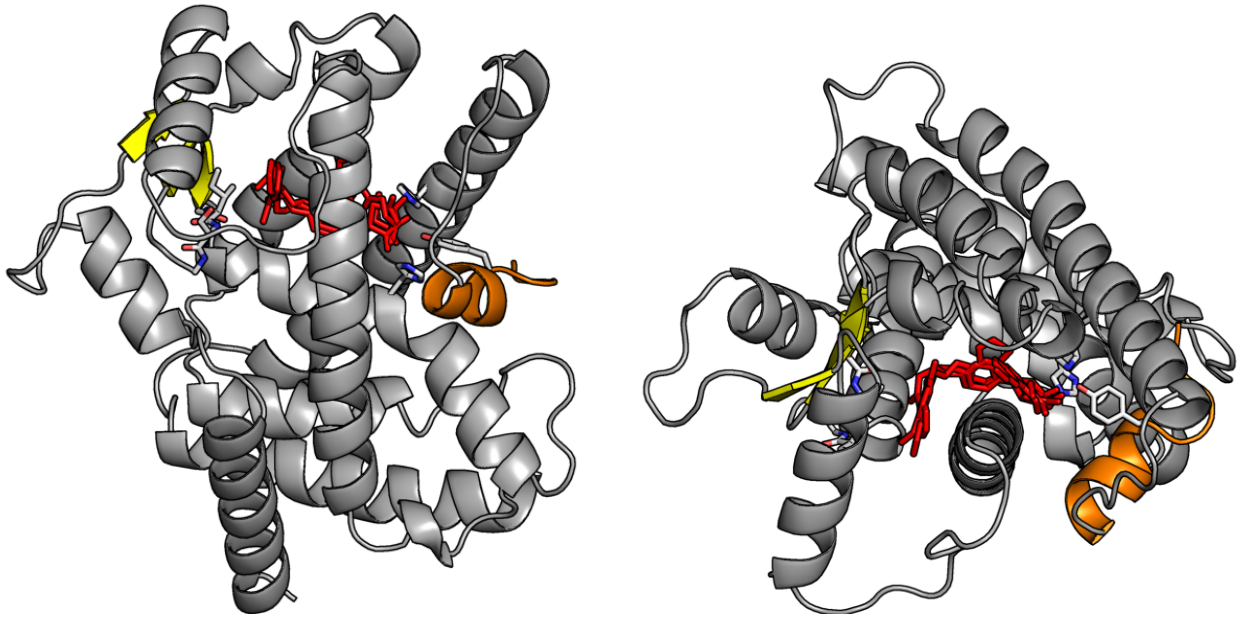

(a)

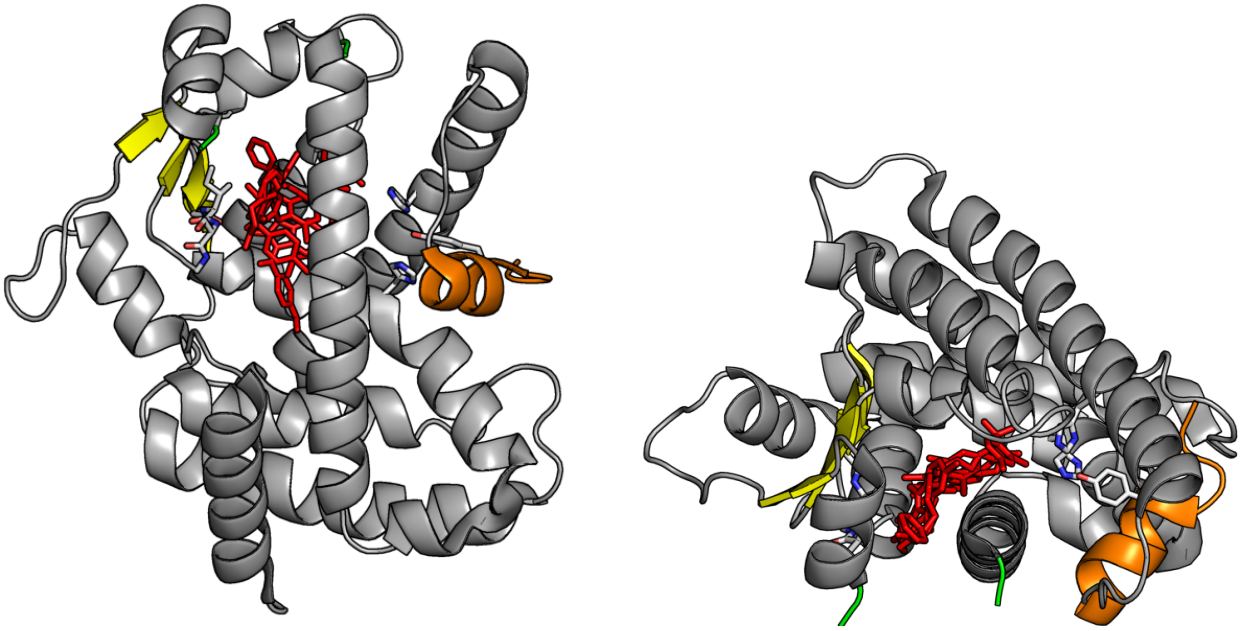

(b)

Figure 5.8. The general binding modes of PPARγ classical agonists and partial agonists. *Top*: The agonists are colored red to visualize their general position in the PPARγ LBP. Their head groups extend into the AF-2-pocket and stabilize helix 12 (orange) through the formation of a network of hydrogen bonds commonly involving the residues His323, His449 and Tyr473, shown as sticks to the right. The tails of larger agonists also extend into the Ω-pocket where they may interact with the β-sheets (yellow sheets and grey sticks). *Bottom*: The partial agonists are colored red to visualize their general position in the PPARγ LBP. The partial agonists occupy the Ω-pocket and do not interact with helix 12 (orange) in the AF-2 pocket. Rather, they stabilize helix 3 and the β-sheet region (yellow sheets and grey sticks), commonly through interactions with the residues Ile341 and/or Ser342. The residues 340 - 343 of the lower β-sheet are drawn as grey sticks, with the sidechains of Ile341 and Ser342 facing the pocket. The first and last residues of the Ω-loop, the central portion of which is not resolved in the structure, are shown in green. The PPARγ structures shown were taken from PDB ID: 2PRG[21] (*top*) and PDB ID: 2Q5S[164] (*bottom*) and visualized with PyMOL.[13]

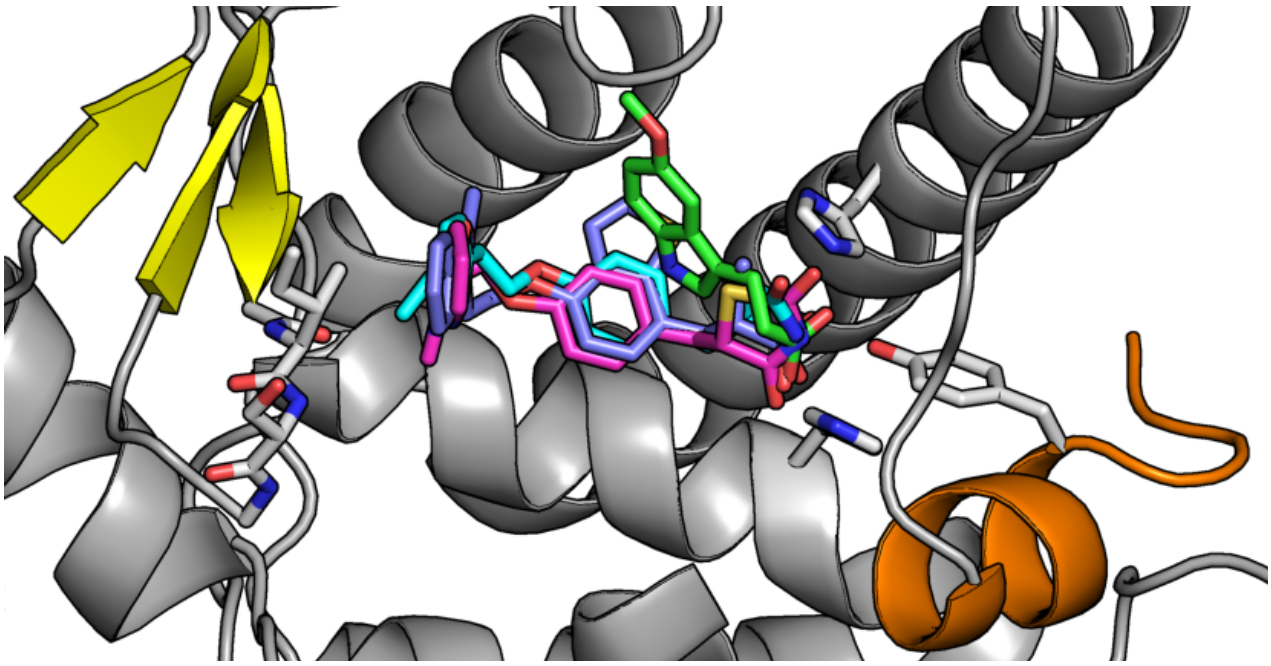

(a)

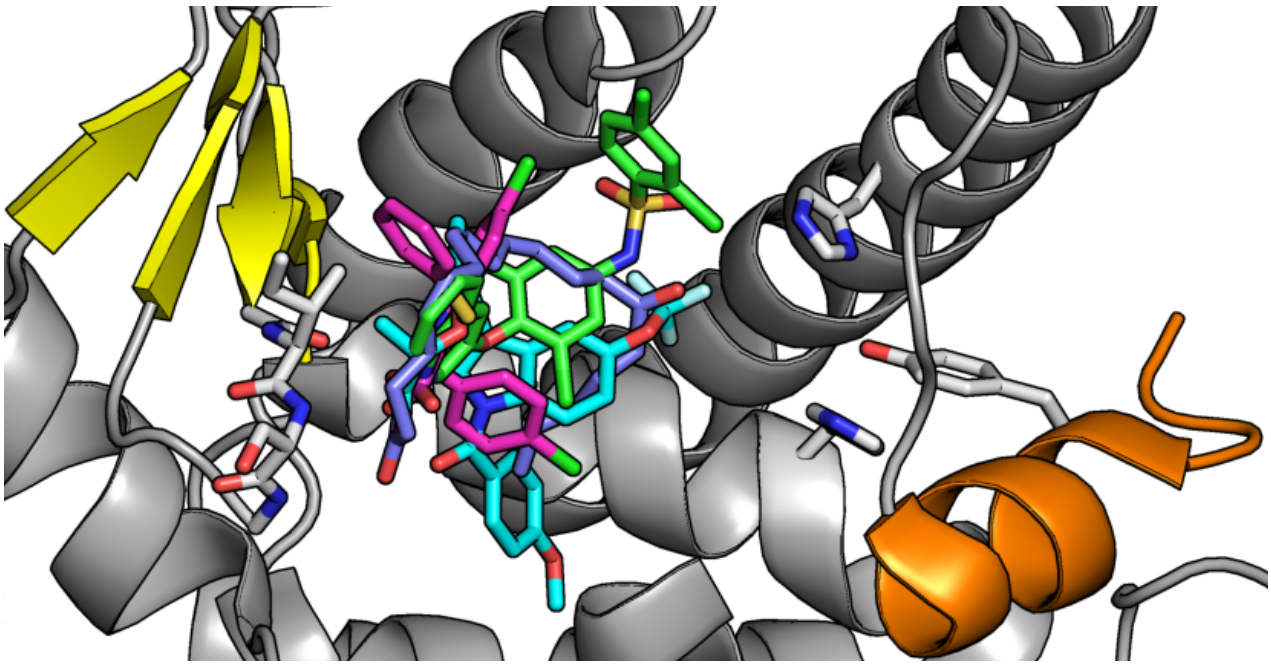

(b)

Figure 5.9. An expanded view of the binding modes of PPARγ classical agonists and partial agonists. The AF-2 residues His323, His449 and Tyr473 are shown as sticks to the right. The residues 340 - 343 of the lower β-sheet are drawn as sticks, with the sidechains of Ile341 and Ser342 facing the pocket. *Top*: The shown agonists are: rosiglitazone (**3**, magenta, PDB ID: 2PRG), pioglitazone (**11**, cyan, PDB ID: 2XKW), the dual PPARα/γ agonist aleglitazar (**17**, purple, PDB ID: 3G9E) and the pan-PPAR agonist indeglitazar (**1**, green, PDB ID: 3ET0). The pose shown for pioglitazone (**11**) is one of two alternative conformations observed, the second of which had the TZD head group directed towards the opening of the pocket between the β-sheets and helix 3. *Bottom*: The PPARγ partial agonists nTZDpa (**39**, magenta, PDB ID: 2Q5S), MRL24 (**42**, cyan, PDB ID: 2Q5P), INT131 (**38**, green, PDB ID: 3FUR) and 15-oxo-ETE (**23**, PDB ID: 2ZK4). The Helix 2', the Ω-loop and helix 3 (residues 276 - 287) are hidden to improve the visibility of the LBP. The PPARγ structures shown were taken from PDB ID: 2PRG[21] (*top*) and PDB ID: 2Q5S[164] (*bottom*) and visualized with PyMOL.[13]

suggest that the Ω-pocket represents a functionally distinct binding site from the AF-2 pocket. These and other studies have demonstrated that the Ω-pocket binding site is functional even when the AF-2 pocket is occupied by a ligand.[24,168–170] Importantly, discrete binding curves for the Ω-pocket-binding ligands could also be obtained, after covalent modification of the reactive, central cysteine residue on helix 3 (Cys285), by the electrophilic antagonists GW9662 (**47**), T0070907 (**48**) (see chemical structures in Figure 5.16 in section 5.5), as well as by endogenous oxo-fatty acids 5-oxo-ETE and 15-oxo-ETE (**23**). These results contribute to a view of the PPARγ Ω-pocket as an independent ligand binding site.[14,57]

In a more general perspective, solvent probes have shown clustering in 10 hot spots of the PPARγ LBP, attesting to the many possible points of ligand interactions.[171] Indeed, in addition to the studies mentioned above, the available PPARγ crystallographic data show yet other complexes with multiple ligands.[39,172,173] From an evolutionary perspective, the apparent indiscriminateness of the PPARγ LBP may rather be an adaptive trait, that not only serves to maintain sensitivity towards a broad spectrum of endogenous structures (even larger ones), but that also retains the possibility for smaller ligands to collectively activate the receptor through simultaneous binding.

5.3.2 Ligand-regulated Phosphorylation of PPARγ

The above described studies on PPARγ partial agonists were recontextualized by the discovery of the regulation of a new PTM site in the PPARγ LBD. In 2010, Choi et al. demonstrated the cyclin dependent kinase 5 (Cdk5)-mediated phosphorylation of PPARγ Ser273 (Ser245)[ix] and a connection between a high level of phosphorylated Ser273 (pSer273) and obesity, in both mice and humans.[x] Importantly, they also demonstrated a correlation between the ligand-dependent inhibition of this phosphorylation and the regulation of a distinct set of genes, including genes that are commonly dysregulated in obesity (e.g. adipsin and adiponectin). Notably, in their studies, these effects were brought about by MRL24 (**42**, Figure 5.7), a compound that displayed only a partial activation of transcription in a PPARγ reporter gene assay and that does not directly stabilize helix 12 in the AF-2 (see Figure 5.9, bottom).[164] By HDX-MS, Choi et al. could also show that the binding of **42** protected helix 3, the β-sheets and the P-loop against deuterium incorporation. Conversely, although the potent PPARγ classical agonist rosiglitazone (**3**) (see Figure 5.2), also inhibited Ser273 phosphorylation, its binding to PPARγ induced a broader set of genes. This set included genes linked to fluid retention and hallmark genes of adipogenesis, linked to an increase in adipose tissue mass, both of which are side effects observed with the TZD class of PPARγ agonists.[88]

Several PPARγ partial- and non-agonists have been shown to inhibit phosphorylation of Ser273, among them, the natural products amorfrutin 1 (**27**),[174] ionomycin (**31**),[175] chelerytrine (**32**)[176] (see Figure 5.6) and the ginseng saponins pseudoginsenoside F11[177] and pro-

[ix] Ser273, used by the Choi et al., corresponds to PPARγ2 numbering,[10] which is coherent with the discovery of this PTM in adipocytes. The larger part of the PPARγ literature, however, uses PPARγ1 numbering. Thus, while this particular residue will consequently be referred to as Ser273, other references to residue numbers in PPARγ, will correspond to those of the UNIPROT sequence of PPARγ1.

[x] This is an example of a regulatory PTM occurring on an NR, as briefly mentioned in Section 4.1.

topanaxatriol.[178] Also among them are the synthetic partial agonists BVT.13 (**36**), nTZDpa (**39**),[88] GQ-16 (**35**),[161] (see Figure 5.7) telmisartan,[179] Mbx-102 (*R*-metaglidasen)[88] and F12016.[180] The similar binding modes of several of these PPARγ ligands (see Figure 5.8 and Figure 5.9), further support that binding to the Ω-pocket and/or the β-sheet region is conducive to inhibition of Ser273 phoshorylation.

In recent studies, the origin of the regulation of a distinct subset of genes by the phosphorylation of Ser273, has been linked to the interaction of PPARγ pSer273 with the coregulator protein thyroid hormone receptor associated protein 3 (Thrap3/TRAP150). Choi et al. could show that the interaction of phosphorylated PPARγ with Thrap3 was both sensitive to ligand treatment with MRL24 (**42**), SR1664 (**44**) (see Figure 5.7) and rosiglitazone (**3**), as well as to a mutation of Ser273 to alanine. In addition, they demonstrated that knockdown of Thrap3 expression, in both cultured adipocytes and in mice, resulted in increased expression of adipsin and adiponectin.[181] While the region of Thrap3 that was necessary for its interaction with phosphorylated PPARγ could be narrowed down,[181] it is uncertain whether this coregulator binds to the canonical coregulator binding site. Interestingly, it has been demonstrated that the expression of both the pSer273-inhibited genes adipsin and adiponectin,[88] as well as classical adipogenic genes such as *Ap2/Fabp4* and *Sreb-1c*, is dependent upon a functional helix 12. This is based on the observation that a PPARγ Glu471Gln mutant, which is believed to be incapable of binding coactivator proteins,[182] was also incapable of inducing the transcription of all of these genes in mice.[183]

In sum, these results delineate a separation of the mechanisms through which ligands can affect the transcriptional regulation by PPARγ. They also offer an explanation as to how ligands displaying weak classical agonism can potently improve metabolic parameters in obese humans, with greatly diminished side effects, compared to TZDs.

5.3.3 Allosteric Stabilization of the AF-2 by PPARγ Partial Agonists

In studies on PPARγ partial agonists that bind exclusively to the Ω-pocket, it has been observed that several of these induce a certain degree of transcriptional activation (transactivation). A likely hypothesis holds that this reflects an allosteric stabilization of the AF-2 region and thus of the canonical coactivator binding site. As was shown with PA-082 (**45**, Figure 5.7), partial agonists may influence the affinity profile of PPARγ for coactivator proteins, allowing it to retain binding to PGC-1α, while not recruiting the SRC and CPB families of coactivators.[184] The origin of the AF-2 stabilization caused by Ω-pocket-binding partial agonists and its effects on coregulator recruitment is not entirely clear. Nonetheless, the stabilization of helix 12 may correlate with the ability of a ligand to stabilize LBP residues on helix 3 and in the Ω-loop.

The residues Arg288 and Phe363 have been suggested to mediate such a stabilization.[29,185] Through the backbone of helix 3, the dynamics of the residues in the LBP are connected to those of the residues on the opposite (solvent-exposed) side of the helix. The residue Lys301 is involved a coactivator binding charge-dipole interaction referred to as the "charge clamp".[21,186]

Additionally, residues such as Phe282, Phe287 and Gln286 may interact in a stabilizing or destabilizing manner with the loop between helix 11 and helix 12.[29,66,90] Finally, the reactive cysteine residue, Cys285, holds a particular position, as the formation of a covalent bond between this residue and an electrophilic ligand may be envisioned to have a profound effect on the dynamics of helix 3.

Furthermore, the Ω-loop is often stabilized significantly by PPARγ partial agonists.[161–165] Interestingly, MD-simulations indicate that a change in the dynamic patterns of the Ω-loop, caused by the binding of a partial agonist, may explain both the previously proposed function of the Ω-loop as a gatekeeper to the Ω-pocket, as well as its role in the stabilization of the loop between helix 11 and helix 12.[187]

Taken together, these observations may indicate that the development of Ω-pocket-binding PPARγ ligands, with negligible potential for AF-2-mediated transcriptional activation of adipogenic genes, will require a more detailed understanding of the mechanisms of the networks of allosteric stabilization in the PPARγ LBD.

5.3.4 Clinical Trials with a PPARγ Partial Agonist

The compound INT131 (**38**, T0903131, T131, AMG131) (see Figure 5.7) was introduced in 2004 as a high-affinity PPARγ ligand, designed to minimize the side effects observed with TZDs[188–190] (see Section 5.2.2). For instance, treatment of rats with **38** had been shown to increase circulating adiponectin levels.[188,191,192] INT131 was submitted to clinical trials in T2DM patients in 2009,[xi] in which it improved glycemic control in the treatment groups. While its usage was associated with a mild weight gain, compared to the placebo groups, this was the only reported side effect of statistical significance. The weight gain was also lower than that caused by pioglitazone (**11**). In terms of its effects on bone density, a parameter on which the TZDs produce a negative impact, the described clinical trials were not statistically powered to conclude on the effects of INT131 (**38**).[193,194] A study in mice, however, indicates that **38** is able to normalize bone parameters offset by diet-induced obesity.[195]

Even though INT131 (**38**) appeared to be a promising clinical candidate for improving glycemic control in patients with T2DM, InteKrin Therapeutics Inc. filed a drug repurposing patent for INT131 in August 2014,[196] redirecting it towards the treatment of multiple sclerosis (MS).[197] Thus, a clinical trial with INT131 in patients suffering from Recurring Remitting MS (RRMS) was commenced in 2015.[xii] This potential indication for the use of PPARγ ligands is linked to the finding of high levels of PPARγ in the cerebrospinal fluid of MS patients,[198] combined with the roles of PPAR activation in neuroprotection and remyelination.[199,200] In light of the demonstrated separate induction of classical agonism and/or inhibition of Ser273 phosphorylation by PPARγ ligands, the neuroprotective effects of PPARγ modulation will require further study to determine the involvement of each of these mechanisms. In this context, as noted by Choi et al., it is intriguing that the non-phosphorylatable Ser273Ala PPARγ mutant induced an upregulation of the *Ahnak* protein and of proteolipid protein 1

[xi] See identifiers NCT00631007 and NCT00952445 at `http://clinicaltrials.gov/`

[xii] See identifier NCT02638038 at `http://clinicaltrials.gov/`

(*Plp1*), both of which are involved in myelination.[88]

5.3.5 Phosphorylation of the PPARα and PPARβ/δ LBDs and Ligands with Alternative Binding Modes

The observation that a PTM (LBD phosphorylation) modulates PPARγ target gene expression is paralleled by observations from the context of PPARα-regulated transcription. In a human hepatoma cell line, it was demonstrated that the protein kinase C (PKC)-mediated phosphorylation of Ser179 in the linker region and/or[xiii] Ser230 in the LBD (see Figure 5.12) markedly affected the transcription of PPARα target genes such as *CPT1a* and *PPARA*. Thus, inhibition of PKC reduced both basal expression and that induced by the PPARα agonists pirinixic acid (WY14643,[201] **49**) and GW7647 (**50**) (see Figure 5.10), suggesting that phosphorylation of PPARα is important for its ability to induce transcription of these genes.[202]

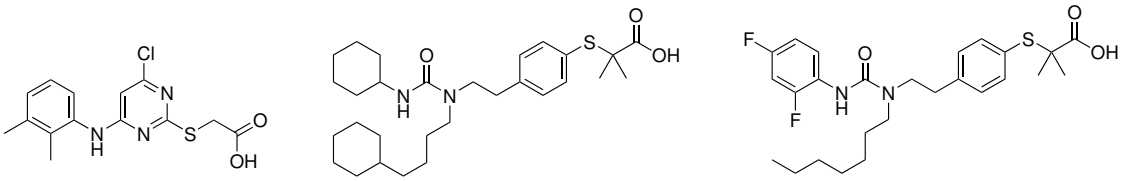

WY14643 (**49**) GW7647 (**50**) GW9578 (**51**)

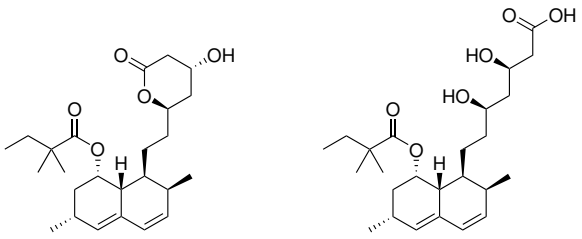

Simvastatin (**52**) Simvastatin β-hydroxy acid (**53**)

Figure 5.10. PPARα ligands shown to modulate the phosphorylation of the PPARα Ser179 and/or Ser230 by PKC.

In another study, the ability of PPARα ligands to inhibit the lipopolysaccharide (LPS)-induced expression of pro-inflammatory NF$\kappa\beta$ target genes *iNOS*, *IL-6* and *TNF*α was investigated. The inflammatory response to LPS also involves activation of PKC which phosphorylates PPARα. However, upon treatment of PPARα with the agonist GW9578 (**51**) or simvastatin (**52**)[203,204] (the actual ligand may be its hydrolysis product **53**, see Figure 5.10), a ligand- and PPARα-dependent decrease in the transcription of *iNOS* was observed. A similar effect was also observed upon pharmacological inhibition of PKC.[205] The observed effect was thus likely caused by a stronger tendency towards transrepression of the NF$\kappa\beta$-p65 transcription factor complex by ligand-bound PPARα.[80,205,206] In line with these results, the

[xiii] According to the cited works, both Ser179 and Ser230 are sites of PKC phosphorylation. Therefore, the non-phosphorylatable Ser→Ala double mutant was used in these studies. The effects of phosphorylation at exclusively one of these serines are thus unknown.

authors demonstrated that the non-phosphorylatable double mutant (Ser179Ala, Ser230Ala) could also repress the transcription of a GAL4-p65 chimeric reporter, even in the presence of a constitutively active form of PKC. This indicates that PKC-mediated phosphorylation of PPARα was inhibited by ligand binding.[205] Together, these results indicate that some PPARα target genes are regulated by both ligand binding and PTMs (serine phosphorylation), and that the binding of the described ligands has an inhibitory effect on the PKC-mediated phosphorylation of PPARα Ser179, Ser230 or both.

Recently, a new region of ligand binding in the PPARα LBP was described for pirinixic acid (WY14643, **49**). X-ray crystallographic data of PPARα in complex with **49**, revealed that while **49** did bind to the AF2-pocket and stabilized helix 12 as a classical PPAR agonist, a second molecule of **49** bound to a site between helix 3, the Ω-loop and the β-sheet region (see Figure 5.11). Subsequent molecular dynamics (MD) simulations demonstrated a stabilizing effect on the Ω-loop and the P-loop, in response to the presence of the second molecule of **49**.[207]

With the Ω-loop and the β-sheet region as common denominators, these findings thus indicate a mechanism of stabilization of the P-loop in PPARα, that appears to be analogous to the demonstrated mechanism of ligand-induced stabilization of the P-loop in PPARγ.[88] Taken together with the observation that stabilization of the β-sheet region correlates to the ability of PPARγ ligands to inhibit the phosphorylation of Ser273 (see Figure 5.12),[88] further studies should seek to determine whether stabilization of the β-sheet region in PPARα is indeed instrumental to the modulation of PPARα phosphorylation, as described above.

In PPARβ/δ, on the other hand, a regulatory site of phosphorylation in the P-loop has yet to be demonstrated.[74,208] Nonetheless, the presence of several solvent-exposed, phospho-

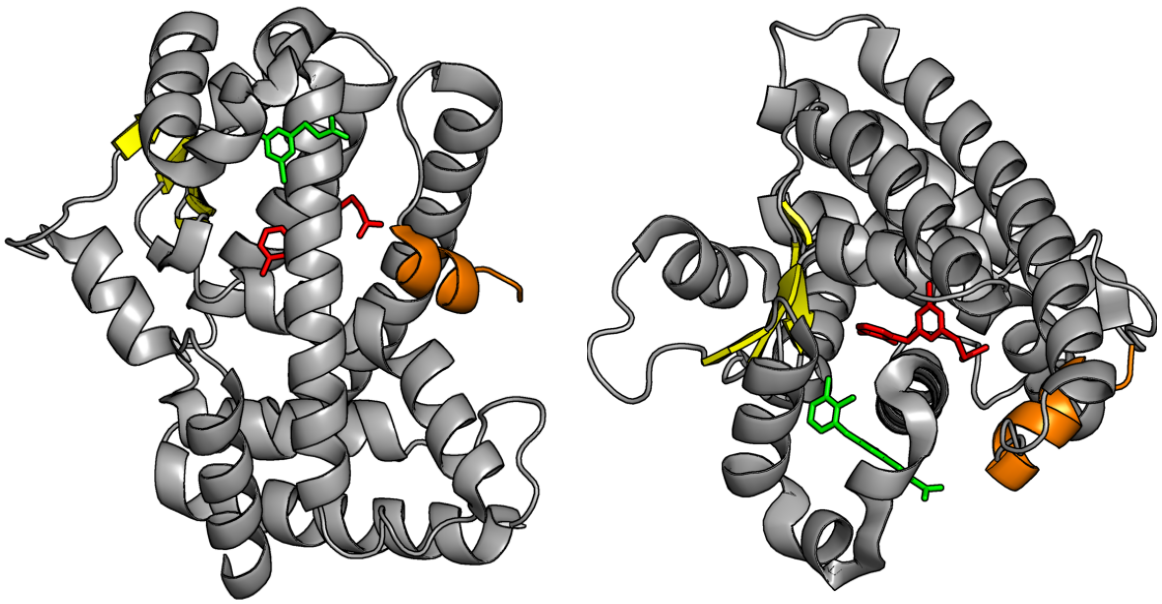

Figure 5.11. Two molecules of WY-14643 (**49**) bound to the PPARα LBP. The molecule occupying the classical agonist pose, in which it stabilizes helix 12 in the AF-2 pocket is colored red. The second molecule occupying the alternative binding site under the Ω-loop is colored green. The PPARα structure shown was taken from PDB ID: 4BCR[207] and visualized with PyMOL.[13]

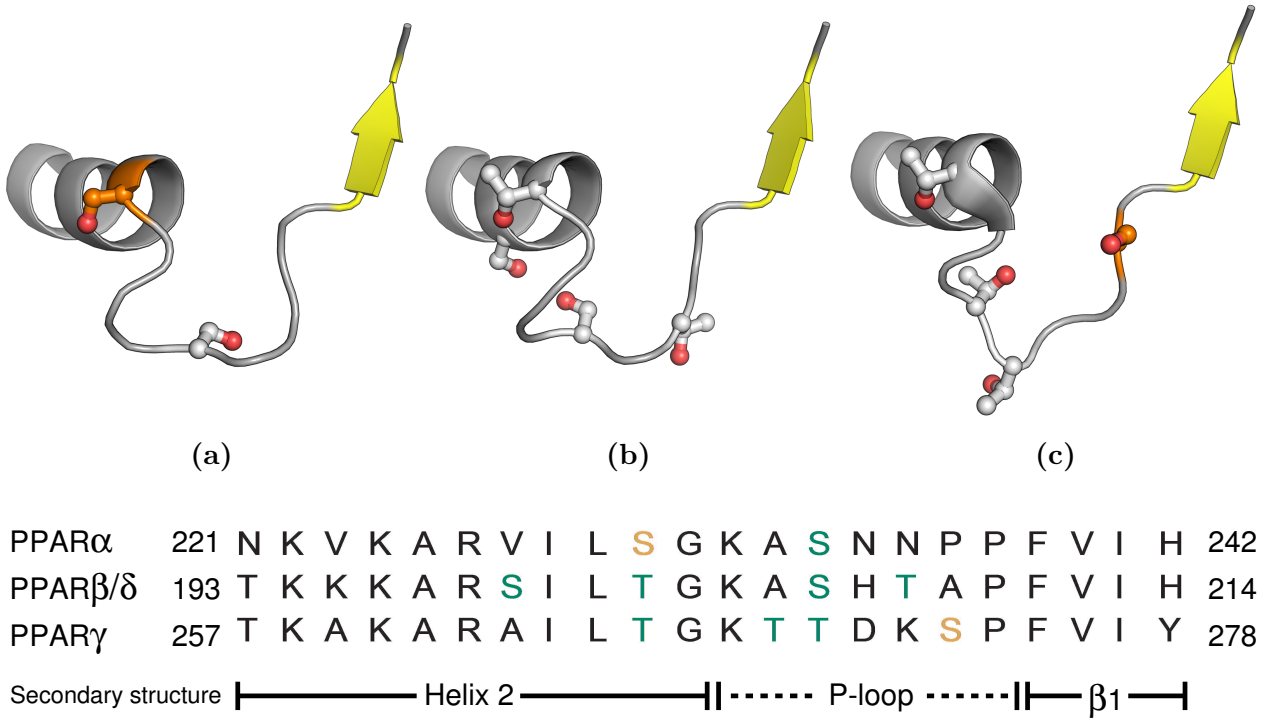

Figure 5.12. *Top*: The P-loops of PPARα (a), PPARβ/δ (b) and PPARγ (c) are shown, flanked by helix 2 and the first β-sheet (in yellow) on either side. The solvent-exposed, phosphorylatable residues shown in grey and the known sites of phosphorylation in PPARα (Ser230) and PPARγ (Ser273) are shown in orange, both in ball and stick representation. *Bottom*: The sequences of PPARα, PPARβ/δ and PPARγ of the structures shown above, with their residue numbering (UNIPROT canonical sequences for PPARα and PPARβ/δ, and PPARγ2 numbering for PPARγ)[10] and secondary structure indicated. Phosphorylatable residues towards the end of helix 2 and the in P-loop (serines and threonines) are shown in green. Known sites of phosphorylation (PPARα Ser230 and PPARγ Ser273) are shown in orange.

rylatable residues in the P-loop of PPARβ/δ (see Figure 5.12), suggests that the occurrence and roles of PTMs in this region merit further study.

In the context of PPARβ/δ agonistic ligands with alternative binding modes, high-affinity PPARβ/δ ligands that do not bind to the AF-2 pocket have also been reported.[209,210] These ligands display binding to helix 3 and the Ω-pocket of PPARβ/δ (see Figure 5.13). The intriguing differential transcriptional outcomes of treatment of PPARγ with Ω-pocket-binding ligands compared to ligands that bind to the AF-2 pocket, warrant genomewide transcriptional analyses of PPARβ/δ in complex with ligands of this understudied class. In the context of the classical PPARβ/δ agonist GW501516 (**20**), such studies have previously provided exquisite insight into the complex transcriptional regulation by PPARβ/δ in WPMY-1 myofibroblasts.[211]

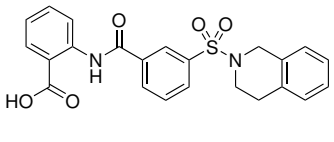

GW9371 (**54**)

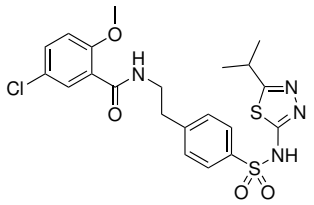

Compound 6 (**55**)

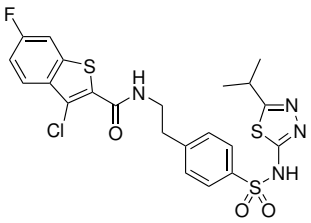

Compound 11t (**56**)

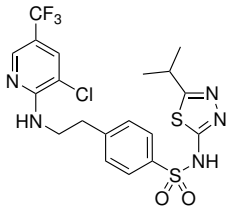

Compound 20a (**57**)

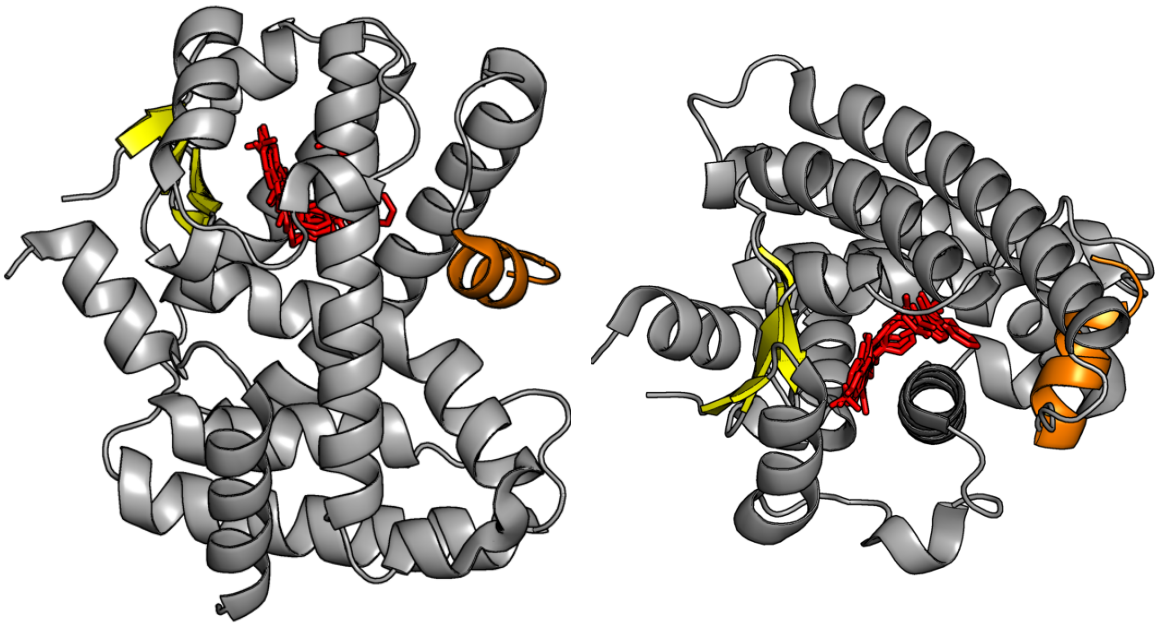

Figure 5.13. *Top*: PPARβ/δ partial agonists binding to the Ω-pocket. *Bottom*: The PPARβ/δ structure shown was taken from PDB ID: 2XYX[209] and visualized with PyMOL.[13]

5.4 PPAR Antagonistic Ligands

5.4.1 Inverse Agonists - the AF-2-pocket Revisited

The development of ligands for PPARγ that are capable of inhibiting the phosphorylation of Ser273, have in recent years focused on ligands binding to the Ω-pocket, and in particular, to the β-sheet region. In the realm of PPAR antagonism on the other hand, the view of helix 12 as a crucial region of stabilization in the mode of action of classical *agonists*, spawned the hypothesis that a ligand-induced *destabilization* of helix 12 could confer antagonism.[212] Based on this strategy, antagonists of all three PPAR subtypes have been successfully developed (see Figure 5.14).[35,90,213–217] These antagonists have typically been structurally akin to their agonist counterparts, except for the incorporation of larger, more sterically bulky head groups. While their antagonism of agonist-induced activity in PPAR reporter assays has been demonstrated, x-ray structural data to evaluate the actual binding poses of these antagonists in the respective PPAR LBPs, as well as their effects on helix 12, are scarce. As the only structural data of its kind, the GW6471:PPARα:SMRT complex (PDB ID: 1KKQ)[xiv] demonstrates the disruptive nature of the head group of GW6471 (**58**) on the position of helix 12. Furthermore, treatment of the PPARs with these ligands has been shown to confer upon their respective targets, a greater affinity for corepressors (such as SMRT or NCoR), attesting to the functional character of their inhibition of AF-2-mediated agonism.[35,90,213]

In cellular systems, it has been observed that treatment of PPARα or PPARγ with certain members of this class of ligands decreases the expression of genes induced by classical agonists to subbasal levels, thus earning the ligands a status as inverse agonists.[90,214,215,217] In PPARγ, the mechanisms behind the observed basal or constitutive expression of its target genes may involve a ligand-independent recruitment of coactivators by apo-PPARγ, such as that of PGC-1α.[218,219] The constitutive recruitment of other coactivators, including p300, may be involved in the basal expression of the *aP2/FABP4* gene in adipocytes.[220] Both PGC-1α interaction and *aP2/FABP4* expression are dependent on helix 12.[183,186] A destabilization of helix 12 by PPARγ inverse agonists, with concurrent recruitment of corepressor proteins, is thus a likely mechanism of repression of both these types of basal expression.

5.4.2 Clinical Outlooks for PPARγ Inverse Agonists

The currently available data on the ligand-dependent PPARγ modulation, suggests that the antidiabetic effects of PPARγ ligands owe to their ability to inhibit phosphorylation of Ser273 and is likely not linked to their abilities as classical, AF-2 mediated agonists. At a time before these data were available, the development of PPARγ inverse agonists as pharmacotherapeutics may naturally have been avoided, based on a concern that such ligands would cause severe metabolic side effects. While today, these concerns may be less relevant with respect to the regulation of glucose metabolism by PPARγ, systemic AF-2 mediated inverse agonism would likely have negative consequences on lipid storage and metabolism.

In some aspects however, inverse agonistic properties are indeed beneficial. As men-

[xiv] See Figure 2.6 in chapter 2 for the effects on the position of helix 12.

(a)

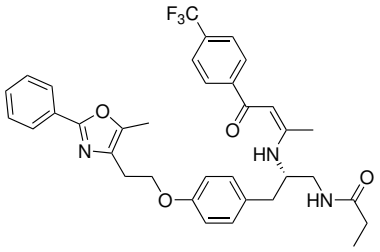

GW6471 (**58**)

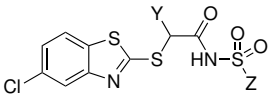

Compound 4g (**59**); Y = Ph, Z = Ph
Compound 2c (**60**); Y = *n*Pr, Z = Me
Compound 2e (**61**); Y = *n*Bu, Z = Me
Compound 2g (**62**); Y = Ph, Z = Me

(b)

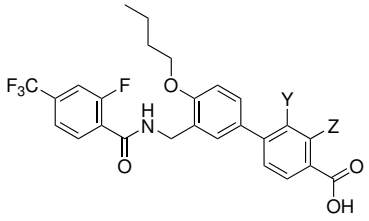

Compound 3a (**63**); Y = H, Z = H
Compound 3g (**64**); Y = F, Z = H
Compound 3h (**65**); Y = Me, Z = H
Compound 3i (**66**); Y = H, Z = Me

(c)

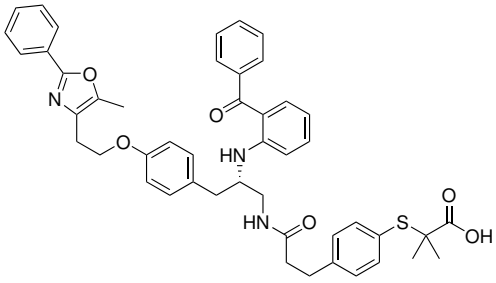

GSK5737 (**67**)

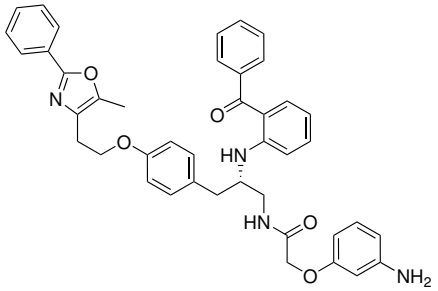

GSK5775 (**68**)

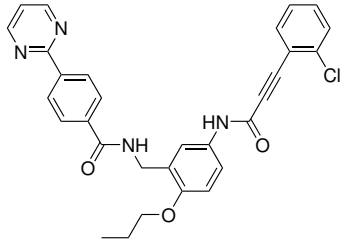

Compound 9p (**69**)

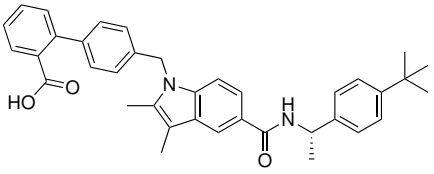

SR2595 (**70**)

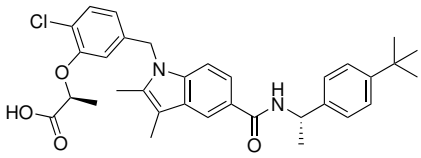

SR10221 (**71**)

Figure 5.14. Antagonists against PPARα (a), PPARβ/δ (b and PPARγ (c), designed to perturb the folding of helix 12 and thus inhibit the formation of a coactivator binding site.

tioned in Section 5.2.2, a detrimental side effect of the use of members of the TZD family of PPARγ classical agonists as antidiabetic drugs, was their negative impact on bone density, seen particularly in women.[123] In contrast, the promotion of osteogenesis by the PPARγ inverse agonist SR2595 (**70**) (see Figure 5.14) has been demonstrated. Consistent with an inhibition of PPARγ classical agonism, the authors could also show that the SR2595-induced upregulation of bone morphogenetic proteins *BMP2* and *BMP6* was similar to that induced by siRNA-mediated PPARγ knockdown.[90] These results may thus hold promise for the future utility of **70** and other reported PPARγ inverse agonists such as GSK5737 (**67**), GSK5775 (**68**)[217] and compound 9p (**69**)[213] (see Figure 5.14).

5.5 Covalent Reactivity of the PPARs

Another important embodiment of the ligand-dependent modulation of the PPARs, involves the nucleophilic reactivity of a cysteine residue, conserved throughout the PPARs, which is located on helix 3, centrally in the binding pocket (see Chapter 2). The ability of the thiol moiety of this cysteine residue to react with electrophilic substrates of both endogenous and exogenous origin, has been demonstrated. However, while numerous examples of ligands that bind covalently to PPARγ can be found in the literature, reports of such events from PPARα and PPARβ/δ are more scarce. In this section a brief survey of the known covalent ligands of the PPARs will be given.

5.5.1 Covalent Ligands of PPARα

In the case of PPARα, the only reported example of covalent modification by a ligand involves the PPARγ selective antagonist GW9662 (**47**) (see Figure 5.16). Interestingly, in PPARα, the covalent binding of **47** conferred partial agonism in a GAL4-PPARα reporter gene assay. However, this effect was not observed with full-length PPARα on an LFABP promoter in HEK293-cells.[221]

5.5.2 Covalent Ligands of PPARγ

The transcriptional outcome of covalent modification of PPARγ have ranged from agonism to antagonism. Covalent PPARγ agonists include oxo-[29,64,65] and nitro-metabolites[66,67] of fatty acids, the 15-deoxy-$\Delta^{12,14}$-prostaglandin J2 (**72**)[222,223] (see Figure 5.15 and the chemical structures in Appendix A) and some synthetic ligands[224,225] (see Figure 5.16). The covalent modification of PPARγ by the oxo- and nitro-fatty acids induce partial agonism, with transcriptional acitivies ranging from approximately 10 - 60% of those induced by PPARγ full agonists. These differences in transcriptional activity may be connected to the ability of the carboxylate head group in each fatty acid to stabilize helix 12. Such a stabilization may depend on the distance from the site of covalent attachment to the carboxylate head group, as well as on the flexibility of the carbon chain leading to the head group. The said distance is dictated by the location of the nucleophilic attack by Cys285 on each fatty acid, i.e. the β- or δ-carbons of the dienones present in the oxo-fatty acids, or the β-carbon in

the α,β-unsaturated nitro-fatty acids.[xv] Combinations of these factors likely produce the range of effects observed with covalently binding fatty acids, from the more strongly agonistic 6-oxo-OTE (**73**) and 6-oxo-THA (**74**), to the near antagonistic 8-oxo-ETE (**75**)[29,64–67] (see Figure 5.15). An extreme example of a distance mismatch may be represented by 15-oxo-ETE (**23**) (see Figure 5.15), the carboxylate head group of which does not engage in interactions with helix 12, plausibly due to the length and rigidity of the carbon chain between the carboxylate and the site of nucleophilic attack by Cys285. The rather strong partial agonism seen upon treament of PPARγ with 15-oxo-ETE,[29] may thus owe to an allosterically induced stabilization of helix 12, caused by its multiple interactions with residues on helix 3 and in the Ω-pocket (see also Section 5.3.3). In summary, the covalent binding of fatty acid metabolites may be of physiological importance, as several of the oxo-fatty acids display inductions of transcription that exceed those of their hydroxy-analogues by up to an order magnitude.[64]

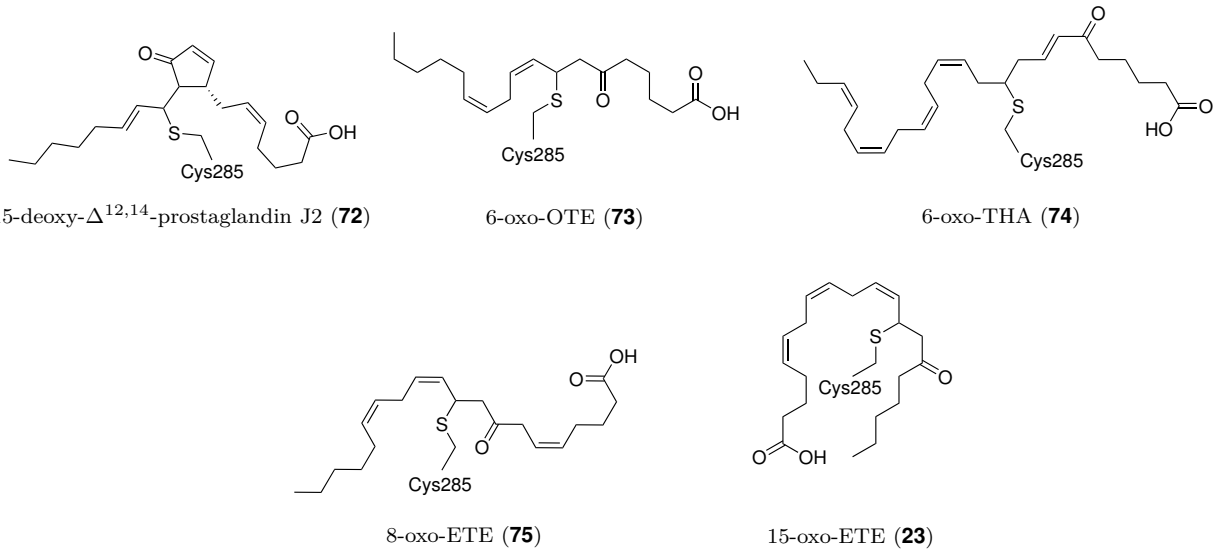

Figure 5.15. Covalent binding of selected endogenous oxo-fatty acids by PPARγ. The structures and poses of **72**–**75** were taken from PDB IDs: 2ZK1, 2VV4, 3X1I, 2ZK3 and 2ZK4, respectively.

Among the covalently binding PPARγ ligands of synthetic origin, the compound L-764406 (**76**) (see Figure 5.16) was shown to be partial agonist in a GAL4-PPARγ reporter assay and in measurements of *Ap2/Fabp4* mRNA levels in 3T3-L1 preadipocytes.[224] Recently, a PPARγ covalent partial agonist, that is a structural hybrid between the antagonist GW9662 (**47**) and a naturally sourced ethyl cinnamate, has been developed. The cinnamic ester tail of Compound 5 (**77**) (see Figure 5.16) was designed to bind to the Ω-pocket and its relatively higher induction of adiponectin compared to *Ap2/Fabp4*,[225] may be indicative of a ligand profile that is similar to other Ω-pocket-binding PPARγ partial agonists (see also Section 5.3.1).

Covalent antagonists (see Figure 5.16) of PPARγ have held a prominent position in studies of the function of PPARγ. As the covalent attachment of a ligand centrally in the LBP

[xv] Corresponding to either 1,4- or 1,6 conjugate additions for the oxo-fatty acids and 1,4-conjugate additions for the nitro-fatty acids.

may block the access to the AF-2 pocket, the effect of treatment of PPARγ with antagonists such as GW9662 (**47**),[221] and T0070907 (**48**),[226] has been observed as an unresponsiveness to classical agonists. The inhibition of classical agonism naturally encouraged the conclusion that PPARγ-regulated transcription was completely silenced upon treatment with these antagonists. However, as introduced in section 5.3.1, it has recently become clear that the Ω-pocket remains receptive to ligands, even in the presence of such covalent ligands. As demonstrated by Hughes et al.,[57] this finding may indicate that the conclusions reached in studies, in which covalent antagonists such as GW9662 (**47**) or T0070907 (**48**) have been employed to rule out the involvement of PPARγ or ligand binding to PPARγ, may need to be reconsidered in light of the new data.

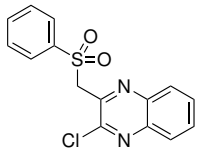

L-764406 (**76**)

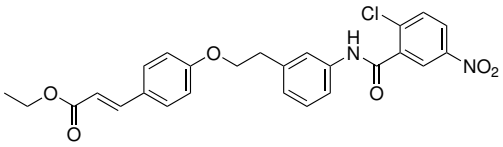

Compound 5 (**77**)

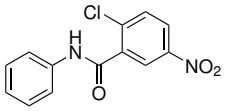

GW9662 (**47**)

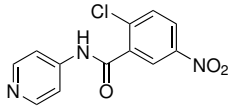

T0070907 (**48**)

Figure 5.16. Covalent PPARγ partial agonists and antagonists.

5.5.3 Covalent Ligands of PPARβ/δ

Covalent agonists of PPARβ/δ have not been described thus far. On the other hand, as noted for PPARα, treatment of PPARβ/δ with the PPARγ-selective antagonist GW9662 (**47**) was also observed to covalently modify the PPARβ/δ LBD. In contrast to its partially agonistic effect in PPARα, treatment of PPARβ/δ with **47** did not elicit transcriptional activation of a GAL4-PPARβ/δ reporter.[221]

GSK3787 (**78**) was identified in a high-throughput screen of a GlaxoSmithKline in-house compound collection and displayed an $IC_{50} = 0.20\,\mu M$ ($pIC_{50} = 6.7$) in a ^{3}H-GW2433[227] displacement assay. Compound **78** failed to induce transcription in a GAL4-PPARβ/δ reporter assay, but completely inhibited transcriptional induction by the agonist GW501516 with an $IC_{50} = 0.13\,\mu M$ ($pIC_{50} = 6.9$). In a subsequent structure-activity relationship (SAR) study, two analogues of GSK3787, Compound 9 (**79**) and Compound 16 (**80**), were found to be slightly more potent binders of PPARβ/δ (see Figure 5.17).

Interestingly, the sulfide analogue of **78**, namely compound **81**, as well as analogues Compound 19 (**82**) and Compound 20 (**83**), respectively bearing either a 5-methyl group or a hydrogen in place of the 5-trifluoromethyl group on the pyridine ring, were inactive in the same assay. The requirement of an electron-poor pyridine ring poised Shearer et al. to investi-

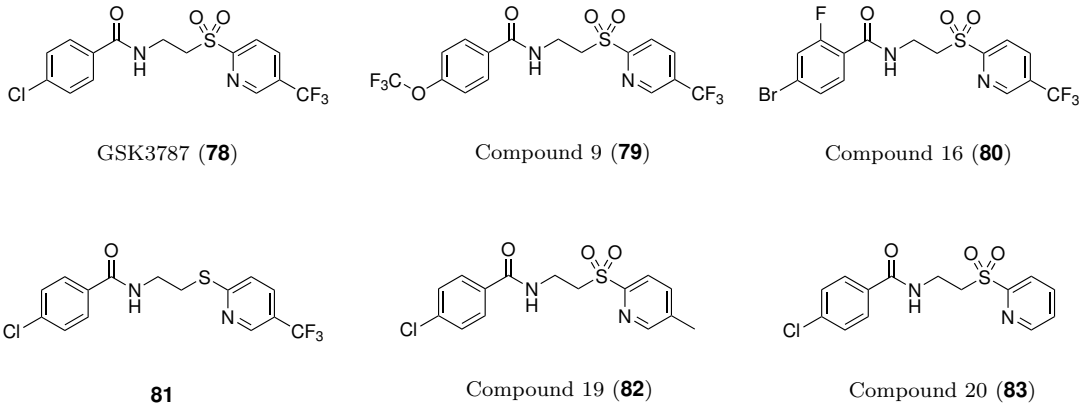

Figure 5.17. GSK3787 (**78**) and analogues.

gate the possibility of covalent binding to PPARβ/δ. Indeed they found that both GSK3787 (**78**) and Compound 9 (**79**), augmented the mass of PPARβ/δ as seen by LC-MS analysis. Subsequent LC-MS/MS analysis of PPARβ/δ treated with GSK3787 (**78**) identified the residue bearing the added mass as Cys249.[228] However, despite its apparent selectivity towards PPARβ/δ in a ligand displacement assay (>50 times versus PPARα and PPARγ),[228] another study found that treatment of PPARγ with **78**, at pharmacologically relevant concentrations, did antagonize agonist-induced effects on transcription and coactivator recruitment. Interestingly, on its own, GSK3787 (**78**) profiled as a PPARγ partial agonist, based on its effects in a reporter assay and on coregulator recruitment.[229]

5.6 Motivations and Backgrounds of Study

In the context of the developments of PPAR ligands described in the preceding sections, a more detailed background for the studies presented in this thesis is given below.

PPARβ/δ is highly expressed in psoriatic lesions[50,230] and PPARβ/δ antagonism has recently been shown to have a beneficial effect in models of psoriasis.[231] Notably, GSK3787 (**78**) was among the PPARβ/δ antagonists used in this study and required less frequent dosing, likely due to its covalent binding to PPARβ/δ.

GSK3787 (**78**) represents a chemical entity of interest with regards to its reported covalent mode of action.[228] However, **78** displayed less than desirable selectivity for PPARβ/δ.[229] Thus, in order to be able to employ covalent modification of Cys249 in the PPARβ/δ LBP as a means to pharmacological antagonism of PPARβ/δ in cells that also express PPARγ, the development of new analogues of **78** is warranted. Papers I and II, presented in Chapter 6, widen the scope of the SAR around this class of PPARβ/δ antagonists, aiming to increase their selectivity for PPARβ/δ.

In a broader context, PPARβ/δ inverse agonists[xvi] have been demonstrated to inhibit invasion by human breast cancer cells in model systems[89] and normalize abberrant PPARβ/δ-

[xvi] The terminology is used based on corepressor recruitment. No structural data regarding the interactions of these ligands (see Chapter 7) with helix 12 are available.

dependent gene expression patterns in ovarian carcinomas.[232] While the roles of PPARβ/δ in the pathophysiologies of cancers are incompletely understood,[146,147] these results furnish interesting endpoints for the further development of PPARβ/δ antagonistic ligands. The PPARβ/δ antagonistic ligands reported to date, span a wide range of chemical structures. Little is known about their binding modes and interactions with the PPARβ/δ LBP. Paper III, presented in Chapter 7, aims to on shed light on the mode of action of a selection of the reported antagonistic ligands, with a particular focus on their possible electrophilic reactivity towards the reactive cysteine residue, Cys249.

Returning to the context of PPARγ, the many x-ray crystallographic studies of PPARγ in complex with ligands, accumulated through nearly two decades of PPARγ research, furnish structural data that may reflect the distinct patterns of stabilization of PPARγ observed upon treatment with classical agonists or partial- and non-agonists with dynamic techniques such as NMR and HDX-MS. A collective analysis of these structural data may thus elucidate general trends in the structural consequences of the binding of ligands from the different classes. While these trends may be obscured by the apparent small variation observed between the crystal structures and by the crystal environment, a dimensionality-reducing statistical treatment of the data, could reveal such trends.[233–235] Paper IV, presented in Chapter 8, evaluates the utility of principal component analysis of the atomic coordinates and dihedral angles of PPARγ contained within the x-ray crystallographic data in the public domain.

The motivations for the studies delineated above are connected through the ongoing elucidation of the structure and function of the ligand-binding pockets of each PPAR subtype. Covalent ligands of the PPARs can attach relatively small molecular fragments to reactive cysteines in their ligand binding pockets. This likely inhibits the access of other ligands to the AF-2 pocket, a region responsible for one type of agonistic PPAR modulation - the *classical* agonism. However, as described in Section 5.3.1, the newly demonstrated modes of modulation of PPARγ involve other parts of the ligand-binding pocket and this type of modulation is apparently not inhibited by the presence of such covalently attached ligands. Thus, a translation of these findings to PPARβ/δ presents an opportunity to use PPARβ/δ covalent antagonists as research tools to study similar alternative modes of ligand-dependent modulation of PPARβ/δ.

Part II

Results & Discussion

6 Papers I and II: Synthesis and Biological Evaluations of PPARβ/δ Antagonists

Antagonism of PPARβ/δ by covalent modification of Cys249 in the LBP represents a powerful strategy to oppose the effects of classical PPARβ/δ agonists. However, due to the irreversible nature of the mode of action of GSK3787 (**78**)[228] (see also Section 7.3), its affinity for PPARγ,[229] albeit weak, hampers its usefulness as a pharmacological tool to selectively study the effects of PPARβ/δ antagonism in cells expressing all three PPARs.

This section describes the synthesis and biological evaluation of new analogues of **78**, in an effort to produce a more selective member of the 5-trifluoromethyl-2-sulfonylpyridine class of PPARβ/δ antagonists. The new antagonists were thus prepared by modifying the arylamide moiety of **78**, while maintaining its electrophilic 5-trifluoromethyl-2-sulfonyl group intact.

6.1 Syntheses of Key Intermediates

The ammonium salt intermediates employed in the syntheses of the amides presented in this chapter (see Scheme 6.1) were prepared essentially as reported for the preparation of GSK3787 (**78**).[228] Thus, in DMF, and in the presence of triethylamine (Et_3N), 5-trifluoromethyl-2-mercaptopyridine (**84**) or 2-mercaptopyridine (**85**) was alkylated with *tert*-butyl (2-bromoethyl)-carbamate (**86**). The resulting sulfides **87** and **88** were then oxidized to their corresponding sulfones, **89** and **90**, using potassium peroxymonosulfate triple salt (Oxone®) in aqueous acetone, in the presence of sodium hydrogen carbonate ($NaHCO_3$) (see Scheme 6.1).

For the syntheses of CC618 (**95**) and 5-H-CC618 (**96**) (*vide infra*), deprotection of the *N*-Boc groups of sulfones **89** and **90** was carried out with trifluoroacetic acid (TFA) in acetonitrile, affording key ammonium intermediates **91** and **92** as TFA-salts (see Scheme 6.1).

For the syntheses of the other amides presented in Section 6.5, the *N*-Boc group of sulfone **89** was cleaved with hydrochloric acid in dioxane, affording the key ammonium intermediate **93** as an HCl-salt. A sulfide analogue of **93**, sulfide **94**, for use in the synthesis of the *N*-alkylated amides, presented in Section 6.5, was also prepared. Sulfide **94** was obtained by direct deprotection of the *N*-Boc-group in sulfide **87** with hydrochloric acid in dioxane.

6.2 Design and Synthesis of CC618 and 5-H-CC618

CC618 (**95**, ClogP = 4.85[i]) was designed as a structural hybrid between the potent PPARβ/δ agonist GW501516 (**20**, ClogP = 6.01[i]) and the antagonist GSK3787 (**78**, ClogP = 3.51[i]).[ii] It was envisioned that a combination of the phenylthiazole tail of **20** in combination with the linker moiety and electrophilic head group of **78** could harvest some of the affinity of **20** for the PPARβ/δ LBP, while maintaining the antagonism displayed by GSK3787.[237] We also prepared an analogue of CC618 (**95**), 5-H-CC618 (**96**), lacking the 5-trifluoromethyl group

[i]The ClogP-values were calculated with ChemBioDraw® Ultra 13.[236]
[ii]This compound was first prepared by Dr. Calin Ciocoiu Steindal.[237]

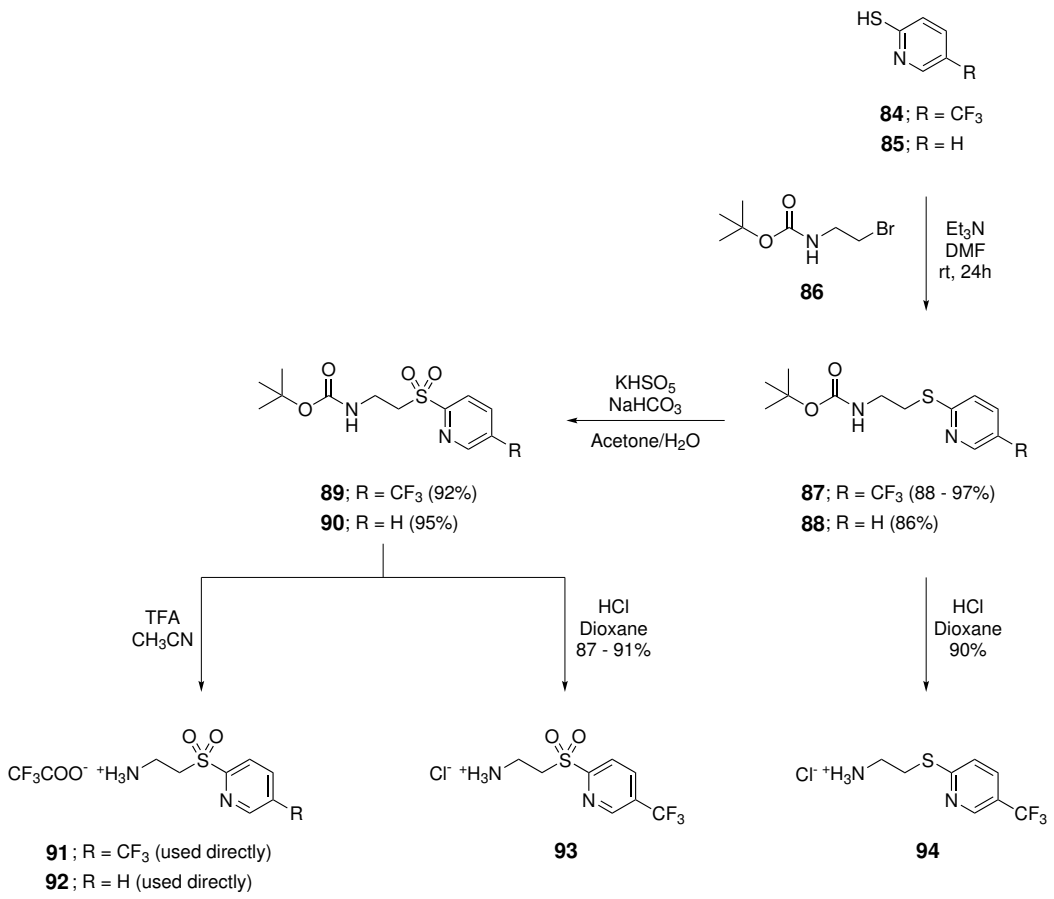

Scheme 6.1. Synthesis of key intermediates.

on the pyridine ring. As treated in Section 5.5.3, Shearer et al. observed that Compound 20 (**83**), an analogue of GSK3787 (**78**) lacking the 5-trifluoromethyl group on the pyridine ring, was inactive as an antagonist.[228] 5-H-CC618 (**96**) was therefore prepared to investigate whether this result owed exclusively to the higher electron density on the pyridine ring of **83**, or to specific interactions of **83** with the PPARβ/δ LBP.

Thus, a phenylthiazole ester was prepared by a Hantzsch-type cyclization of thioamide **97** and ethyl 2-chloroacetoacetate (**98**) in refluxing ethanol. The resulting ester **99** was hydrolyzed to acid **100**, with aqueous sodium hydroxide in ethanol. The acid **100** and either TFA-salt **91** or **92** were then assembled under peptide coupling conditions using *N*,*N*'-dicyclohexylcarbodiimide (DCC) and 1-hydroxybenzotriazole (HOBt) (see Scheme 6.2).

6.3 Biological Evaluations of CC618

We pursued the characterization of CC618 (**95**) as a PPARβ/δ antagonist in three different *in vitro* biological assays (see Figure 6.1, Figure 6.2 and Figure 6.3). Firstly, to determine whether **95** was a competent antagonist of PPARβ/δ, we evaluated its ability to inhibit transcription induced by the agonist GW501516 (**20**) in a GAL4-PPARβ/δ luciferase reporter gene assay in Cos-1 cells.[238,239,iii] To our delight, CC618 (**95**) antagonized the effect of 4 nM of GW501516 with an $IC_{50} = 10.0\,\mu M$ ($pIC_{50} = 5.0$) - a comparable potency to that of GSK3787

[iii] These results were provided by Prof. Hilde Nebb, Department of Nutrition, Institute of Basic Medical Sciences, University of Oslo, and Steinar M. Paulsen, University of Tromsø.

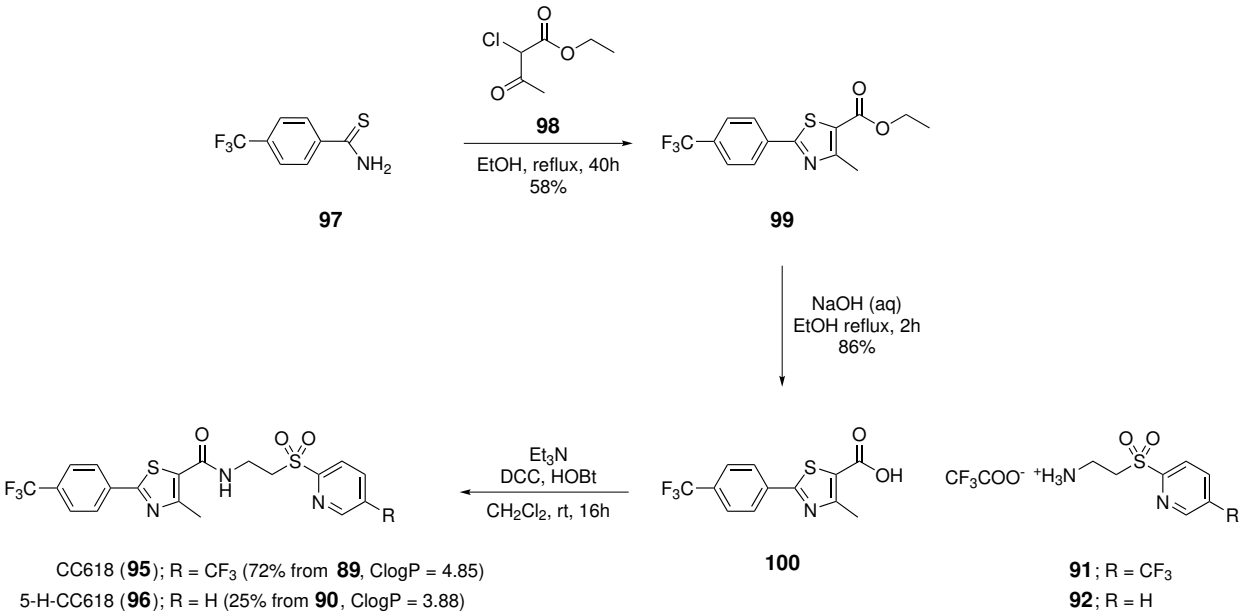

Scheme 6.2. Synthesis of CC618 (**95**) and 5-H-CC618 (**96**). The ClogP-values were calculated with ChemBioDraw® Ultra 13.[236]

(**78**), which displayed an $IC_{50} = 5.0\,\mu M$ ($pIC_{50} = 5.3$) (see Figure 6.1a). 5-H-CC618 (**96**), on the other hand, was inactive as an antagonist, supporting the notion that an electron-poor pyridine ring is required for antagonist activity (see Figure 6.1b). Neither **95** nor **78** displayed *agonistic* effects in the same assay, when administered on their own (see Figure 6.1c). In an analogous assay with PPARα, high concentrations ($10 - 100\,\mu M$) of CC618 (**95**) displayed weak to moderate inhibition of transcription induced by $200\,\mu M$ of bezafibrate (**7**). In PPARγ, GSK3787 (**78**) and CC618 (**95**) displayed similar properties and at higher concentrations ($20 - 150\,\mu M$), both compounds weakly inhibited transcription induced by $10\,\mu M$ of rosiglitazone (**3**) (see Supplementary Data of Paper I in Appendix B).

Secondly, we sought to support our hypothesis that CC618 (**95**) antagonized PPARβ/δ through the mechanism proposed for GSK3787 (**78**). To this end, we treated human recombinant PPARβ/δ with $10\,\mu M$ of either **95** or **78** for a period of 15 minutes. The resulting mixtures were trypsinized and subsequently analyzed with high-performance liquid chromatography (HPLC) coupled to tandem mass spectrometry (MS/MS). Upon MS/MS of the tryptic peptides containing Cys249, obtained from either treatment, an increase in the mass of Cys249 corresponding to the formation of an *S*-(5-(trifluoromethyl)pyridin-2-yl)cysteine was observed (see Figure 6.2 and Section 7.2 for more details about the assay). This result demonstrated that CC618 (**95**) and GSK3787 (**78**) share a similar mode of action, with respect to their covalent modification of Cys249 in the PPARβ/δ LBP.

Finally, although not presented in Paper I, we also investigated the effects of CC618 (**95**) and GSK3787 (**78**) in an assay that quantifies the ^{14}C-oleic acid oxidation induced by the PPARβ/δ agonist GW501516 (**20**) in primary human skeletal myotubes.[240,iv] A high expression level of PPARβ/δ relative to the other PPARs has been observed in skeletal muscle

[iv] This assay was performed by Prof. G. Hege Thoresen, Department of Pharmaceutical Biosciences, School of Pharmacy, University of Oslo, as part of the MURES collaboration.

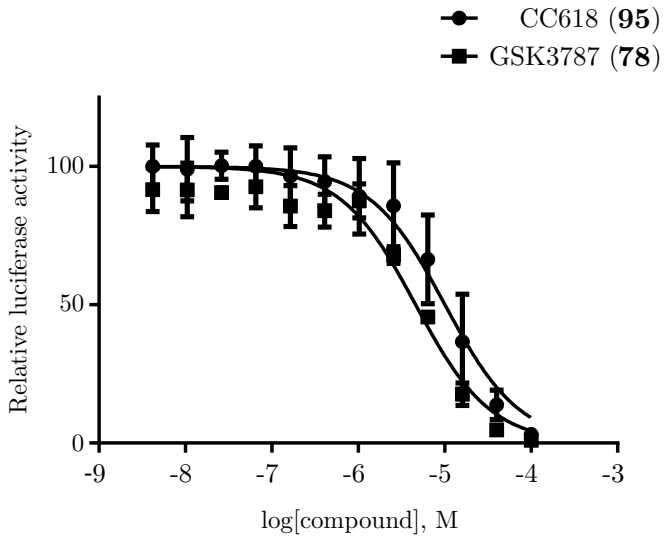

(a)

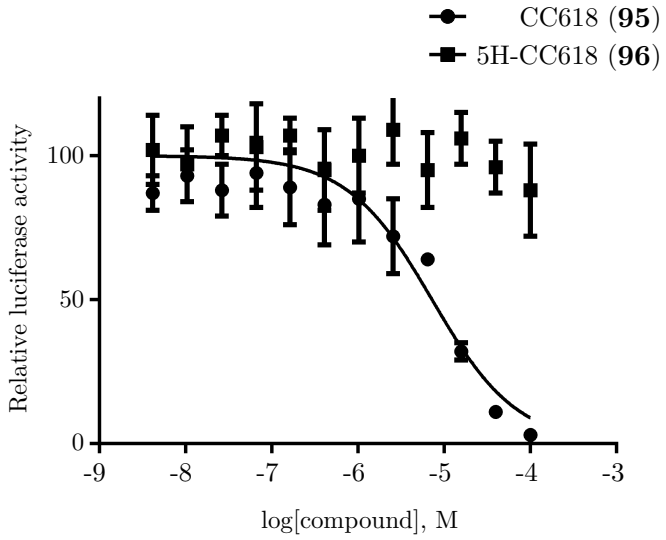

(b)

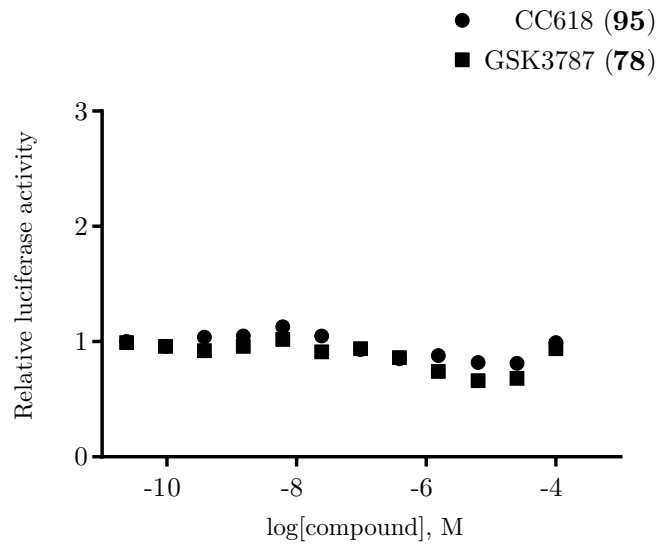

(c)

Figure 6.1. The antagonistic effects of (a) CC618 (**95**) or GSK3787 (**78**), or (b) CC618 (**95**) or 5H-CC618 (**96**) on Luc protein expression in Cos-1 cells, induced by 4 nM GW501516 (**20**). (c) The agonistic effects of CC618 (**95**) or GSK3787 (**78**) administered alone in the same assay.

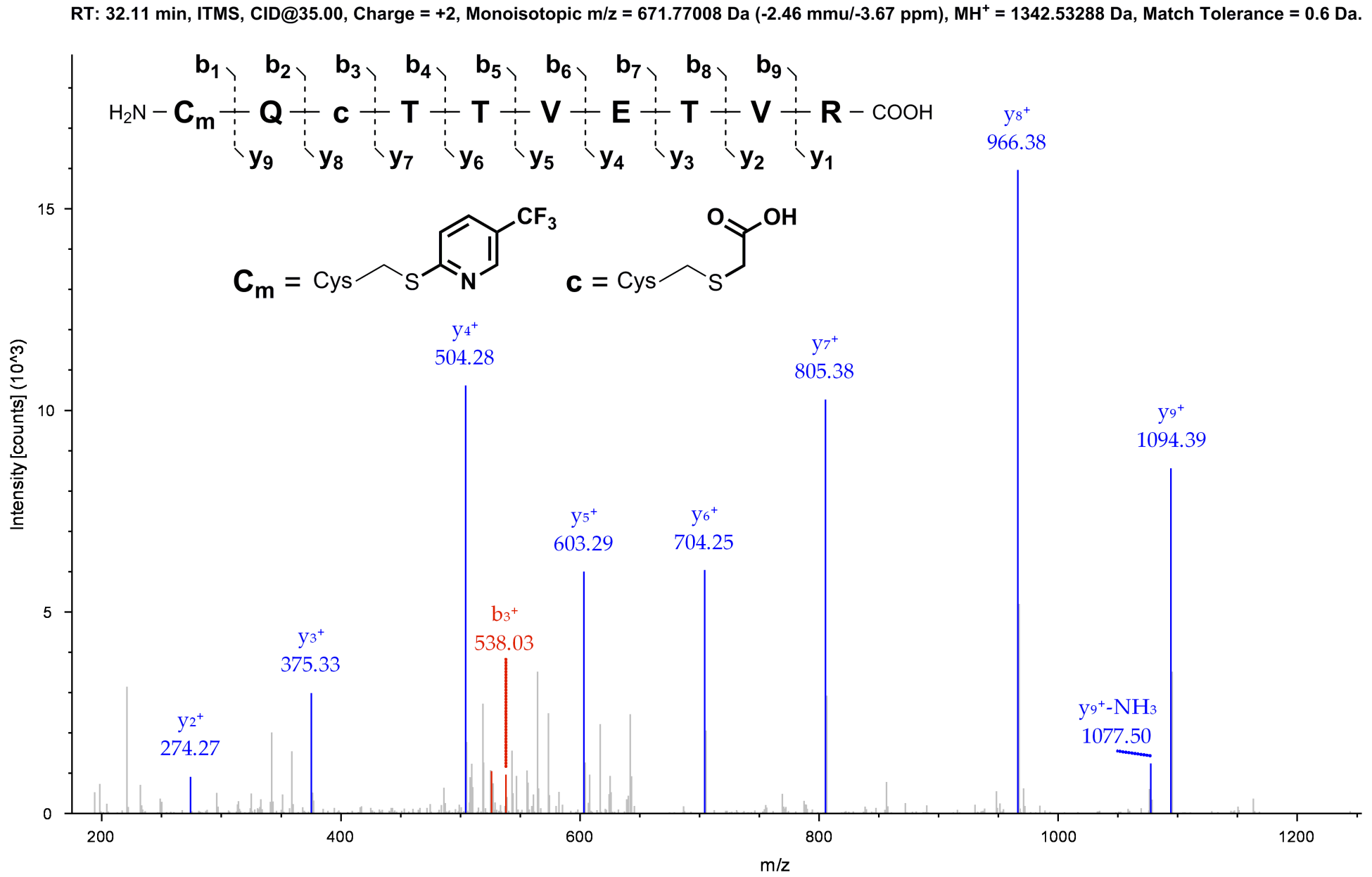

Figure 6.2. Representative MS/MS spectrum of the fully tryptic peptide $C_mQcTTVETVR$ (residues 249 – 258, C_m = modified Cys249, c = carboxymethylated Cys251), obtained from tryptic digestion of human PPARβ/δ after incubation with 10 µM of CC618 (**95**). Comparison of the masses of the tryptic peptide MH^+ and ion $y9^+$, indicates that Cys249 has an increased mass of 145.13369 Da corresponding, within the match tolerance, to the addition of a 5-trifluoromethyl-2-pyridyl fragment and the loss of the thiol hydrogen atom.

cells[241,242] and the agonistic effects of **20** on oleic acid oxidation are well established.[238,243–245] Thus, after treatment with 10 nM of **20**, the cells were exposed to 100 nM or 1000 nM of either CC618 (**95**) or GSK3787 (**78**) for 96 hours. Subsequent trapping of the released $^{14}CO_2$ and quantification by scintillation, demonstrated that both antagonists reduced the agonist-induced oxidation of oleic acid by approximately 20%. However, of these moderate effects, only the reduction observed with CC618 (**95**) reached statistical significance (see Figure 6.3).

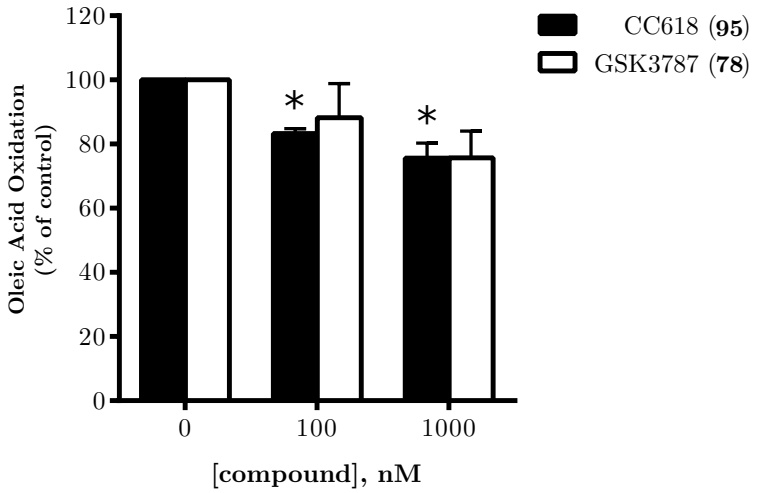

Figure 6.3. The effects of CC618 (**95**) and GSK3787 (**78**) on the ^{14}C-oleic acid oxidation induced by 10 nM of the PPARβ/δ agonist GW501516 (**20**) in primary human skeletal myotubes ($n = 3$, *p > 0.05 versus control by Student's paired t-test)

6.4 New 5-trifluoromethyl-2-sulfonylpyridine PPARβ/δ Antagonists

In order to pursue our goal of increasing the PPARβ/δ-selectivity of 5-trifluoromethyl-2-sulfonylpyridine antagonists, we expanded the scope of the structure-activity relationship (SAR) study performed by Shearer et al. in connection with their report on GSK3787 (**78**). Thus, a series of alkyl- and arylamides,[v] N-alkylated arylamides[vi] and arylketones were synthesized and evaluated in TR-FRET-based ligand displacement assays in the three PPARs. In this section, an overview of the syntheses of the putative PPARβ/δ ligands will be presented, followed by a brief introduction to the TR-FRET methodology. Finally, the results from the TR-FRET assays will be described.

6.5 Synthesis of New PPARβ/δ Antagonists

The syntheses of alkyl- and arylamide analogues of GSK3787 (**78**) were carried out by acylation of the common ammonium intermediate **93** with commercially available acyl chlorides and carboxylic acids. Thus, in an initial batch of compounds, alkyl- and arylamides **101** – **109** were prepared by acylation of **93** with acyl chlorides in tetrahydrofuran (THF), in the presence of Et_3N (see Scheme 6.3).

[v] Compounds **101** – **109** were first prepared by Cecilie Xuan Trang Vo[246] and later resynthesized.
[vi] Compounds **111**, **112** and **113** were first prepared by Marthe Amundsen[247] and later resynthesized.

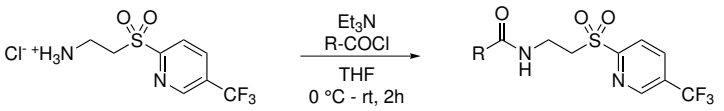

93 **101 - 109**

#	R =	Yield (%)[a]	ClogP
101	*iso*-propyl	42	1.73
102	*tert*-butyl	53	2.13
103	adamantyl	94	3.55
104	phenoxymethyl	73	2.79
105	phenyl	60	2.60
106	4-methoxyphenyl	82	2.80
107	4-fluorophenyl	67	2.94
108	pyridin-3-yl	69	1.84
109	naphth-2-yl	63	3.77

[a]Isolated material.

Scheme 6.3. Synthesis of alkyl- and arylamides **101** – **109**. The ClogP-values were calculated with ChemBioDraw® Ultra 13.[236]

In the subsequent batches of compounds, we focused our efforts on synthesizing analogues of naphth-2-yl amide **109**, as this compound displayed reasonably high affinity for PPARβ/δ (see details in Section 6.7). To explore the chemical space around **109**, we investigated four modifications to the naphth-2-yl amide motif. These included *N*-alkylation of the naphth-2-yl amide **109**, exchange of the amide N – H group for CH_2, saturation of the distal naphthalene ring and exchange of the naphthalene ring carbons for nitrogen. The scopes of the latter three groups were expanded to include a naphth-1-yl series, in addition to the napht-2-yl series.

Firstly, we sought to prepare *N*-alkylated analogues of **109**. These were prepared by alkylation of the sulfide analogue of naphth-2-yl amide **109**, sulfide **110**, obtained by acylation of ammonium intermediate **94** (see Scheme 6.1) with 2-naphthoyl chloride, since direct *N*-alkylation of naphth-2-yl amide **109** was not successful (see Scheme 6.4). Given the strong base used to deprotonate the amide nitrogen in the attempted alkylations of either **109** and **110**, the encountered difficulties with **109** could have been caused by a levelling effect on the part of
the more acidic protons in the α-methylene group of sulfone **109**, compared to those of sulfide **110**. Such an effect could thus have limited the available concentration of the amide nucleophile. In continuation, by directly submitting the crude *N*-alkylated sulfides to persulfate oxidation in aqueous acetone, the *N*-methyl, -ethyl and -benzyl naphth-2-yl amides **111** – **113** could be isolated (see Scheme 6.4).

Secondly, in order to increase the flexibility of the chain between the naphthalene ring system and the 5-trifluoromethyl-2-sulfonylpyridine group, we wanted to prepare a ketone analogue of naphth-2-yl amide **109**. We also prepared its naphth-1-yl congener. Thus, starting from 2- and 1-bromonaphthalenes **114** and **115**, lithium-halogen exchange with *n*-butyllithium in THF at -78 ℃ formed lithium naphthalenides **116** and **117**. Nucleophilic ring-opening of γ-butyrolactone (**118**) by **116** or **117**, afforded the 4-hydroxyketones **119** and

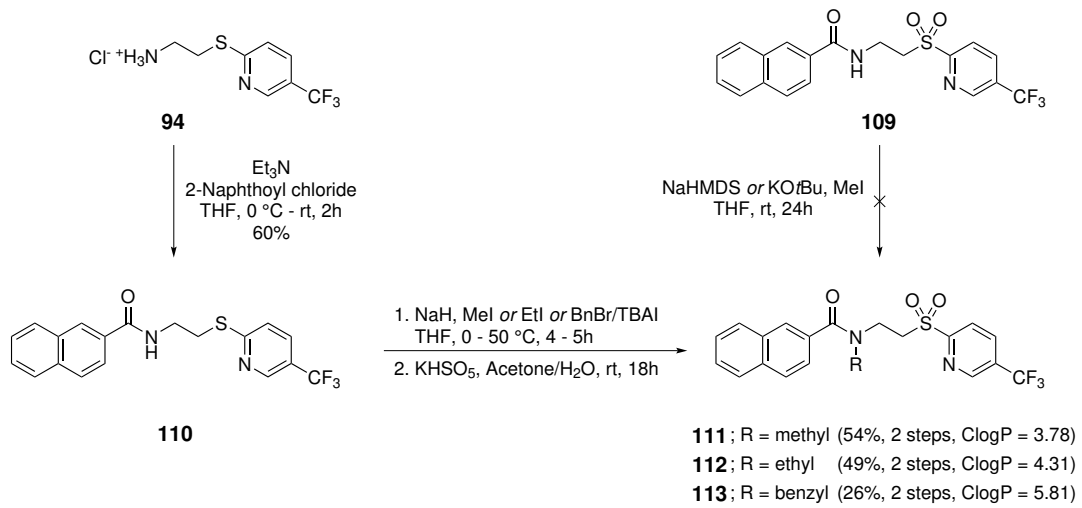

Scheme 6.4. Synthesis of the *N*-alkylated naphth-2-yl amides **111** – **113**. The ClogP-values were calculated with ChemBioDraw® Ultra 13.[236]

120 (see Scheme 6.5). By thin layer chromatographic (TLC) analysis, the reaction with **118** appeared to take place cleanly. However, the alcohols **119** and **120** decomposed to complex mixtures upon evaporation to dryness under reduced pressure at ambient temperature. The observed decomposition may owe to the formation of furanoid compounds, by an intramolecular cyclization/dehydration mechanism, as observed in the cases of 5-hydroxypentan-2-one (γ-acetopropyl alcohol) and its α-chloro analogue.[248,249]

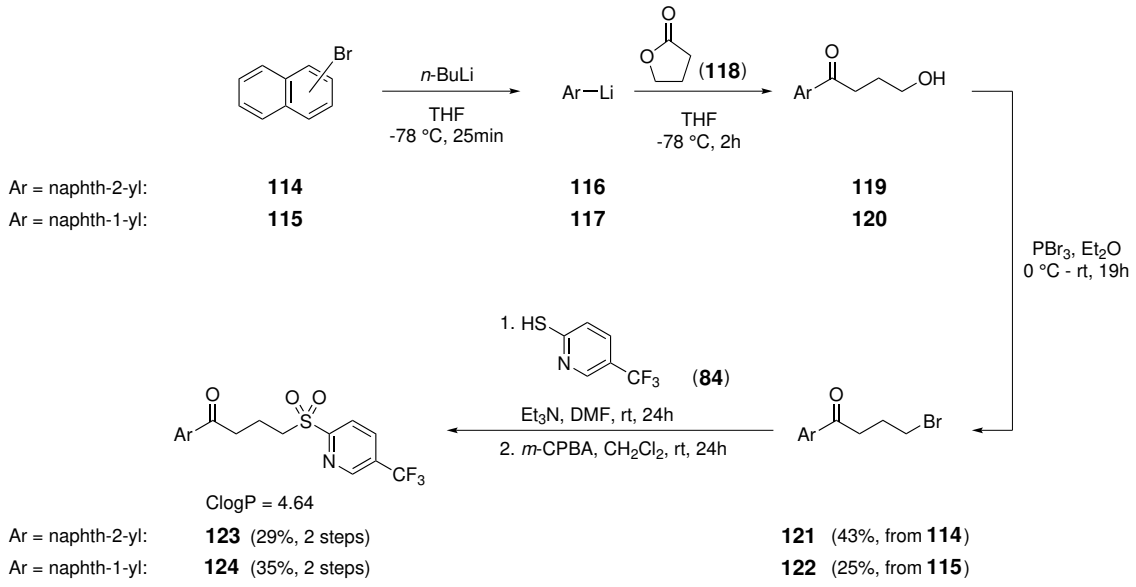

Scheme 6.5. Synthesis of ketones **123** and **124**. The ClogP-values were calculated with ChemBioDraw® Ultra 13.[236]

Thus, the combined diethylether (Et_2O) extracts of each alcohol were concentrated and subsequently treated with phosphorous tribromide (PBr_3). This protocol allowed the isolation of 4-bromoketones **121** and **122** in moderate to low yields, comparable to those obtained in

alternative preparations.[250,vii] Alkylation of 5-trifluoromethyl-2-mercaptopyridine (**84**) with bromide **121** or **122**, followed by direct oxidation of the resulting crude sulfides with 3-chloroperbenzoic acid (*m*-CPBA) in dichloromethane (CH_2Cl_2), afforded the sulfones **123** and **124** (see Scheme 6.5).

Finally, we prepared two series of compounds that included semi-saturated 5,6,7,8-tetrahydronaphthyl-, quinolinyl- and isoquinolinyl amides. The bulk of these amides were prepared by treating their corresponding carboxylic acids in CH_2Cl_2, with the peptide coupling reagent *O*-(benzotriazol-1-yl)-*N*,*N*,*N*',*N*'-tetramethyluronium hexafluorophosphate (HBTU), in the presence of 2 equivalents of *N*,*N*'-diisopropylethylamine, and subsequently adding in the ammonium intermediate **93** (Route A, Scheme 6.6). The naphth-2-yl series included the 5,6,7,8-tetrahydronaphth-2-yl amide **125**, as well as quinolinyl- and isoquinolinyl amides **126** – **132**. Of these, the quinolin-2-yl amide **126** was prepared by acylation of ammonium intermediate **93** with quinaldoyl chloride in CH_2Cl_2, in the presence of tribasic potassium phosphate (K_3PO_4) (Route B, Scheme 6.6). In the naphth-1-yl series, the parent napht-1-yl amide **133** was also prepared from its corresponding acyl chloride using this protocol. The remainder of the series, prepared under the above described peptide coupling conditions, consisted of the 5,6,7,8-tetrahydronaphth-1-yl amide **134**, as well as quinolinyl- and isoquinolinyl amides **135** – **141** (see Scheme 6.6).

6.6 Introduction to TR-FRET

In short, FRET-based assays make use of the ability of an excited fluorophore (the donor) to non-radiatively relax by transferring energy to a nearby fluorophore (the acceptor), which subsequently may relax by emission. The resonance energy transfer (RET) between the fluorophores is held to be a long-range dipolar interaction and it is affected by the quantum yield of the donor, the overlap of the emission spectrum of the donor and the absorbtion spectrum of the acceptor, the relative orientations of the transient donor/acceptor dipoles and the distance between them. Given a suitable selection of the donor/acceptor pair, the phenomenon is indeed highly sensitive to the distance between the fluorophores, with the magnitude of the RET being proportional to r^6, in which r is distance between the fluorophores. Thus, the measured FRET between a single donor and a single acceptor may be used to determine the distances between macromolecules or between domains within a macromolecule.[251]

In a parallel application, using a donor-labelled protein and a fluorescent ligand of the protein as the acceptor, a high FRET is observed when the fluorescent ligand (herafter referred to as the tracer ligand) is bound to the LBP of the protein. While the magnitude of the observed FRET is a function of several factors, the details of which are beyond the scope of this text, an important contributor to the observed FRET is the greater average proximity of the bound tracer ligand to the donor, compared to the tracer ligands freely diffusing in the solution outside the LBP. In these multiple acceptor assays, the use of a time-resolved

[vii] From a report by Tada, Hiratsuka, and Goto (1990):[250] In THF, 2- or 1-lithium naphthalenide, obtained by lithium-halogen exchange, was added copper(I) iodide. The resulting Gilman-type reagent was then treated with 4-bromobutanoyl chloride.

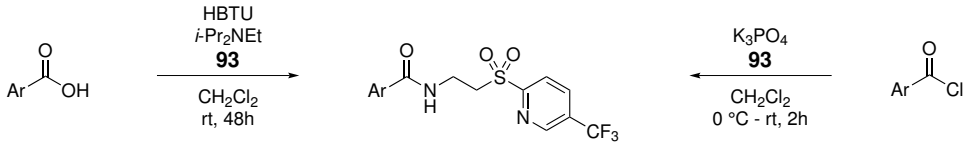

#	Ar =	naphth-X-yl series, X =	Procedure	Yield (%)[a]	ClogP
125	5,6,7,8-tetrahydronapht-2-yl	2	A	80	4.17
126	quinolin-2-yl	2	B	62	3.58
127	quinoline-7-yl	2	A	42	3.04
128	isoquinolin-7-yl	2	A	41	2.83
129	isoquinolin-6-yl	2	A	29	2.83
130	quinolin-6-yl	2	A	21	3.04
131	quinolin-3-yl	2	A	67	3.23
132	isoquinolin-3-yl	2	A	35	3.37
133	naphth-1-yl	1	B	37	3.77
134	5,6,7,8-tetrahydronaphth-1-yl	1	A	80	4.17
135	quinolin-8-yl	1	A	77	3.04
136	isoquinolin-8-yl	1	A	31	2.83
137	isoquinolin-5-yl	1	A	42	2.83
138	quinolin-5-yl	1	A	69	3.04
139	quinolin-4-yl	1	A	73	3.23
140	isoquinolin-4-yl	1	A	55	3.02
141	isoquinolin-1-yl	1	A	59	3.37

[a]Isolated material.

Scheme 6.6. Synthesis of 5,6,7,8-tetrahydronaphthyl-, quinolinyl- and isoquinolinyl amides **125**–**141**. The ClogP-values were calculated with ChemBioDraw® Ultra 13.[236]

format (TR-FRET) is necessary to distinguish the FRET-induced emission of the bound tracer ligand from the background emission. Thus, in this system, the effect of introducing a ligand that competes with the tracer ligand for binding to the LBP, is a reduction in the FRET-induced emission of the tracer ligand. Furthermore, since not all the energy used to excite the donor is transferred by FRET to the tracer ligand, some is emitted by the donor itself. In TR-FRET-based ligand displacement assays, the quantification of the tracer ligand displacement can favourably be determined as the ratio of the tracer ligand emission to the donor emission. This serves to correct for differences in the volume of each assay well (and thus the absolute number of donors and acceptors, given a homogenous solution), as well as for fluoroscence quenching effects caused by the competitor ligands.[252,253]

A statistical parameter commonly used to assess the quality of TR-FRET screening data, the Z'-factor,[254] was calculated for all the assays presented, and its values and a discussion of the quality of the obtained TR-FRET data can be found in the Supplementary Material of Paper II (see Appendix B).

6.7 Results from the TR-FRET-based Ligand Displacement Assays

As introduced in the previous section, the TR-FRET-based assays employed here quantify the ability of a competitor ligand to displace a tracer ligand from the LBPs of the PPARs. In the case of the 5-trifluoromethyl-2-sulfonylpyridine antagonists, their covalent mode of action

leads to non-equilibrium binding kinetics. Generally, barring situations in which ligand binding and tracer ligand displacement do not correlate with a covalent mode of action, a ligand possessing even a low affinity for the PPAR LBPs will thus, given enough time, completely displace the tracer ligand by covalent modification of the available protein. The mode of action of the 5-trifluoromethyl-2-sulfonylpyridine antagonists thus made the observation of our assays through time of interest, in order to collect data that were suggestive of the kinetics of the event of covalent modification of the central cysteines in the PPAR LBPs. Consequently, the ligand displacement assays presented here, were measured at four time points (30 minutes, 1 hour, 2 hours and 24 hours).

6.7.1 TR-FRET Assays with PPARβ/δ

For the TR-FRET assays with PPARβ/δ, we selected the following reference compounds: the agonist GW501516 (**20**), the antagonists GSK3787 (**78**) and CC618 (**95**), and the recently introduced inverse agonist DG172 (**143**). In an initial screening, we evaluated the alkyl- and arylamides **101** – **109** (see Figure 6.4). The alkylamides displayed markedly lower affinities for the PPARβ/δ LBP compared to the arylamides, the best of which were the 4-substituted benzamides **106** and **107** and more interestingly the naphth-2-yl amide **109**. It is notable that although all of the reference compounds displayed a more rapid displacement of the tracer ligand from the PPARβ/δ LBP, the naphth-2-yl amide **109** displayed a similar (and likely complete) displacement of the tracer ligand after 2 hours.

Based on the result with naphth-2-yl amide **109**, we synthesized a variety of analogues (*vide supra*). The effect of *N*-substitution on the affinity of analogues of GSK3787 (**78**) for PPARβ/δ has not been reported. Thus, we submitted the *N*-methyl-, *N*-ethyl- and *N*-benzyl naphth-2-yl amides **111**, **112** and **113** to the TR-FRET assay. Unfortunately, none of these compounds were more potent than their parent, the *N*-H naphth-2-yl amide **109**. In continuation, neither the naphth-2-yl ketone **123**, nor the naphth-1-yl ketone **124** presented improved affinities over that of **109** (see Figure 6.4). The decrease in the affinity of compounds **111** – **113**, **123** and **124** for PPARβ/δ, upon *N*-alkylation or exchange of the N – H group for CH_2, respectively, may owe to changes in the conformational spaces of the ligands, but may also indicate that the amide N – H group is of importance in the binding mode of naphth-2-yl amide **109**.

Consequently, the focus was turned towards making changes to the naphthalene ring system. We evaluated two series of analogues, **125** – **132** and **134** – **141**, of the naphth-2-yl amide **109** or its naphth-1-yl regioisomer **133**, respectively (see Figure 6.5). In general, the TR-FRET assays with the 5,6,7,8-tetrahydronaphthyl-, quinolinyl- and isoquinolinyl amides, demonstrated that the series derived from naphth-1-yl amide **133** contained fewer ligands with significant affinity for PPARβ/δ than the series derived from naphth-2-yl amide **109**. In the naphth-1-yl series, only the parent naphth-1-yl amide **133** caused a significant displacement of the tracer ligand after 1 hour. Among the analogues of naphth-2-yl amide **109**, the 5,6,7,8-tetrahydronaphth-2-yl amide **125**, the quinolin-2-yl amide **126**, the quinolin-6-yl amide **130**

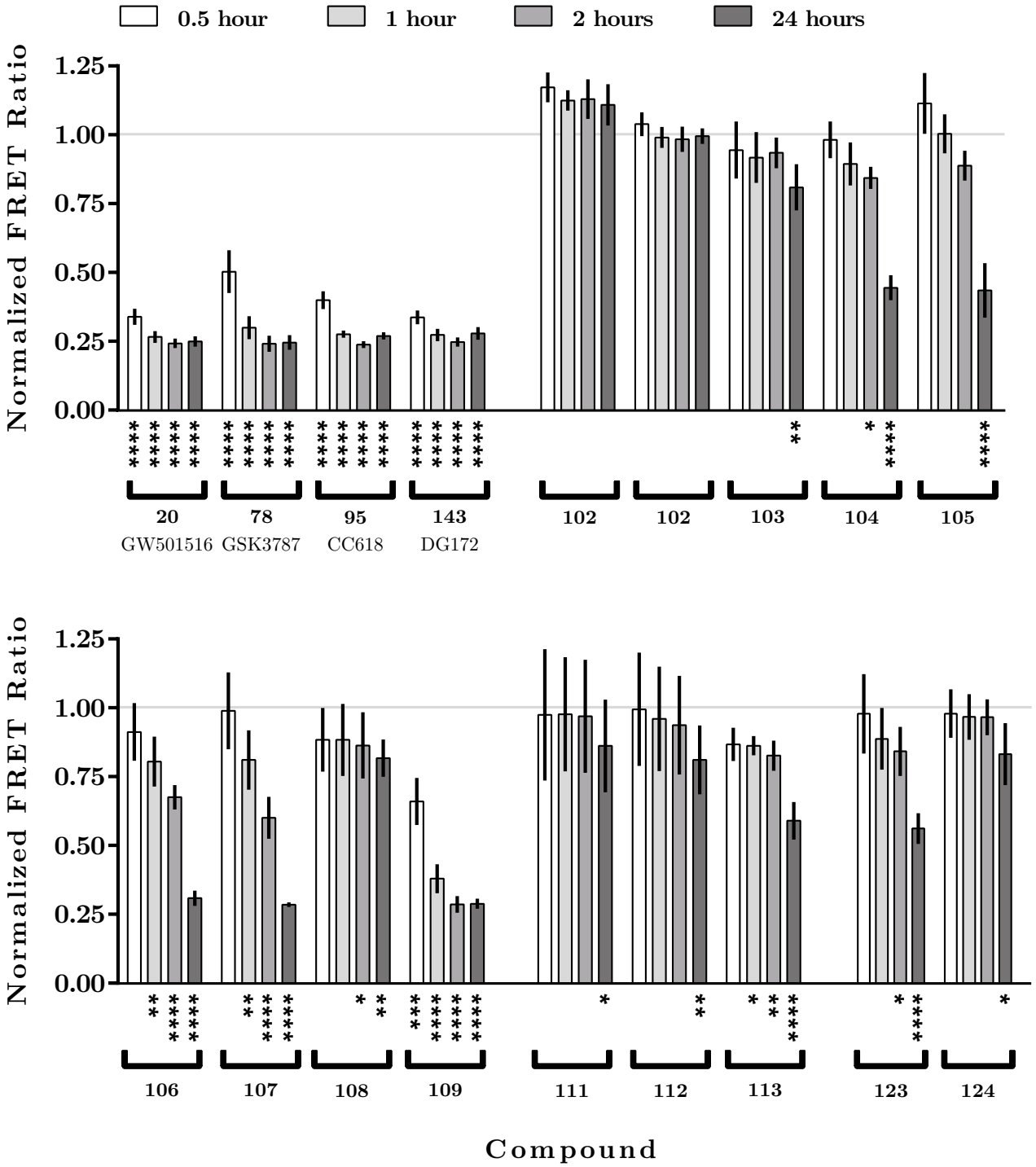

Figure 6.4. Displacement of 20 nM of the fluorescent tracer ligand Fluormone Pan PPAR Green from the LBP of PPARβ/δ by 1 µM of GW501516 (**20**), GSK3787 (**78**), CC618 (**95**), DG172 (**143**) or each of the alkyl- and arylamides **101** – **109**, the *N*-substituted naphth-2-yl amides **111** – **113** or the ketones **123** and **124**. The results are expressed as the ratio of the acceptor emission at 520 nm to the donor emission at 495 nm, normalized by dividing this ratio on the corresponding ratio of the control wells (2% v/v DMSO, $rw = 20$) at each given time point. The values represent means ±SD obtained with the positive control GW501516 (**20**) ($rw = 16$), GSK3787 (**78**), CC618 (**95**) and DG172 (**143**) ($rw = 8$), and with the test compounds **101** – **109**, **111** – **113**, **123** and **124** ($rw = 4$), in which rw equals the number of replicate wells from a single independent experiment ($n = 1$). Values that were significantly lower than negative control wells, by *t*-test, are marked (*P < 0.05), (**P < 0.01), (***P < 0.001), (****P < 0.0001).

and the quinolin-3-yl amide **131** all caused significant tracer ligand displacements after 1 hour of incubation. After 24 hours, the displacements caused by **125** and **131** were near complete (see Figure 6.5), by comparison with those caused by the reference ligands (see Figure 6.4).

6.7.2 Determination of IC_{50}-values

We thus proceeded to determine IC_{50}-values for the new compounds **109**, **125** and **131**, as well as for the reference antagonistic ligands GSK3787 (**78**), CC618 (**95**) and DG172 (**143**). This analysis demonstrated potencies for tracer ligand displacement in the micromolar range for **109**, **125** and **131** (see Table 6.1). It is notable that the IC_{50}-values obtained with the 5-trifluoromethyl-2-sulfonylpyridine antagonists decrease with time. This is an expression of the decreasing relative concentration of free receptor, caused by the covalent modification of PPARβ/δ by the antagonists (see Figure 6.6). A similar time-dependent increase in the apparent potency of the ligands was observed by Schopfer et al. for the EC_{50}-values obtained upon treatment of PPARγ with α,β-unsaturated nitro-fatty acid agonists, that bind covalently to Cys285.[67] The similarly decreasing IC_{50}-values observed with compounds **109**, **125** and **131** support the assumption that they share the covalent mode of action of GSK3787 (**78**) and CC618 (**95**).

Table 6.1. IC_{50}-values (nM) determined by nonlinear regression analyses of the observed displacement of the tracer ligand from PPARβ/δ LBP at time points from 20 minutes to 24 hours.

	IC_{50} (nM)					
Compound	**20 min**	**40 min**	**1 hour**	**2 hours**	**3 hours**	**24 hours**
109	1931	930	751	448	320	-[c]
125	4221	1961	1528	907	598	271[b]
131	-[c]	17611	6815	2322	1431	241
GSK3787 (**78**)	1329	825	648	284	233	1.21[b]
CC618 (**95**)	949[b]	581	423	301[b]	284[b]	-[c]
DG172 (**143**)	29.0	30.4	32.7[a]	37.0	40.1	48.0

[a] Previously determined after 1 hour by Lieber et al. as 26.9 nM.[255]
[b] Curve fit was ambiguous.
[c] Curve fit did not converge.

6.7.3 TR-FRET Assays with PPARα and PPARγ

Having demonstrated that the naphth-2-yl amide **109**, the 5,6,7,8-tetrahydronaphth-2-yl amide **125** and the quinolin-3-yl amide **131** displayed reasonable affinities for PPARβ/δ, we submitted these ligands, as well as GSK3787 (**78**) and CC618 (**95**) to TR-FRET assays with PPARα and PPARγ. None of the ligands displayed significant ability to displace the

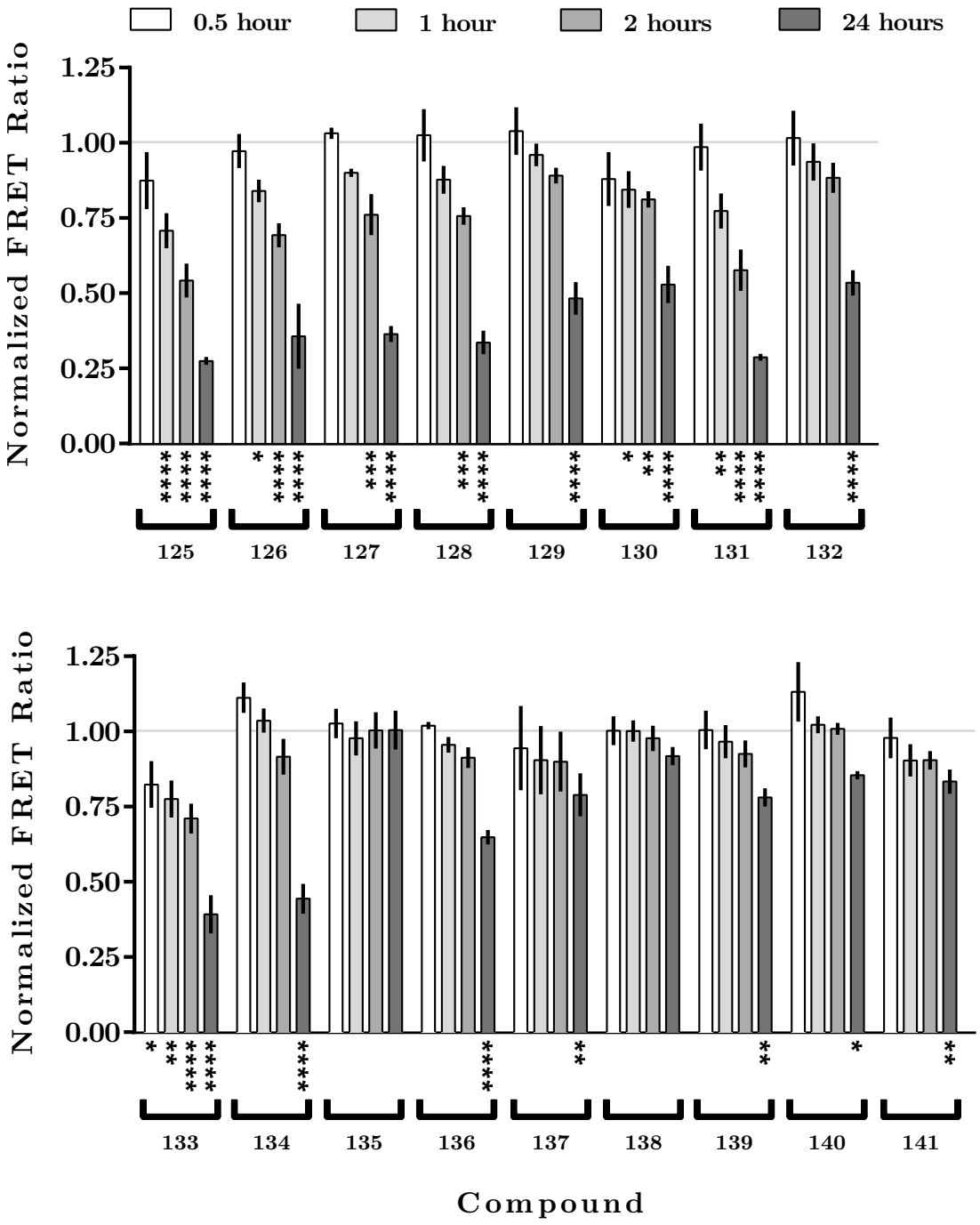

Figure 6.5. Displacement of 20 nM of the fluorescent tracer ligand Fluormone Pan PPAR Green from the LBP of PPARβ/δ by 1 µM of the 5,6,7,8-tetrahydronaphthyl amides **125** or **134**, the naphth-1-yl amide **133** or the quinolinyl- and isoquinolinyl amides **126** – **141**. Detailed information regarding the assay and the figure are found in the legend of Figure 6.4.

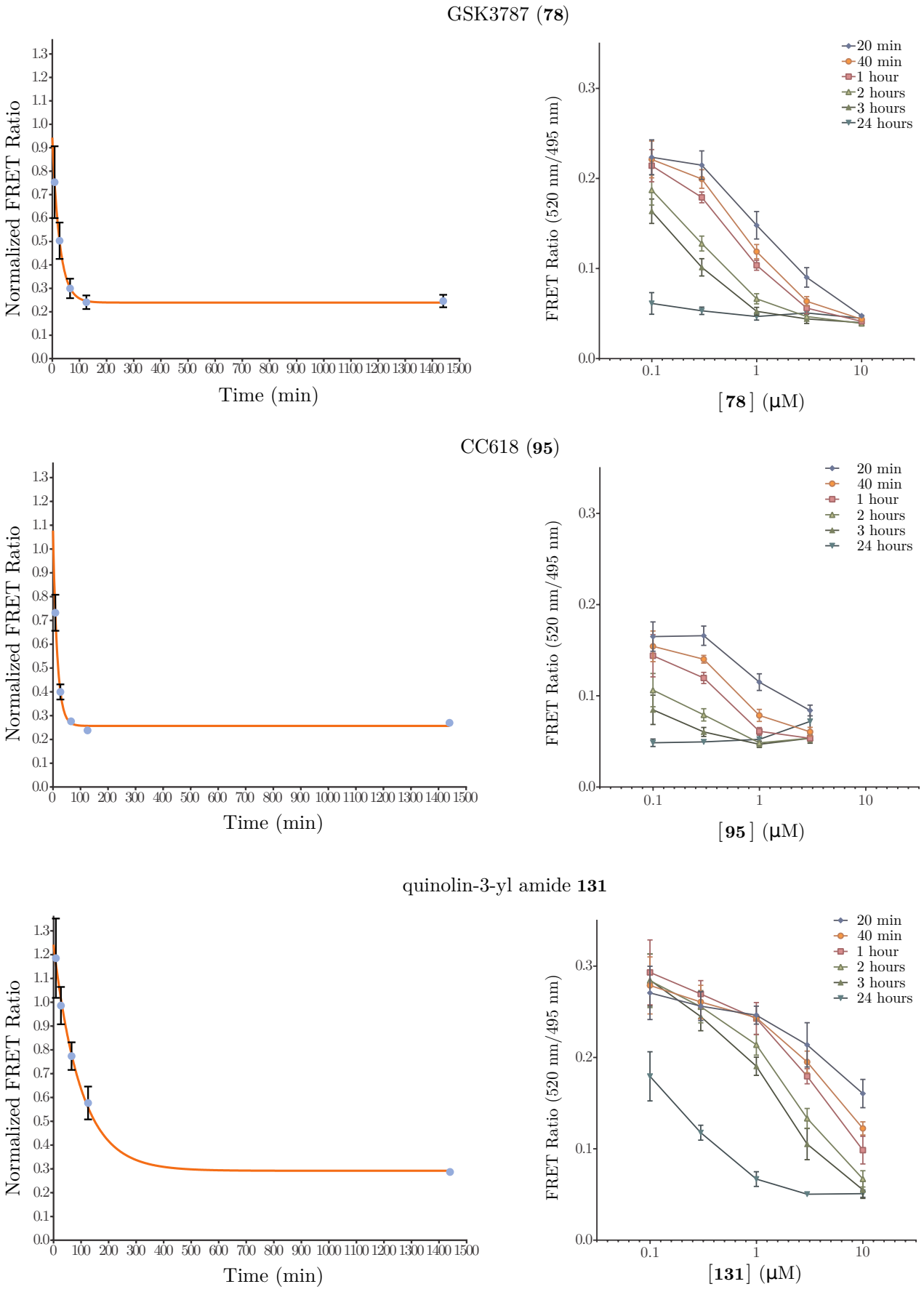

Figure 6.6. Effects on the displacement of the tracer ligand from the PPARβ/δ LBP, by covalently modifying antagonists. *Left*: The time-dependent displacements of the tracer ligand caused by GSK3787 (**78**), CC618 (**95**) and quinolin-3-yl amide **131**. *Right*: IC_{50}-measurements of the same ligands at different time points, showing their apparent increasing potency.

tracer ligand from the LBP of PPARα (see Figure 6.7a). On the other hand, our TR-FRET assay results with GSK3787 (**78**) corroborates its previously reported effects on PPARγ, and indicates that our hybrid antagonist CC618 (**95**) represents a marginal improvement in selectivity (see Figure 6.7b). Among the new ligands, the naphth-2-yl amide **109** and the 5,6,7,8-tetrahydronaphth-2-yl amide **125** both displayed comparable or greater affinities for PPARγ than GSK3787 (**78**). On the other hand, quinolin-3-yl amide **131** did not significantly displace the tracer ligand from the LBP of PPARγ.

In the TR-FRET assays with PPARα and PPARγ, we did not observe clear indications of a time-dependent consumption of the free proteins (see the Supplementary Material of Paper II in Appendix B), as was demonstrated with PPARβ/δ (see Figure 6.4 and Figure 6.5). Thus, the observed effects on PPARα and PPARγ after 1 hour were largely unchanged after 24 hours. However, a time-dependent consumption of the free proteins, by covalent modification, may be obscured by the relatively low affinity of the new antagonists for PPARα and PPARγ. In the case of PPARγ, its instability in the TR-FRET assay after more than six hours of observation, as noted in the assay manual,[256] may also have influenced the results.

Nonetheless, although it is uncertain whether the 5-trifluoromethyl-2-sulfonylpyridine class of PPARβ/δ antagonists display a covalent mode of action in PPARγ, this hypothesis is supported by the relatively high sequence similarity of the PPAR LBDs (see Section 2.1) and the demonstrated reactivity of the homologous cysteine in PPARγ (Cys285) towards similar ligands (e.g. the PPARγ-selective antagonist GW9662 (**47**, see Section 5.5). Assuming a covalent mode of action, the reported partial agonism observed upon treatment of PPARγ with GSK3787 (**78**),[229] may be interpreted on the background of the partial agonism induced by the reported covalent PPARγ ligand L-764406 (**76**).[224] Both GW9662 (**47**) and **76** attach relatively small molecular fragments centrally in the PPARγ LBP. The different functional outcomes observed upon treatment PPARγ with these ligands (antagonism vs. partial agonism) indicate that the structure of the *S*-aryl cysteinyl sulfides resulting from covalent modification with either ligand, influences the transcriptional activity of their complexes with PPARγ. This influence appears to be subtype specific, as treatment of PPARα with the PPARγ antagonist GW9662 (**47**) resulted in partial agonism, as observed in a GAL4-PPARα reporter gene assay. This effect was not observed with either PPARβ/δ or PPARγ.[221]

6.8 Conclusions

Our efforts to synthesize and characterize new members of the 5-trifluoromethyl-2-sulfonylpyridine class of PPARβ/δ antagonists resulted in the demonstration that subtle changes in the structure of the ligands can greatly affect their affinity for the three PPARs. The quinolin-3-yl amide **131** represents a new and more PPARβ/δ-selective member of this class of antagonists. While **131** displays a higher IC_{50}-value for tracer ligand displacement from PPARβ/δ after 1 hour (IC_{50} = 6.8 µM/pIC_{50} = 5.2) than its previously reported analogues GSK3787 (**78**, IC_{50} = 0.65 µM/pIC_{50} = 6.2) and CC618 (**95**, IC_{50} = 0.42 µM/pIC_{50} = 6.4), the irreversible mode of action of this class of ligands requires selectivity to be preferred over

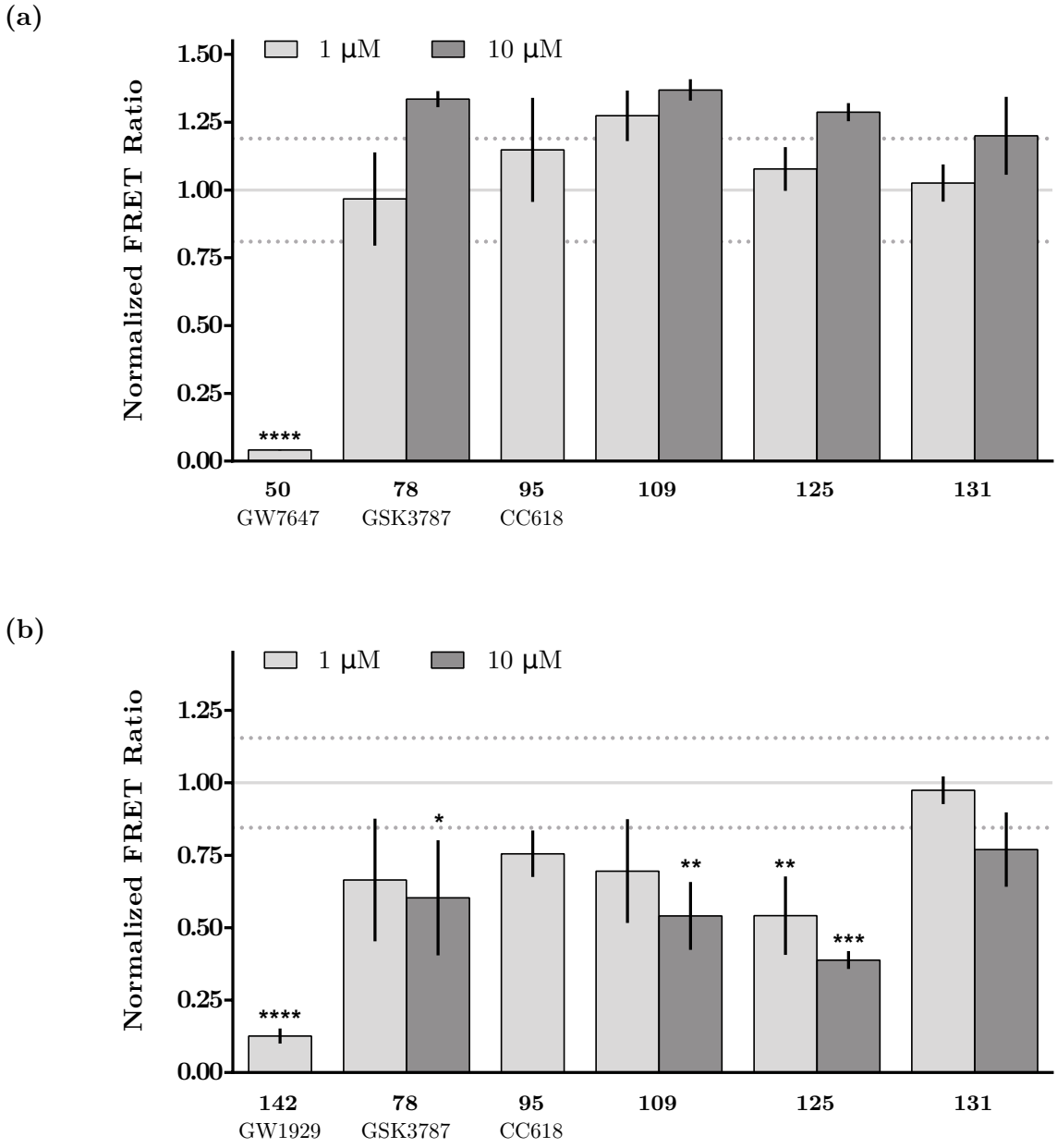

Figure 6.7. Evaluation of the affinity of 1 µM or 10 µM of the compounds GSK3787 (**78**), CC618 (**95**), **109**, **125** or **131** for PPARα (a) or PPARγ (b) after 1 hour. The highest concentration data points for CC618 (**95**) could not be determined due to solubility issues. The results are expressed as the ratio of the acceptor emission at 520 nm to the donor emission at 495 nm, normalized by dividing this ratio on the corresponding ratio of the negative control wells (2% v/v DMSO, rw = 16 in PPARα, rw = 12 in PPARγ). The mean ±SD of the negative control wells are indicated in grey, as solid and dotted lines. The values represent means ±SD obtained with the positive controls GW7647 (**50**, $rw = 8$) in PPARα and GW1929 (**142**, $rw = 8$) in PPARγ, and with the test compounds GSK3787 (**78**), CC618 (**95**), **109**, **125** and **131** ($rw = 4$), in which rw equals the number of replicate wells from a single independent experiment ($n = 1$). Values that were significantly lower than negative control wells, by t-test, are marked (*P < 0.05), (**P < 0.01), (***P < 0.001), (****P < 0.0001).

rapid binding kinetics. In this context, **131** may prove itself as a valuable pharmacological tool, or a starting point for further development of PPARβ/δ-selective 5-trifluoromethyl-2-sulfonylpyridine antagonists. On the other hand, the 5,6,7,8-tetrahydronaphth-2-yl amide **125** may represent a possible starting point for the development of *dual* PPARδ/γ 5-trifluoromethyl-2-sulfonylpyridine antagonists.

7 Paper III: Investigations on the Mode of Action of PPARβ/δ Antagonistic Ligands

In the realm of PPARβ/δ antagonistic ligands, assays based on TR-FRET have become popular in the determination of the affinity of a ligand for the receptor relative to a fluorescent tracer ligand, but also in the characterization of the affinity of the resulting PPARβ/δ:ligand complex for oligopeptides derived from the nuclear receptor-binding motifs of coregulator proteins. The latter format of these assays has the ability to shed light on the molecular events occurring after ligand binding, but prior to a modulation of transcription. Particularly, TR-FRET data from studies of PPARβ/δ antagonistic ligands have made possible a distinction between inverse agonists and silent antagonists. These observations form a background for further studies into the mode of action of PPARβ/δ antagonistic ligands, seeking to elucidate the structural components involved in these differences. To date, no x-ray crystallographic determination of the structure of PPARβ/δ in complex with its reported antagonists has been published. Thus, other methodologies must be employed to further our understanding of the interactions between the PPARβ/δ LBP and the antagonistic ligands.

7.1 Structural Evaluation of PPARβ/δ Antagonistic Ligands

Encouraged by the wide range of electrophiles observed to react with Cys285 in PPARγ, in combination with the report by Shearer et al. on the covalent modification of PPARβ/δ by GSK3787 (**78**) (see Section 5.5.3),[228] it was desirable to investigate the mode of action of a selection of the reported PPARβ/δ antagonists, with a focus on the possible involvement of covalent interactions with Cys249 in PPARβ/δ. This selection was based on an evaluation of possible sites of electrophilic reactivity in the ligands, guided by their respective accounts and the chemical literature. Thus, in the following, the PPARβ/δ antagonists reported to date are briefly reviewed and their structures are evaluated focusing on potential sites of electrophilic reactivity.

7.1.1 Sulindac sulfide, Indomethacin and FH535

Apparently, the first report of PPARβ/δ antagonism appeared in 1999, six years after the discovery of the PPARβ/δ receptor in Xenopus and in humans.[257,258] He et al. reported that sulindac sulfide (**144**) and indomethacin (**145**) (see Figure 7.1) antagonized the effect of carbaprostacyclin (cPGI), a stabilized synthetic analogue of the short-lived, endogenous PPAR agonist prostacyclin (PGI_2),[260] on PPARβ/δ.[259] Later work by Jarvis, Gray, and Palmer supported the PPARβ/δ antagonism of the former, by showing that **144** could suppress the GW501516-induced transcription of a liver-type fatty acid-binding protein (L-FABP) reporter construct.[261] Both antagonistic ligands also display significant affinity for PPARγ.[259,261] The structures of these NSAIDs, however, do not suggest that they contain electrophilic sites, capable of reacting with a thiolate.

Handeli and Simon reported that the (*N*-phenyl)phenylsulfonamide FH535 (**146**) (see Figure 7.1) antagonized agonist-induced responses in PPARβ/δ- and PPARγ-driven GAL4 reporter gene assays.[262] The structure of **146** bears similarity to that of GW9662 (**47**) (see Figure 5.16), a covalent antagonist of PPARγ, which also covalently modifies PPARα and PPARβ/δ.[221] FH535 (**146**) contains an electron-poor 2,5-dichlorobenzenesulfonamide moiety. In a chemical context, 2-halosulfonamides have been used to prepare 2-alkylthiobenzenesulfonamides through nucleophilic aromatic substitution of the halide by alkylthiolates.[263–265]

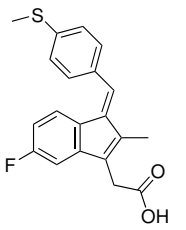

Sulindac sulfide (**144**)

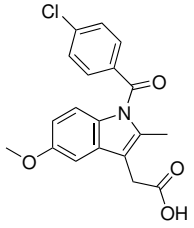

Indomethacin (**145**)

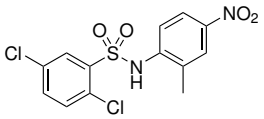

FH535 (**146**)

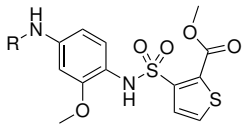

GSK0660 (**147**); R = Phenyl
ST247 (**148**); R = *n*-Hexyl
PT-S58 (**149**); R = *t*-Butyl
Compound 10b (**150**); R = *n*-Butyl
Compound 10h (**151**); R = *iso*-Pentyl
Compound 10l (**152**); R = Benzyl

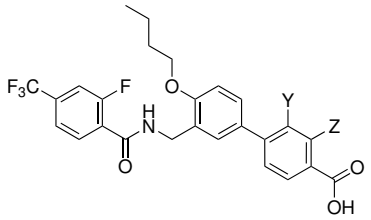

Compound 3a (**63**); Y = H, Z = H
Compound 3g (**64**); Y = F, Z = H
Compound 3h (**65**); Y = Me, Z = H
Compound 3i (**66**); Y = H, Z = Me

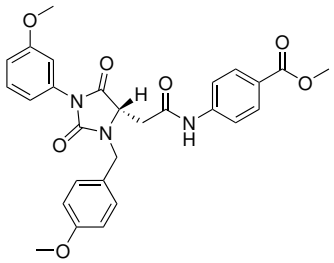

Compound 9 (**153**)

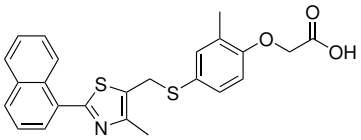

SR13904 (**154**)

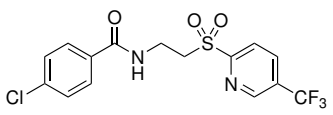

GSK3787 (**78**)

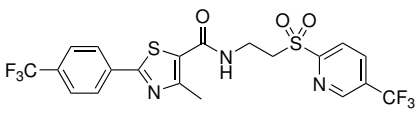

CC618 (**95**)

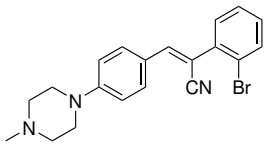

DG172 (**143**)

Figure 7.1. Overview of the PPARβ/δ antagonists reported to date.

Interestingly however, the antagonistic effect of FH535 (**146**) on transcription, induced by the agonist cPGI, was not diminished in a PPARβ/δ Cys249Ala mutant.[262] This result indicates that covalent bond formation to Cys249 is not involved in the mode of action of FH535 (**146**).

7.1.2 GSK0660 and its Recent Analogues

A report of a highly PPARβ/δ-selective antagonist was first published in 2008 by Shearer et al., in which a high-throughput screening hit named GSK0660 (**147**) (see Figure 7.1) displayed high affinity and selectivity for PPARβ/δ in ligand displacement assays, but did not induce transcription in a GAL4-PPARβ/δ reporter assay.[266] More recent reports by Naruhn et al. and Toth et al., describe SAR studies, in which GSK0660 was used as a lead compound. These studies resulted in the discovery that a replacement of GSK0660's *N*-phenyl tail for *N*-alkyl- or *N*-alkylaryl chains, produced a series of compounds with significantly greater affinities for PPARβ/δ (see Figure 7.1).[267,268] Of these, ST247 (**148**), was shown to be an inverse agonist, with respect to a repression of PPARβ/δ target gene expression to subbasal levels[89] and an enhanced corepressor recruitment to PPARβ/δ.[267] Interestingly, the *tert*-butyl analogue PT-S58 (**149**), although a potent competitor in a ligand displacement assay, inhibited both agonist-induced coactivator recruitment and inverse agonist-induced corepressor recruitment. This ligand thus profiled as a silent antagonist of PPARβ/δ.[267] An improved analogue of ST247 in terms of plasma stability, PT-S264, has been announced, but its structure has yet to be published.[232,269]

In a chemical context, it has been shown that 3-halothiophene-2-carboxylates may undergo nucleophilic aromatic substitutions with thiolates,[270] although these reactions proceed in higher yields with added copper metal or with the corresponding benzothiophenes as substrates (see Figure 7.2).[271,272] Furthermore, the reactivity of electron-poor arylsulfonamides, such as nitrobenzenesulfonamides, towards thiolates, has been studied and exploited in the synthetic preparation of the corresponding amines - a reaction that also produces 2- or 4-

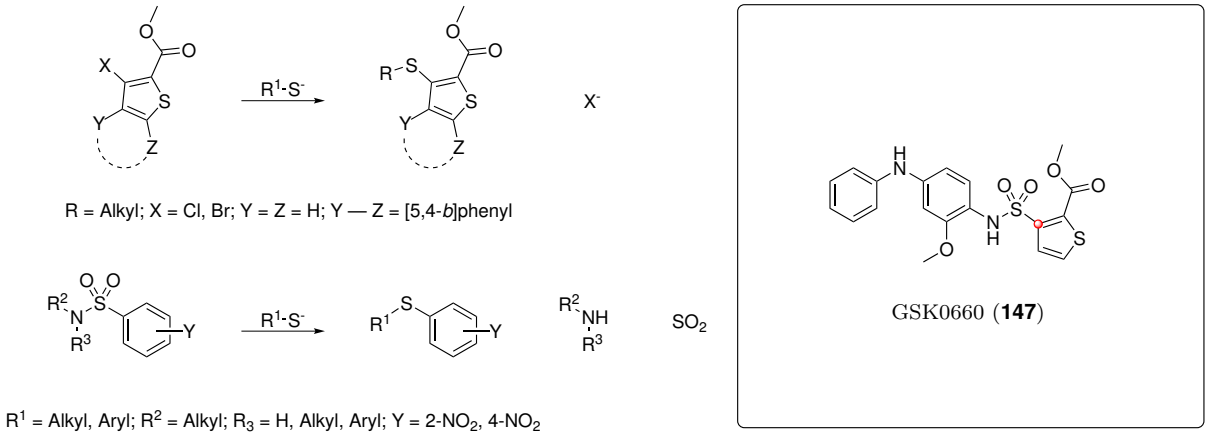

Figure 7.2. Nucleophilic aromatic substitution reactions of electron-poor 3-halo(benzo)thiophenes and nitrophenylsulfonamides. The carbon atom in GSK0660 (**147**) hypothesized to be reactive towards thiolates is marked with a red bullet.

nitrophenylsulfides, through a nucleophilic aromatic substitution mechanism (see Figure 7.2).[273–277]

With both the mentioned reactivity patterns in mind, it seemed prudent to consider the possibility that the methyl 3-sulfamoylthiophene-2-carboxylate head group of GSK0660 (**147**) may be reactive towards a nucleophilic cysteine residue. Although analogues of **147** with higher affinity for PPARβ/δ exist, the structures of these analogues differ from **147**, only in the terminal aniline *N*-substituent (see Figure 7.1). These structural differences are not likely to cause significant changes in the chemical reactivity of their common methyl 3-sulfamoylthiophene-2-carboxylate head-groups. A ligand with higher affinity for the PPARβ/δ LBP may, however, achieve poses that are more suited for a reaction with Cys249 to occur. Nevertheless, **147** was deemed representative of its class of PPARβ/δ antagonists, and was thus included in the study presented in Paper III.

7.1.3 A Virtual Screening Hit and Carboxylic Acids

Also in 2008, following a virtual screening campaign, Markt et al. synthesized and evaluated a series of putative PPAR modulators in ligand displacement and GAL4-PPAR reporter assays, among them Compound 9 (**153**) (see Figure 7.1). This compound was shown to be an antagonist of PPARβ/δ, as well as a partial agonist of PPARγ.[278] The following year, Zaveri et al. reported that the carboxylic acid SR13904 (**154**) (see Figure 7.1) antagonized agonist-induced PPARβ/δ- and PPARγ-driven transcription and that the ligand displayed an anti-proliferative effect on cell lines from various carcinomas.[279] However, the structures of neither Compound 9 (**153**) nor SR13904 (**154**) suggest that they should be reactive towards thiolates.

The design of PPAR antagonists based on a destabilizing interaction with helix 12 was introduced in Section 5.4.1. Using this strategy, Kasuga et al. designed the carboxylic acids named 3a, 3g, 3h and 3i (**63** - **66**) (see Figure 7.1), analogues of the potent PPARβ/δ agonist TIPP-204.[280] These biphenylcarboxylic acids displayed high affinities for PPARβ/δ, but weak transcriptional induction in a GAL4-PPARβ/δ reporter assay. They were also shown to be functional antagonists of PPARβ/δ target gene expression.[216] Chemically, the 2-fluoro-4-(trifluoromethyl)benzamide moiety, common to the tails of these ligands, could plausibly be reactive towards thiolates. This is based on the findings that 2-fluoro-4-(trifluoromethyl)benzaldehydes[281] and 2-fluoro-4-halobenzamides[282,283] all undergo nucleophilic aromatic substitution with thiolates, to furnish the corresponding 2-sulfides. However, a published x-ray crystal structure determination of PPARβ/δ in complex with the agonist TIPP-204, which carries the same 2-fluoro-4-(trifluoromethyl)benzamide moiety, did not indicate a covalent interaction with Cys249, although in its observed binding pose, the putatively electrophilic carbon of TIPP-204 is located within 4 Å of the Cys249 sulfur atom.[284] Thus, although the binding poses of the carboxylic acids 3a, 3g, 3h and 3i (**63** - **66**) in the PPARβ/δ LBP, and consequently the reactivities of their 2-fluoro-4-(trifluoromethyl)benzamide moieties, may differ from those of TIPP-204, these antagonists were not included in our study.

7.1.4 GSK3787, CC618 and DG172

As introduced in Section 5.5.3, Shearer et al. reported the discovery and characterization of GSK3787 (**78**) (see Figure 7.1) – an antagonistic ligand that was found to covalently modify PPARβ/δ.[228] Our group recently disclosed CC618 (**95**) (see Figure 7.1), a PPARβ/δ-selective antagonist with similar *in vitro* effects to those of GSK3787 (see Section 6.3).[285] On the basis of their reported reactivities towards Cys249 in PPARβ/δ, these ligands were included in the study. The reactivity of **78** and **95** can be rationalized in the context of similar 2-sulfonylpyridines, which undergo nucleophilic aromatic substitutions with thiolates (see Figure 7.3).[286,287]

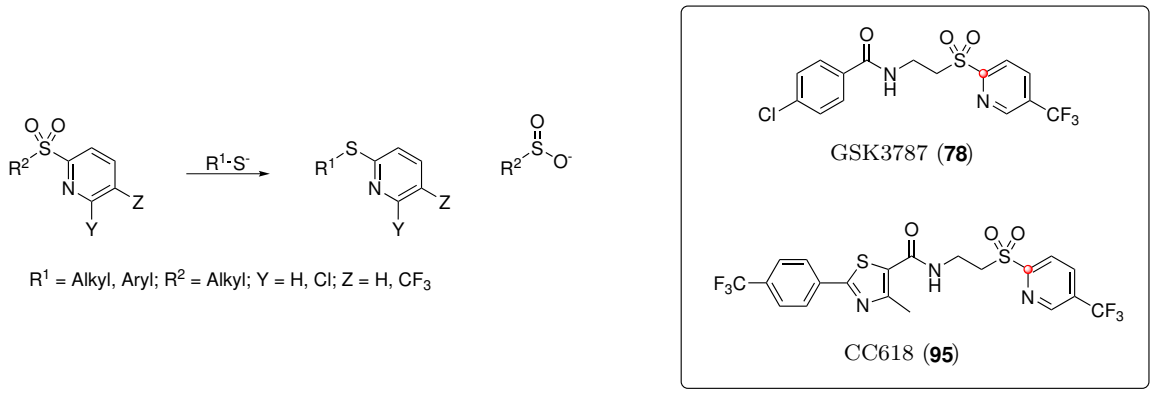

Figure 7.3. Nucleophilic aromatic substitution reactions between 2-sulfonylpyridines and thiolates. The carbon atoms shown to be reactive towards thiolates are marked with red bullets.

The cyanostilbene DG172 (**143**) (see Figure 7.1) is a potent antagonist and inverse agonist of PPARβ/δ, in terms of its competition with agonists[255] and the induction of subbasal levels of PPARβ/δ target gene expression, respectively.[89] In analogy to the inverse agonists derived from GSK0660 (**147**), TR-FRET analysis demonstrated that **143** is also able to enhance the affinity of PPARβ/δ for a peptide derived from the corepressor SMRT.[255]

The report on DG172 (**143**) also describes the evaluation a series of compounds with stilbene skeletons that lacked the electron-withdrawing nitrile group on the central alkene moiety. These stilbene analogues were significantly less potent binders of PPARβ/δ, indicating that the acrylonitrile moiety in DG172 is an important contributor to its affinity for PPARβ/δ.[255] Taken together with the well-established reactivity of activated acrylonitriles towards 1,4-conjugate addition of thiolates (see Figure 7.4),[288–293] the possible involvement of covalent interactions in the binding mode of DG172 merited further study.

7.2 Chemical and Biological Assays

Based on the presented evaluation of electrophilic motifs present in the PPARβ/δ antagonists reported to date, the four ligands GSK0660 (**147**), GSK3787 (**78**), CC618 (**95**) and DG172 (**143**) were selected for the study presented in Paper III. In order to shed light on the reactivity of these ligands towards Cys249 in the PPARβ/δ LBP, both chemical and biological assays were employed (*vide infra*).

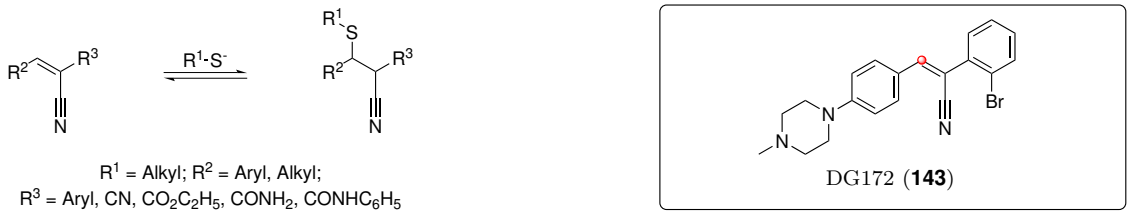

Figure 7.4. Reversible 1,4-conjugate additions of thiolates to activated acrylonitriles. The carbon atom in DG172 (**143**) hypothesized to be reactive towards thiolates is marked with a red bullet.

Initially, LC-MS/MS experiments were performed on trypsinized PPARβ/δ after treatment with each of the ligands. This assay sought to detect the tryptic peptide containing Cys249 and more importantly, determine the mass of the residue at the position of Cys249 by fragmentation of the tryptic peptide. The latter of these pieces of data would demonstrate an increase in mass upon covalent modification of Cys249. When integrated with the data from the chemical assays (*vide infra*), this mass difference could corroborate a mechanistic hypothesis for the reactivity of the ligand under study.

The PPARβ/δ protein used in these assays, was a commercially available, human recombinant PPARβ/δ, at a final protein concentration of $5\,\mu g\,mL^{-1}$ in each assay. The assays employed overnight trypsination, although recent studies indicate that shorter trypsination periods may increase coverage and detection.[294] Using the protocol described in the Electronic Supplementary Information (ESI) of Paper III (see Appendix B), LBD sequence coverages of approximately 50 – 80% were observed. Cys249 is preceded by Arg248 and the tryptic peptide observed with highest confidence in these assays was CQCTTVETVRELTEFAK (residues 249 – 265, see MS/MS spectrum of this peptide from apo-PPARβ/δ in Figure 7.5). This peptide misses one tryptic cleavage after Arg258. The fully tryptic peptide CQCTTVETVR (residues 249 – 258) was also observed, but with a lower intensity.

In continuation, the chemical reactivities of the ligands were evaluated by subjecting them to a model thiol, 2-mercaptoethanol (2-ME), in phosphate-buffered aqueous methanol at physiologically relevant pH (7.2 - 7.8),[295] and subsequently analyzing these mixtures with electrospray ionization mass spectrometry (ESI-MS). This assay provided a low threshold of detection of eventual products and allowed us to reverse the thiol/thiolate to ligand stoichiometry compared to the assay with the PPARβ/δ protein. While high thiol/thiolate to ligand stoichiometries amount to forcing and rather unnatural conditions, they were used as a tool to elicit detectable reaction products. This strategy based itself on a hypothesis that the chemical microenvironment of the PPARβ/δ LBP may present interactions with a ligand that serve to increase its reactivity - interactions that are not reproducible under chemical conditions. Therefore, the use of forcing conditions may identify relevant reaction products, although these may be formed by different reaction pathways (see tables of the obtained m/z-values in the Electronic Supplementary Information of Paper III in Appendix B).

The collective MS data provided findings regarding the reactivity of the ligands, as well as the masses of eventual reaction products. In order to expand our mechanistic understand-

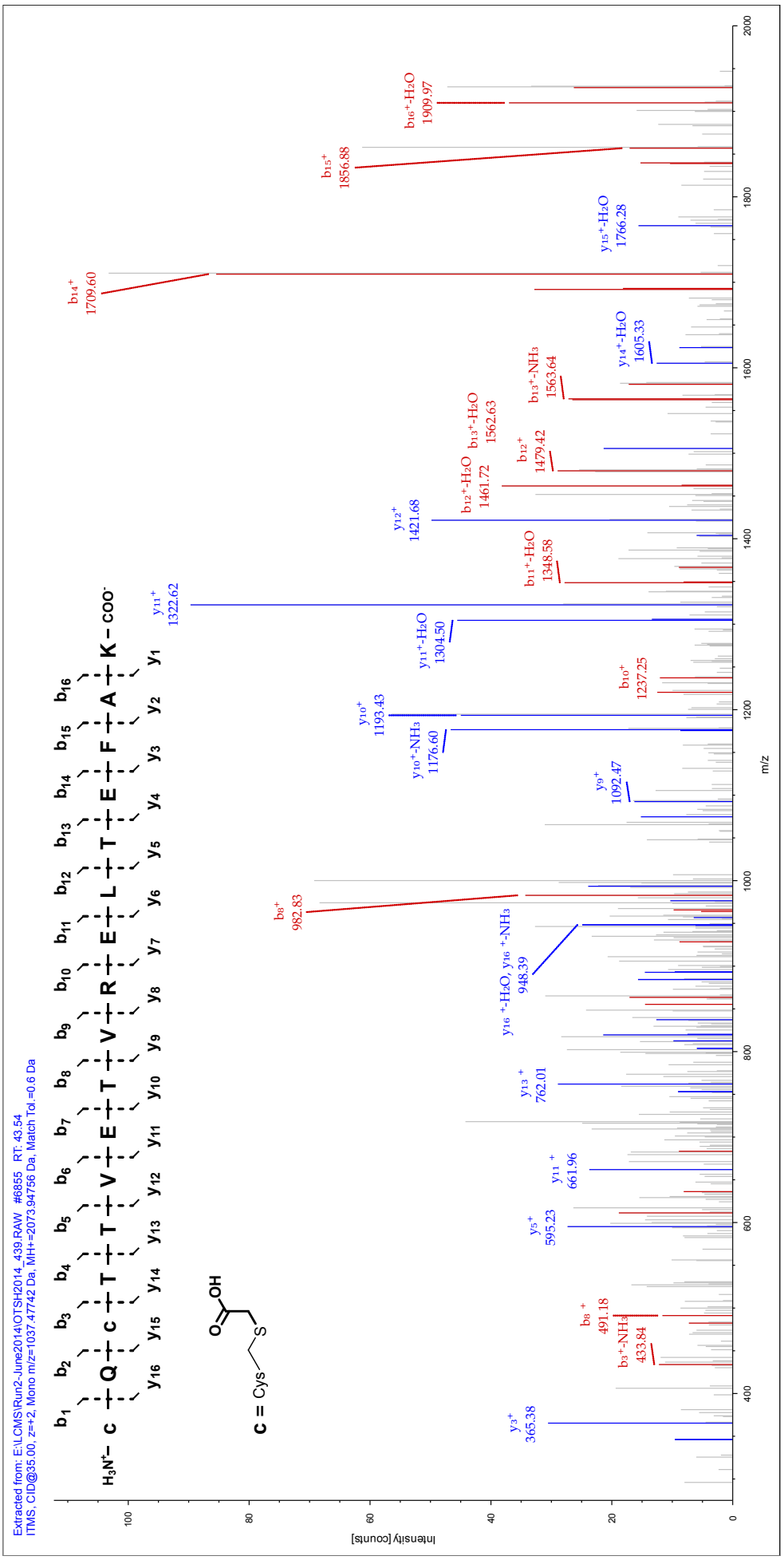

Figure 7.5. Representative MS/MS spectrum of the Cys249 containing peptide CQCTTVETVRELTEFAK from apo-PPARβ/δ, here carboxymethylated on both cysteines.

ing of the formation of these products, we employed ^{1}H-NMR to monitor eventual reactions of the ligands with 2-ME in phosphate-buffered aqueous perdeuterated dimethyl sulfoxide (DMSO-d_6). Although precise kinetic studies were not feasible using the NMR protocol described in the ESI of Paper III (see Appendix B), due to the time lost to tuning/matching and shimming, they provided a qualitative insight into the progress of the reactions between 2-ME and the ligands.

7.3 Results and Ligand Classification

7.3.1 Irreversibly Binding Antagonists

In the protein LC-MS/MS assays we observed covalent modification of Cys249 in PPARβ/δ only in the cases of GSK3787 (**78**) and CC618 (**95**). This result was reported in connection with Paper I (see Section 6.3). The reactivity of their common 5-trifluoromethyl-2-sulfonylpyridine moiety towards thiolates, is coherent with the previously demonstrated reactivity of similar eletron-poor 2-sulfonylpyridines (see Figure 7.3).[286,287] A mechanistic proposal for the reaction of a cysteine thiolate with a 5-trifluoromethyl-2-sulfonylpyridine antagonist can be seen in Figure 7.6.

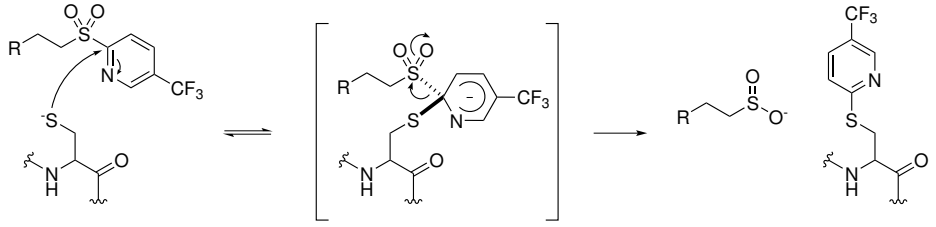

Figure 7.6. A mechanistic proposal for the reaction of a cysteine thiolate and a member of the 5-trifluoromethyl-2-sulfonylpyridine class of PPARβ/δ antagonists.

The mechanistic hypothesis presented in Figure 7.6 was supported by data from the MS/MS of the tryptic peptide containing Cys249 from PPARβ/δ treated with GSK3787 (**78**) or CC618 (**95**). This demonstrated an increased mass of Cys249 corresponding to the formation of a *S*-(5-(trifluoromethyl)pyridin-2-yl)cysteine. However, little is known about the structural consequences of this modification of PPARβ/δ, as no x-ray crystallographic determination of PPARβ/δ in complex with a member of the 5-trifluoromethyl-2-sulfonylpyridine class of antagonists, has been reported.[i] Thus, we employed the covalent docking protocol CovDock,[296] implemented in the Schrödinger Suite,[297] to shed light on this question (see Figure 7.7a). Cys249 is located on helix 3 in a narrow region of the PPARβ/δ LBP between the Ω-pocket and the AF-2 pocket (see Figure 7.7b-c). A structural consequence of covalent modification of Cys249 as a (5-trifluoromethyl)pyridin-2-yl thioether is the positioning of the aryl fragment in the channel leading from the Ω-pocket into the AF-2 pocket (see Figure 7.7).

[i]Cocrystallization of 5-trifluoromethyl-2-sulfonylpyridine antagonists with PPARβ/δ has been arduously pursued by our collaborator Dr. Jademilson Celestino dos Santos, a former member of the The Molecular Biotechnology Group (headed by Prof. Igor Polikarpov), Institute of Physics in São Carlos (IFSC), São Paulo, Brasil. Although crystals of PPARβ/δ treated with the antagonists were obtained, they did not refract well enough for a structure determination.

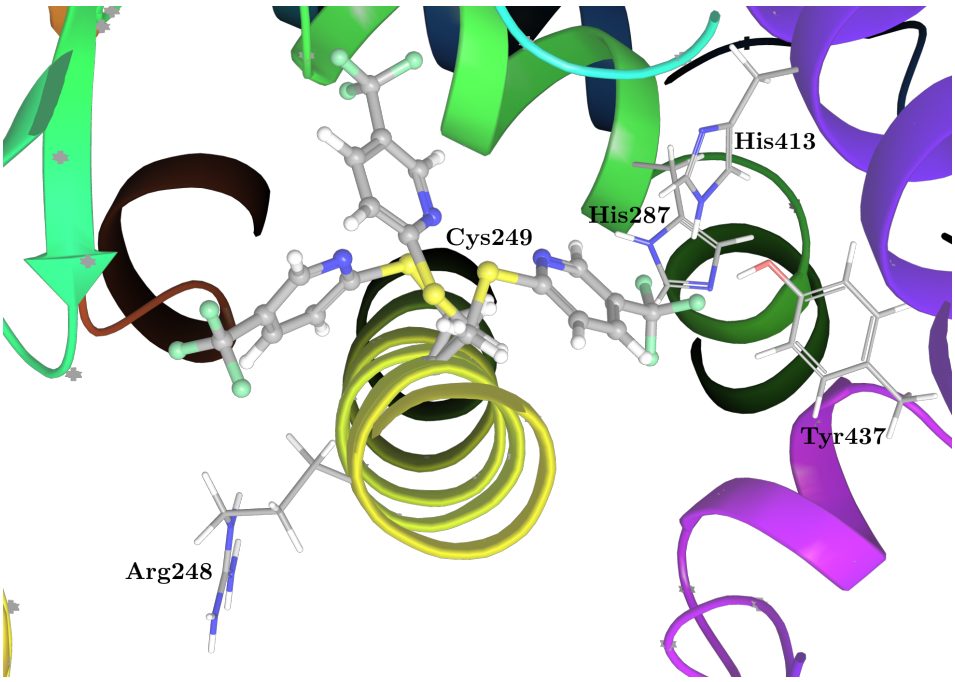

(a)

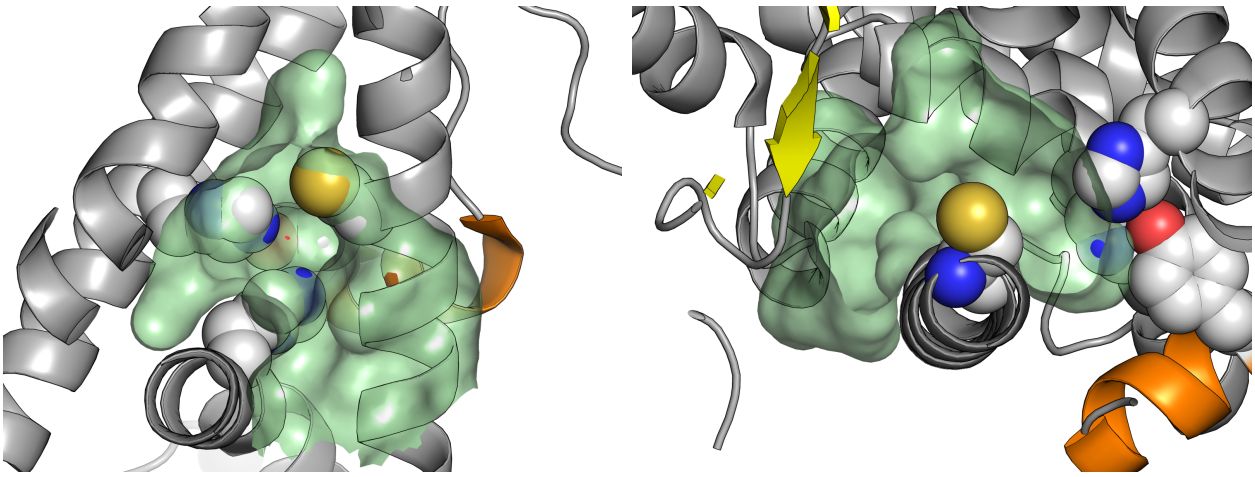

(b) (c)

Figure 7.7. *Top*: (a) The three lowest energy poses from the covalent docking of a 2-fluoro-5-trifluoromethylpyridine probe to PPARβ/δ with CovDock,[296] (see further details in the Supplementary Data of Paper I in Appendix B). *Bottom*: The PPARβ/δ LBP seen from a 90° left rotation of viewing angle 1 (b) and from viewing angle 2 (c) (see 2.2.1 for details on the viewing angles). Cys249 and the key AF-2 pocket residues His287, His413 and Tyr437 are shown as spheres. The pocket surface, seen in pale green, was created with HOLLOW.[16] The PPARβ/δ structure was taken from PDB ID: 3GZ9.

As a functional consequence of treatment of PPARβ/δ with the members of the 5-trifluoromethyl-2-sulfonylpyridine class is the inhibition of transcriptional induction by classical agonists such as GW501516 (**20**), a blockade of the access of agonists to the AF-2 pocket may be the structural basis of the observed antagonism. If seen in context with the demonstrations from PPARγ that covalent modification of the homologous Cys285, by covalent antagonists such as GW9662 (**47**), will inhibit AF-2-mediated agonism, but not Ω-pocket-mediated ligand

binding, it is tempting to speculate that treatment of PPARβ/δ with a 5-trifluoromethyl-2-sulfonylpyridine antagonist will lead to a similar outcome. To date, however, an investigation into whether PPARβ/δ treated with a 5-trifluoromethyl-2-sulfonylpyridine antagonist is still able to bind ligands that predominantly bind to the Ω-pocket of apo-PPARβ/δ (see Section 5.3.5) has not been conducted.

Another way of demonstrating the functional consequences of ligand binding is through differential scanning fluorimetry (DSF). In this assay, the fluorescence of a dye with affinity for the inner, hydrophobic regions of the protein, increases as the protein is denatured by increasing external temperature. The key measurement is referred to as the protein melting temperature, T_m, and is defined as the inflection point on a sigmoidal curve, fitted to the observed fluorescence. While T_m is related to the stabilization of the protein by the ligand, its magnitude is more sensitive to entropically driven binding modes (such as those involving hydrophobic interactions) than to those driven by enthalpy. Thus, the T_m is not directly comparable between different ligands. However, between ligands with similar structures and thus similar physico-chemical properties, such a comparison is justified.[298]

As seen in Figure 7.8,[ii] treatment of the PPARβ/δ LBD with the alkylamides **101** and **102**, that appeared inactive in the TR-FRET assay, does not increase the T_m from that observed upon treatment with vechicle (DMSO). Furthermore, the effect of treatment with the arylamides **105** and **107**, GSK3787 (**78**) or CC618 (**95**), lead to increases in the T_m that correspond to their increasing affinity for PPARβ/δ, as observed in the TR-FRET assays (see Figure 6.4). Interestingly, the inverse agonist GSK0660 (**147**) induces a markedly larger

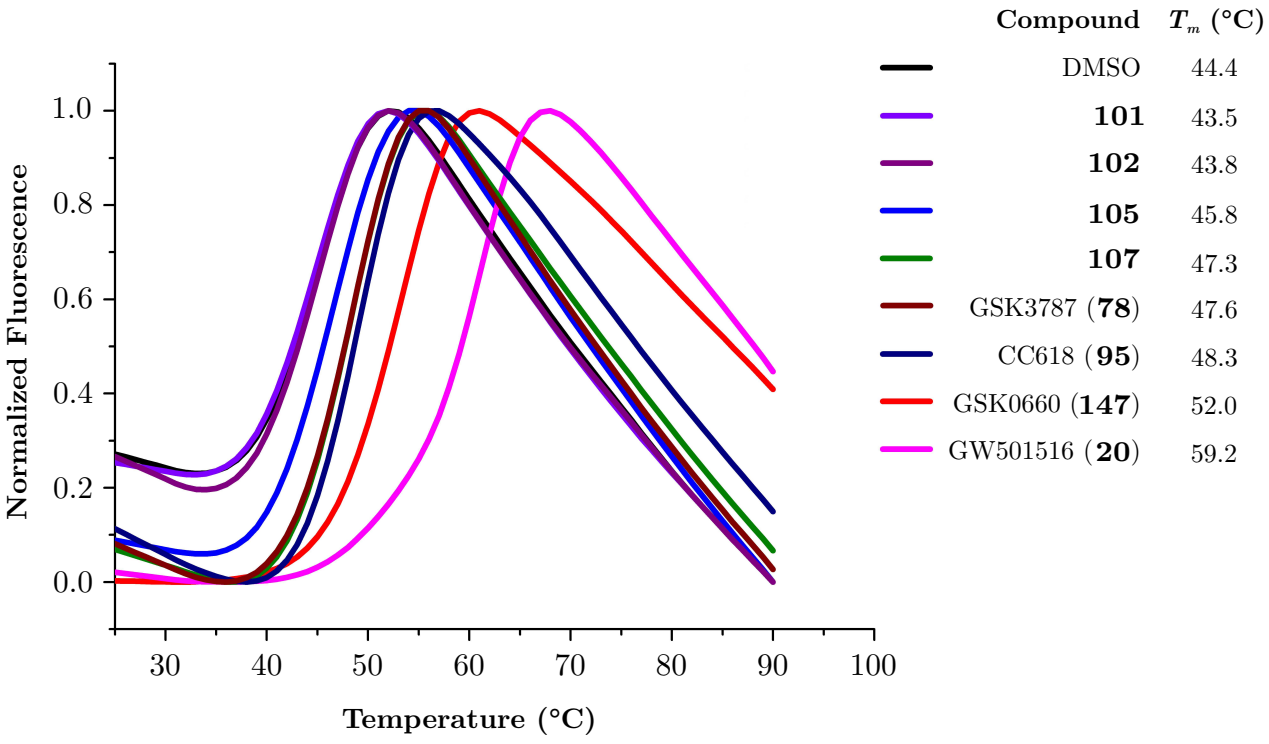

Figure 7.8. Determination of T_m-values for PPARβ/δ treated with the listed compounds by differential scanning fluorimetry (DSF).

[ii] These data are shown with the written permission of Dr. Jademilson Celestino dos Santos, who performed the assay.

increase in the T_m, attesting to either a greater stabilization of PPARβ/δ or a more entropically driven binding mode. Finally, the potent PPARβ/δ agonist GW501516 (**20**) strongly protects the PPARβ/δ LBD from thermal denaturation. Taken together, these data suggest that the T_m observed by DSF correlates to the observed kinetics of binding, as seen in the TR-FRET assays. They also suggest that the covalent modification of Cys249 in PPARβ/δ, stabilizes the LBD towards thermal denaturation, relative to apo-PPARβ/δ.

7.3.2 Reversibly Binding Inverse Agonists

While treatment with neither GSK0660 (**147**) nor DG172 (**143**), appeared to covalently modify Cys249 in PPARβ/δ, **143** was reactive towards 2-ME in both the ESI-MS assay and the NMR assay. In the NMR assay, the extent of the 1,4-conjugate addition to **143** was pH-dependent and we could demonstrate that the reaction proceeds with $> 50\%$ conversion of **143** between pH 7.5 and pH 7.8 (see Figure 7.9) While the addition of DMSO to water is known to increase the basicity of the mixture,[299] it seems unlikely that this phenomenon has significantly skewed the results, given the capacity of the added phosphate buffer (1 M) and the qualitatively similar result obtained in buffered aqueous methanol.

The diverging results obtained with DG172 (**143**) led us to investigate whether the acrylonitrile motif present in **143** is sufficiently activated by its substituents to display a rapidly reversible 1,4-conjugate addition, as has been reported for other highly activated acrylonitriles.[288–293] Thus, to determine whether the addition of 2-ME to DG172 (**143**) is reversible, we took cues from a previous study by Serafimova et al., in which the disappearance/reappearance of the acrylonitrile UV-absorption was monitored during the addition reaction and after dilution of this reaction mixture in phosphate buffer.[290] Under these conditions, the addition of 2-ME to **143** appeared to be slowly reversible (see ESI of Paper III in Appendix B). The reaction did not, however, reverse as quickly as those with more highly activated acrylonitriles.[290] Nevertheless, in the context of PPARβ/δ, interactions between LBP residues and DG172 (**143**) could influence both the rate of addition and elimination of Cys249. Thus, to investigate the possible involvement of a reversible conjugate addition of Cys249 to **143**, we turned to a TR-FRET assay, configured to demonstrate the off-rate of a ligand binding to a receptor.[300–302] In this assay, the rising FRET-induced emission from a fluorescent tracer ligand is monitored as it replaces a ligand in the LBP of the receptor. This curve may then be compared to those of relevant reference compounds for high- or low off-rates i.e. a *bona fide* reversibly binding ligand and an irreversibly binding ligand. When the rate of displacement of DG172 (**143**) from the PPARβ/δ LBP by the fluorescent tracer ligand "Pan-PPAR Green" was compared to those of the reversible agonist GW501516 (**20**) and the covalent, irreversible antagonist GSK3787 (**78**), there was no indication of a decreased off-rate for DG172 (**143**). Furthermore, **143** was similarly displaced when present in a higher concentration (see Figure 7.10).

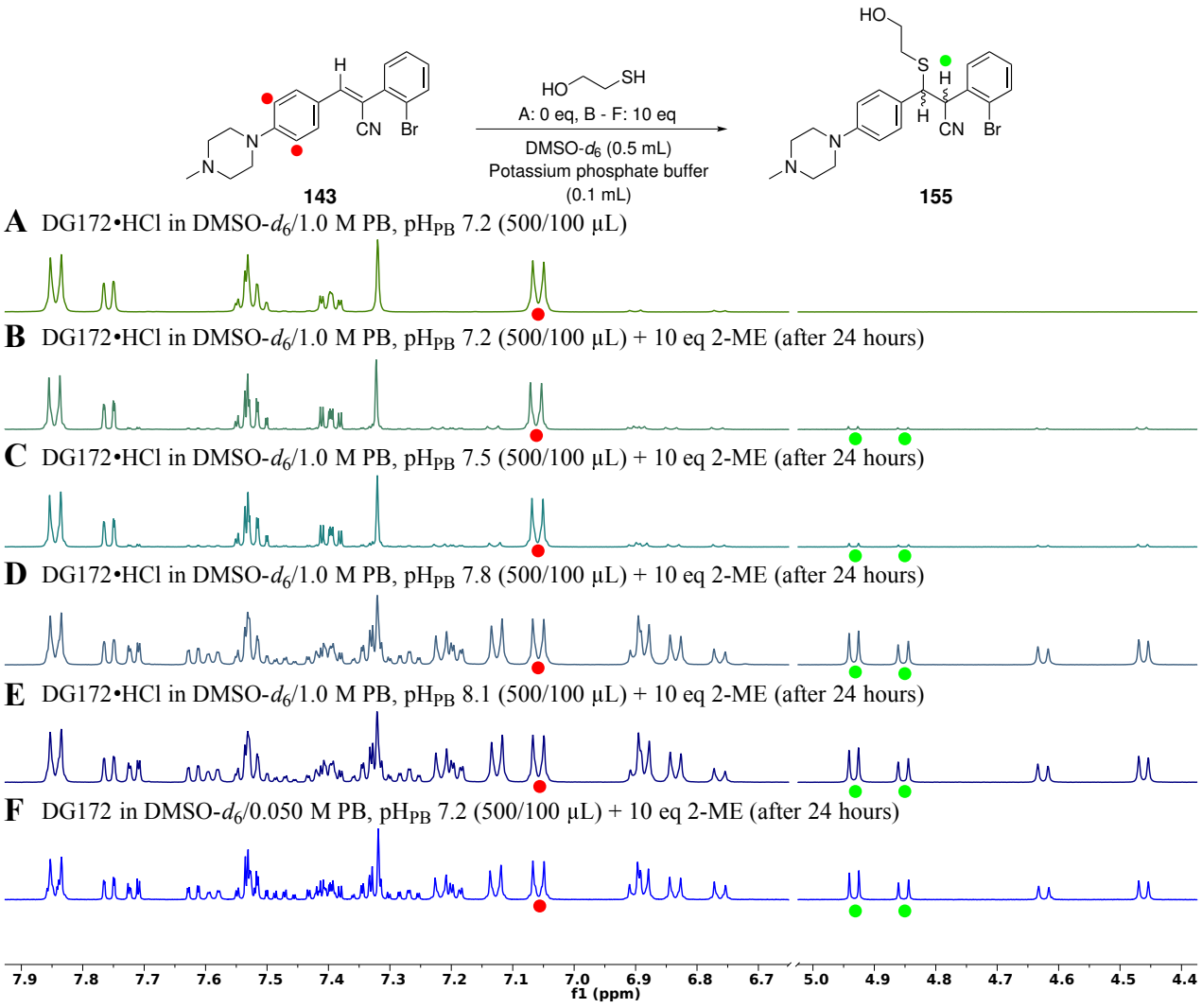

Figure 7.9. ^{1}H-NMR monitoring (split, partial spectrum) of DG172·HCl (**143**·HCl) alone (A), treated with 2-ME (10 eq) in DMSO-d_6/1.0 M potassium phosphate buffer, at increasing pH (7.2 – 8.1, B – E) and DG172 (**143**) treated with 2-ME (10 eq) in DMSO-d_6/0.050 M potassium phosphate buffer (pH 7.2) (F), shown for comparison.

7.4 Conclusions

In summary, the studied antagonistic ligands differ in their interactions with Cys249 in the PPARβ/δ LBP. GSK3787 (**78**) and CC618 (**95**) are covalent, irreversible antagonists of PPARβ/δ. Additionally, the demonstrations of their reactivity towards thiolates in the ESI-MS- and NMR assays, substantiate the hypothesis that their reactions with Cys249 in PPARβ/δ are nucleophilic aromatic substitution reactions. GSK0660 (**147**) and DG172 (**143**), on the other hand, appear to be reversibly binding inverse agonists of PPARβ/δ. Our observations contribute to a mechanistic understanding of the background for the different functional effects observed upon treatment of PPARβ/δ with these antagonistic ligands - from antagonism to inverse agonism.

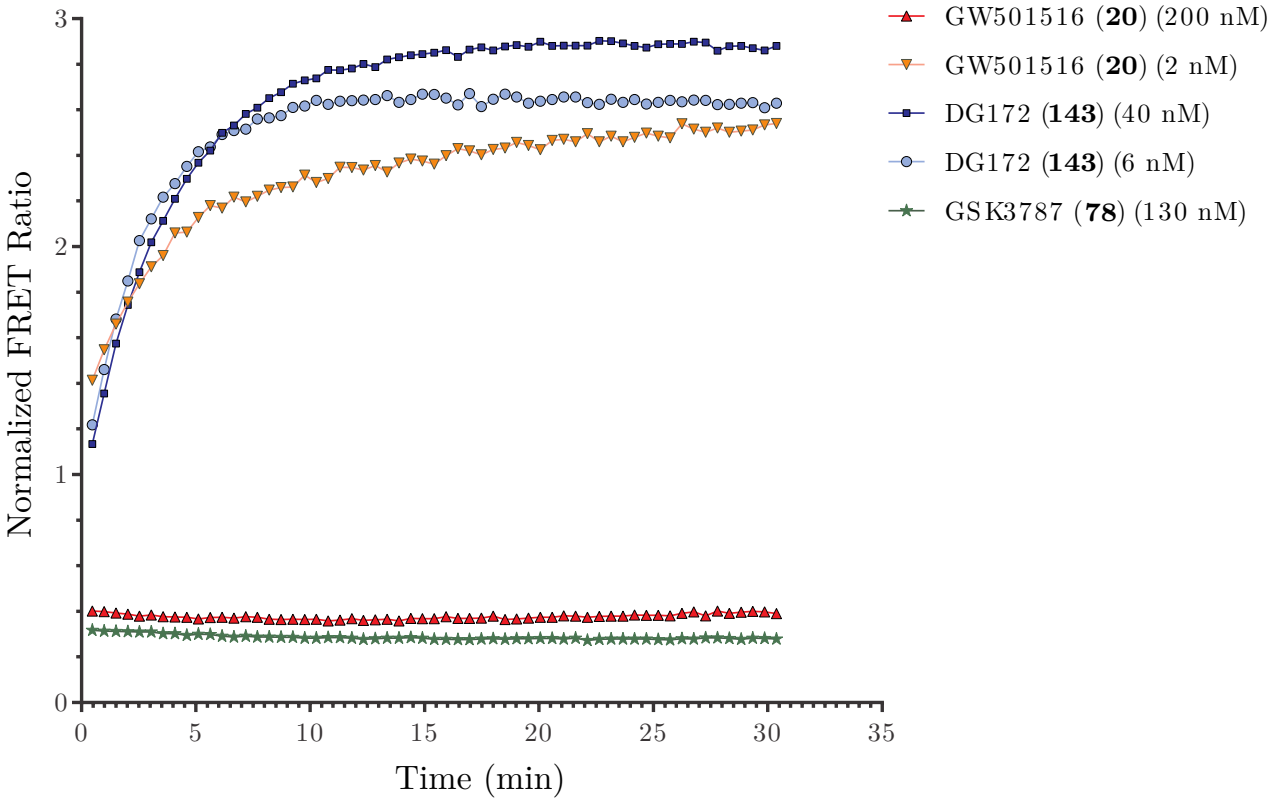

Figure 7.10. Displacement of GW501516 (**20**), DG172 (**143**) and GSK3787 (**78**) from the LBP of PPARβ/δ by the fluorescent tracer ligand Fluormone Pan PPAR Green (100 nM) as a function of time. The normalized FRET ratio represents values from single wells, normalized based on control wells (DMSO, $rw = 2$). The concentrations in parentheses refer to the final concentrations of the ligands after dilution.

8 Paper IV: Principal Component Analyses of PPARγ Structural Data

A considerable number of x-ray crystallographic studies of PPARγ have been reported over the past two decades. The structural data from these studies include PPARγ in complex with a functionally diverse set of ligands, as well as in their absence (apo-PPARγ). In light of the recently demonstrated ligand-dependent inhibition of the Cdk5-mediated phosphorylation of Ser273 (see Section 5.3.2) and the observed allosterically induced agonism by PPARγ ligands that do not directly stabilize helix 12 (see Section 5.3.3), a collective review of these structural data could potentially provide insight into the relative differences of the PPARγ complexes with these ligands and the complexes with classical agonists. A classification of this kind, could serve as a reference for future computational chemistry investigations that aim to discover new ligands of a particular class by molecular docking in PPARγ structures, or that aim to describe the differential dynamics of PPARγ in complex distinct ligands in MD simulations. We thus sought to investigate the feasibility of observing ligand-dependent structural changes in PPARγ by principal component analysis (PCA) of the atomic positions (Cartesian coordinates) (cPCA) and dihedral angles of the protein backbone (dPCA) of the PPARγ structures available in the public domain.

8.1 Principal Component Analysis of Biological Structural Data

The study of protein structures in the crystal phase observes a more static picture of protein dynamics than in-solution studies. While crystal packing must be assumed to limit larger conformational changes such as inter-domain motions, a crystallized protein is often heavily hydrated[303] and retains varying degrees of conformational freedom.[304,305] Indeed, loop regions are often mobile in crystals, in some cases to the point where the positions of their constituent atoms are not resolvable. It has been demonstrated that protein structures in the crystal phase may sample functionally relevant conformational spaces.[233–235] On the other hand, transitions between conformational states of proteins may involve changes in the structure that are too complex in their orientations and magnitudes to be perceived by visual inspection of a set of superimposed structures. To a dataset with high-dimensional variance such as this, the application of PCA can identify the directions of largest variance and recast the data in a coordinate system whose axes are defined by these directions. This way, a description of most of the variance in the dataset can be captured by the first few such axes, called the principal components (PCs).[306] PCA has a history of application in the analysis of protein structure and examples of previously analyzed datasets include the trajectories of atomic positions (as Cartesian coordinates) or backbone dihedral angles from molecular dynamics (MD) simulations[187,307,308] and the atomic positions obtained from x-ray crystallography.[233–235]

An expressed strength of dPCA versus cPCA is rooted in the difficulty of comparing protein positional data. A comparison of atomic positions aims to identify only differences

that can be ascribed to internal motion and not to translations or rotations of the entire protein. To minimize the influence of the latter two, a superimposition of the structures to be analyzed is necessary. This is routinely performed by iteratively aligning the superimposition until a convergence criterion, corresponding to a set maximum RMSD for all the atoms in a structure or an ensemble, relative to each other or to a reference structure, is met. However, it is not certain that the functional differences between protein structures are at their most visible when an ensemble of structures is aligned to minimize the RMSD of *all* the atoms. To the contrary, this may obscure important functional motion. Furthermore, in cases where the magnitude of the differences between the structures are small, compared to the magnitude of e.g. compression of the structure due to crystal packing, the two sources of positional differences may skew a cPCA analysis. dPCA on the other hand is much less sensitive to such confounding effects, as its source of data is defined by the internal coordinates of the protein. Dihedral angles are, as such, an attractive source data for PCA analyses.[309]

8.2 Structural Aspects of PTM Inhibition and Allosteric Stabilization of Helix 12

A common feature of the binding mode of ligands that inhibit the PPARγ PTM involving phosphorylation of Ser273, is their stabilization of the β-sheet region in the Ω-pocket of the PPARγ LBP (see Figure 5.9). This contrasts a principal feature of the binding mode of classical PPARγ agonists, which involves the stabilization of helix 12 in the AF-2 pocket.[164] While several of the partial or non-agonistic PPARγ ligands bind exclusively to the Ω-pocket, several classical agonists of PPARγ, such as rosiglitazone (**3**), partially occupy the Ω-pocket with their tail moieties. Thus, it is possible that the inhibition of Ser273 phosphorylation can be related to a stabilization of the β-sheet region through interactions with the tail moieties of larger ligands, whose head groups bind to the AF-2 pocket. A stabilization of the β-sheet region was indeed observed with HDX-MS of PPARγ treated with rosiglitazone (**3**).[88]

On the other hand, in the case of pioglitazone (**11**), two overlapping molecules of **11** were observed in the crystal structure (PDB ID: 2XKW, chain A). The first of these poses corresponds to the only pose observed with its structural analogue rosiglitazone (**3**) (see Figure 5.2 and PDB ID: 2PRG, 1FM6, 3DZY or 4EMA). In the second pose, **11** is bound parallel to helix 3 in the Ω-pocket, where it interacts with the β-sheet region. This observation suggests that for a given ligand, its stabilization of the β-sheet region, which may be conducive to an inhibition of Ser273 phosphorylation, can be dependent on an equilibrium of multiple binding poses.

As is the case in more than half of the reported crystal structures of PPARγ, the structure with pioglitazone (**11**) contains a PPARγ homodimer, composed of type A and B chains (see Section 2.2.3). Interestingly, **11** is also found in its second pose described above in the type B chain. The observation of multiple binding poses in the type A and -B chains of the crystal structures in which PPARγ is found as a homodimer, is not unique to the case of pioglitazone (**11**). In addition to this phenomenon, there are numerous examples of ligands that are

observed to bind simultaneously in higher stoichiometries. Examples displaying both these phenomena include the structures of PPARγ in complex with the synthetic partial agonist T2384 (**37**, PDB ID:3K8S), the NSAID indomethacin (**145**, PDB ID: 4XUM, 3ADS), the serotonin metabolite 5-methoxyindole acetate (PDB ID: 3ADU) and the fatty acids nonanoic acid (**21**, PDB ID: 4EM9, 3SZ1), 9-(*S*)-HODE (PDB ID: 2VSR) and 5-(*R*)-HEPA (PDB ID: 2VV2). These findings suggest that the stabilization of the PPARγ LBP by ligands depends on the concentration of a ligand and, in a physiological context, those of other ligands. The effects of simultaneous binding of multiple ligands to the PPARγ LBP are not well understood. LBP saturation by multiple ligands, particularly the combination of Cys285-modifying covalent ligands with ligands binding to the Ω-pocket, has been linked to a strong activation of PPARγ.[14,57] LBP saturation may also play a role in the degree of activation observed with multiply binding fatty acids.[24,64] On the other hand, in the case of T2384 (**37**), treatment of PPARγ with low concentrations of **37** led to partial activation, while treatment with high concentrations led to antagonism and an increased recruitment of the transcriptional corepressor NCoR.[173] It is unknown whether the observed allosteric stabilization of helix 12 by Ω-pocket-binding partial agonists, in some cases, is connected to the binding of additional equivalents of these ligands in poses that are not observed by x-ray crystallography. It is, however, tempting to speculate that a connection exists between the activation observed by treatment with Cys285-modifying ligands in combination with ligands binding to the Ω-pocket, and the partial agonism displayed by Ω-pocket-binding ligands that display extensive interactions with helix 3 (see also Section 5.3.3). In summary, given the existence of equilibria between multiple poses and the possibility for different degrees of LBP saturation, the data from x-ray crystallography of PPARγ in complex with ligands may not be straightforwardly connected to the observed biological effects of these ligands.

8.3 Data Selection and Analysis Software

The PPARγ structures available in the public domain are heterogenous in terms of the protein chains that make up the crystals. Based on our initial analyses of the whole dataset (see Paper IV in Appendix B), a subset of the structures were selected for closer comparison. The selected dataset contained 78 structures of PPARγ homodimers, nearly all of which crystallized in the C 1 2 1 space group. Their data were collected from the respective crystals at 100 ± 10 K and spanned resolutions 1.8 – 2.9 Å (average 2.3 Å). The PCA analyses restricted themselves to the type A chains. The atomic positions (in Cartesian coordinates) of the backbone heavy atoms (N, C_α, C, O) or their dihedral angles (ϕ, ψ, ω) were used as input for the cPCA and dPCA, respectively. As the P-loop, the Ω-loop and the three C-terminal residues (see Section 2.2.1) are highly mobile and infrequently resolved in the PPARγ crystal structures, these regions were excluded. This ensured a high occupancy (98.7%) of the residue selection (210 – 238, 245 – 260 and 276 – 474, PPARγ1 numbering) throughout the final dataset.

We obtained the PPARγ structural data from the PDB_REDO databank,[310,311] which contains optimized and consistently refined data from entries in the RCSB Protein Data

Bank.[5] The PDB-files were parsed with the functions implemented in the Python software package ProDy (ver. 1.6.1),[312] which was also used for the cPCA analyses and to produce plots of these. Additionally, ProDy was used to produce a PDB-file of the reference structure (apo-PPARγ, PDB ID: 2ZK0) and an ordered pseudo-trajectory of the structures of the ensemble in DCD-format. The Visual Molecular Dynamics (VMD) software (ver. 1.9.1)[313] was used to parametrize the protein topology (CHARMM36 version, July 2012)[314] of the PDB-file and output the reference structure in PSF-format. The PSF- and DCD-files were then used as input for the software Carma (ver. 1.4),[315] which performed the dPCA analyses. The numerical results were read back into Python and plotted using the plotting functions in ProDy or the standard Python equivalents (matplotlib). An in-house program, written in Python, was used to coordinate the efforts of the above mentioned softwares (Python, ver. 2.7.6).[316]

8.4 Results from the PCA Analyses

Upon completion of the calculations, the structures were plotted along their principal components (PCs) in order to observe whether the transformation of the dataset along the axes of its largest variances could yield a separation of the structures. Subsequently, the data points corresponding to each structure in these plots were colored according to external parameters, such as the ability of a ligand to inhibit phosphorylation of Ser273, or internal structural parameters, such as the presence of contacts (cutoff distance 3.0 Å) of their ligands with specific regions of the LBP, the B-factors of these regions or the distances between heavy atoms in the structure envisioned to capture ligand-induced structural differences.

In general, the cPCA analyses yielded a poor separation of the structures, when plotting them along the first two principal components (PC1 and PC2). However, within this distribution, a moderate correlation with the presence of ligand contacts with Tyr473 in helix 12 (see Paper IV in Appendix B), as well as with the B-factors of Tyr473 was observed (see Figure 8.1, top). A similar trend was not observed when focusing on ligand contacts with a selection of residues from the β-sheet region or the B-factors of these residues (see the Supporting Information of Paper IV in Appendix B). The residues Arg357 and Glu460 form an ionic network, which also involves Glu276 on helix 3. The interaction of Phe360 with Arg357 was shown to be a critical component in the stabilization of helix 12, observed as a marked change in the crystallized conformation of helix 12 in a Phe360Leu mutant. This PPARγ mutant displayed an impaired ability to activate transcription.[317] Interestingly, a correlation could be found between the distributions along cPC1 and cPC2, and the distance between the residues Arg357 and Glu460 (see Paper IV in Appendix B). This correlation corresponded to the stabilization of helix 12, observed in the B-factors of Tyr473, as described above (see Figure 8.1, top).

In the dPCA analysis of the final dataset, a separation of the structures into three rough clusters was observed from the plot of the structures along the three first principal components, dPC1 – dPC3. In Figure 8.1 (bottom), the structures are colored according to the reported ability of the ligands to inhibit phosphorylation of Ser273.[24,88,161,175,176,179,318,319] No

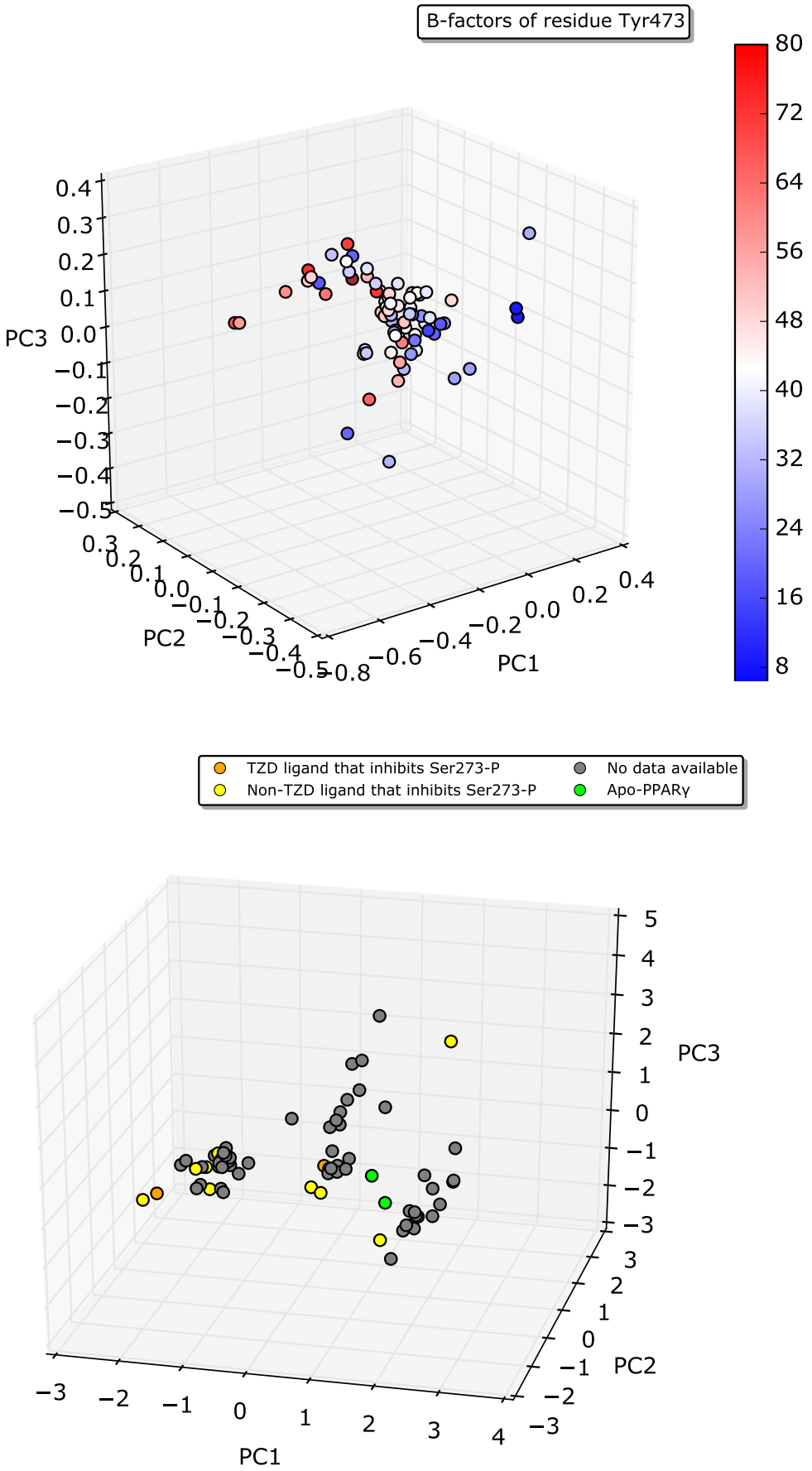

Figure 8.1. cPCA and dPCA analyses of the final dataset of PPARγ structures shown as plots of the structures along the three first principal components, PC1 – 3. *Top*: cPCA. The structures are colored according to the B-factors of Tyr473. *Bottom*: dPCA. The structures are colored according to their reported ability to inhibit pSer273.[24,88,161,175,176,179,318,319]

particular trend in the coloring of the structures was observed with this or any of the other coloring schemes described above. Nevertheless, the observed clustering in the distribution of the structures is of interest. Firstly, the distributions along dPC1 and dPC2 are non-normal, indicating that it is unlikely that they were calculated based on random or normally distributed data. This, in turn, indicates that they contain structural information. Furthermore, in an NMR-study with PPARγ, Johnson et al. showed that the apo-PPARγ structure likely populates multiple minima in solution and that the populations of much fewer of these minima rose upon the addition of ligand.[30] In another study, using cPCA of MD-trajectories from a $> 400\,\text{ns}$ of simulation of the PPARγ:RXRα heterodimer, Lemkul et al. found that holo-PPARγ could be shown to populate three major minima, separated by $< 3.5\,\text{kJ}\,\text{mol}^{-1}$. dPCA has previously been shown to capture energy minima separated by small barriers,[308] thus it seems possible that the clustering observed here may be a manifestation of subtly different structures with similar energies. The observation that none of our attempts to find a correlation between a membership in one of the clusters and a specific biological effect or structural stability parameter, may be linked to the small energy differences between the clusters. In such a scenario, other forces such as crystal packing may dictate the minimum in which PPARγ crystallizes.

8.5 Conclusions

In summary, PCA analyses of structures of PPARγ from x-ray crystallography have been presented. Our analyses show that trends linked to the stabilization of helix 12 are correlated to the distributions of the structures along cPC1 and, to some degree, cPC2. The analysis thus provides a coarse mapping of the stability of helix 12 in the structural ensemble. This mapping can be of interest to others, in studies aiming to use PPARγ crystal structures as starting points for virtual screening campaigns or molecular dynamics simulations. Furthermore, although the dPCA analysis provided a separation of the structures, no correlating parameter could be found to explain the observed clusters. In future work, it would be of interest to apply dPCA to molecular dynamics simulations of PPARγ, in order to further investigate whether a physically relevant conformational space is in fact sampled by the x-ray crystallographic data.

9 Conclusions and Future Work

Nuclear receptor signaling has been an area of research for more than two decades and will continue to provide the scientific community with challenges for decades to come. With the growing parallel capabilities of biochemical- and bioinformatics tools, genomewide analyses of the transcriptional networks under the influence of each nuclear receptor, in a specific cellular environment, are now becoming available. The combination of these data with knowledge gained from the study of the structures of the nuclear receptors and their ligands, will promote an improved understanding of the influence of small-molecular ligands on the dynamics of the receptors and on the interactions of the receptors with other biochemical components in the transcriptional machinery.

In this work, new members of the 5-trifluoromethyl-2-sulfonylpyridine class of PPARβ/δ antagonists have been synthesized and biologically evaluated. Among them, a new, more PPARβ/δ-selective antagonist, the quinolin-3-yl amide **131**, was discovered. Furthermore, a combination of chemical and biological insights into the mode of action of this class of antagonists have distinguished it as unique among the reported PPARβ/δ antagonistic ligands, in that its members covalently modify a reactive cysteine (Cys249) in the PPARβ/δ ligand-binding pocket. In addition, the evaluations of the structural and functional consequences of covalent modification of Cys249 in PPARβ/δ have spawned collaborations with research groups in Brasil and Finland.

Future work may involve evaluations of the utility of the developed PPARβ/δ antagonists as pharmacological tools, in *in vitro* cultured cells expressing all three PPARs and *in vivo*. In this context, experimental determinations of logP/logD-values should be conducted. Furthermore, the utility of the 5-trifluoromethyl-2-sulfonylpyridine PPARβ/δ antagonists in the development of new PPARβ/δ ligands with alternative binding modes may be investigated.

The last part of this work ventured to apply a well-known and powerful statistical treatment to a body of structural data of PPARγ in complex with a diverse set of ligands. These analyses entailed, as far as this author is aware, the first applications of Cartesian- and dihedral principal component analyses to PPARγ x-ray crystallographic data. While challenges such as heterogeneity in the crystal compositions and small variances within the structural ensemble were imposed by the dataset, some general trends were found. The results provide insight into the structural consequences of PPARγ ligand binding, as well as a promising starting point for future investigations, aiming to apply similar statistical treatments to data from in-solution studies.

In conclusion, the recent discovery of the role of a novel post-translational modification of the PPARγ ligand-binding domain and its implications for the use of PPARγ ligands as treatments for both metabolic- and neurodegenerative diseases, symbolize a new dawn in

the field of PPAR research. Hopefully, the resources spent on the failed developments of PPAR classical agonists as drugs to treat type II diabetes mellitus and its related metabolic complications, will not impede further investments in the development of PPAR ligands. The outcomes of the ongoing clinical trial with the PPARγ partial agonist INT131 (**38**), as treatment for relapsing-remitting multiple sclerosis (RRMS), will likely be decisive for the future of this class of PPARγ ligands. In the contexts of PPARα and PPARβ/δ, the notion that the ligand-dependent modulation of their acitivities may display similar points of divergence, as shown in PPARγ, requires a reevaluation of the transcriptional outcomes of treatment with existing PPARα- and PPARβ/δ ligands that display alternative binding modes, with other endpoints in mind than classical agonism.

References

1. Sladek, F. M. What are nuclear receptor ligands? *Mol. Cell. Endocrinol.* **2011**, *334*, 3–13.
2. Hatchwell, E.; Greally, J. M. The potential role of epigenomic dysregulation in complex human disease. *Trends Genet.* **2007**, *23*, 588–595.
3. Ottow, E.; Weinmann, H. In, Ottow, E., Ed.; Methods and Principles in Medicinal Chemistry 39; Wiley-VCH: Weinheim, 2008; Chapter A Historical Perspective of Modern Drug Discovery, pp 1–23.
4. Perissi, V.; Rosenfeld, M. G. Controlling nuclear receptors: the circular logic of cofactor cycles. *Nat. Rev. Mol. Cell Biol.* **2005**, *6*, 542–554.
5. Berman, H. M.; Westbrook, J.; Feng, Z.; Gilliland, G.; Bhat, T. N.; Weissig, H.; Shindyalov, I. N.; Bourne, P. E. The Protein Data Bank - URL: `http://www.rcsb.org/`. *Nucleic Acids Res.* **2000**, *28*, 235–242.
6. Gadaleta, R. M.; Magnani, L. Nuclear receptors and chromatin: an inducible couple. *J. Mol. Endocrinol.* **2014**, *52*, R137–R149.
7. Germain, P.; Staels, B.; Dacquet, C.; Spedding, M.; Laudet, V. Overview of Nomenclature of Nuclear Receptors. *Pharmacol. Rev.* **2006**, *58*, 685–704.
8. Mangelsdorf, D. J.; Thummel, C.; Beato, M.; Herrlich, P.; Schütz, G.; Umesono, K.; Blumberg, B.; Kastner, P.; Mark, M.; Chambon, P.; Evans, R. M. The nuclear receptor superfamily: The second decade. *Cell* **1995**, *83*, 835–839.
9. Bugge, A.; Mandrup, S. Molecular Mechanisms and Genome-Wide Aspects of PPAR Subtype Specific Transactivation. *PPAR Res.* **2010**, *2010*, 1–12.
10. The UniProt Consortium UniProt: a hub for protein information. *Nucleic Acids Res.* **2015**, *43*, D204–D212.
11. Uppenberg, J.; Svensson, C.; Jaki, M.; Bertilsson, G.; Jendeberg, L.; Berkenstam, A. Crystal structure of the ligand binding domain of the human nuclear receptor PPARγ. *J. Biol. Chem.* **1998**, *273*, 31108–31112.
12. Bourguet, W.; Ruff, M.; Chambon, P.; Gronemeyer, H.; Moras, D. Crystal structure of the ligand-binding domain of the human nuclear receptor RXR-α. *Nature* **1995**, *375*, 377–382.
13. The PyMOL Molecular Graphics System 1.3r1, 2010.
14. Waku, T.; Shiraki, T.; Oyama, T.; Maebara, K.; Nakamori, R.; Morikawa, K. The nuclear receptor PPARγ individually responds to serotonin- and fatty acid-metabolites. *EMBO J.* **2010**, *29*, 3395–3407.
15. Artis, D. R.; Lin, J. J.; Zhang, C.; Wang, W.; Mehra, U.; Perreault, M.; Erbe, D.; Krupka, H. I.; England, B. P.; Arnold, J. Scaffold-based discovery of indeglitazar, a PPAR pan-active anti-diabetic agent. *Proc. Natl. Acad. Sci. U.S.A.* **2009**, *106*, 262–267.
16. Ho, B. K.; Gruswitz, F. HOLLOW: Generating Accurate Representations of Channel and Interior Surfaces in Molecular Structures. *BMC Struct. Biol.* **2008**, *8*, 49–54.
17. Wagner, R. L.; Apriletti, J. W.; McGrath, M. E.; West, B. L.; Baxter, J. D.; Fletterick, R. J. A structural role for hormone in the thyroid hormone receptor. *Nature* **1995**, *378*, 690–697.
18. Parker, M. G.; White, R. Nuclear receptors spring into action. *Nat. Struct. Mol. Biol.* **1996**, *3*, 113–115.
19. Moras, D.; Gronemeyer, H. The nuclear receptor ligand-binding domain: structure and function. *Curr. Opin. Cell Biol.* **1998**, *10*, 384–391.
20. Heery, D. M.; Kalkhoven, E.; Hoare, S.; Parker, M. G. A signature motif in transcriptional co-activators mediates binding to nuclear receptors. *Nature* **1997**, *387*, 733–736.
21. Nolte, R. T.; Wisely, G. B.; Westin, S.; Cobb, J. E.; Lambert, M. H.; Kurokawa, R.; Rosenfeld, M. G.; Willson, T. M.; Glass, C. K.; Milburn, M. V. Ligand binding and co-activator assembly of the peroxisome proliferator-activated receptor-γ. *Nature* **1998**, *395*, 137–143.
22. Cavaillès, V.; Dauvois, S.; Danielian, P. S.; Parker, M. G. Interaction of proteins with transcriptionally active estrogen receptors. *Proc. Natl. Acad. Sci. U.S.A.* **1994**, *91*, 10009–10013.

23. Helsen, C.; Claessens, F. Looking at nuclear receptors from a new angle. *Mol. Cell. Endocrinol.* **2014**, *382*, 97–106.

24. Liberato, M. V.; Nascimento, A. S.; Ayers, S. D.; Lin, J. Z.; Cvoro, A.; Silveira, R. L.; Martínez, L.; Souza, P. C. T.; Saidemberg, D.; Deng, T.; Amato, A. A.; Togashi, M.; Hsueh, W. A.; Phillips, K.; Palma, M. S.; Neves, F. A. R.; Skaf, M. S.; Webb, P.; Polikarpov, I. Medium Chain Fatty Acids Are Selective Peroxisome Proliferator Activated Receptor (PPAR) γ Activators and Pan-PPAR Partial Agonists. *PLoS ONE* **2012**, *7*, e36297–e36306.

25. Fyffe, S. A.; Alphey, M. S.; Buetow, L.; Smith, T. K.; Ferguson, M. A. J.; Sørensen, M. D.; Björkling, F.; Hunter, W. N. Recombinant Human PPAR-β/δ Ligand-binding Domain is Locked in an Activated Conformation by Endogenous Fatty Acids. *J. Mol. Biol.* **2006**, *356*, 1005–1013.

26. Xu, H.; Lambert, M. H.; Montana, V. G.; Parks, D. J.; Blanchard, S. G.; Brown, P. J.; Sternbach, D. D.; Lehmann, J. M.; Wisely, G.; Willson, T. M.; Kliewer, S. A.; Milburn, M. V. Molecular Recognition of Fatty Acids by Peroxisome Proliferator–Activated Receptors. *Mol. Cell* **1999**, *3*, 397–403.

27. Fyffe, S. A.; Alphey, M. S.; Buetow, L.; Smith, T. K.; Ferguson, M. A.; Sørensen, M. D.; Björkling, F.; Hunter, W. N. Reevaluation of the PPAR-β/δ Ligand Binding Domain Model Reveals Why It Exhibits the Activated Form. *Mol. Cell* **2006**, *21*, 1–2.

28. Kleywegt, G. J.; Harris, M. R.; Zou, J.-y.; Taylor, T. C.; Wählby, A.; Jones, T. A. The Uppsala Electron-Density Server. *Acta Crystallogr., Sect. D: Biol. Crystallogr.* **2004**, *60*, 2240–2249.

29. Waku, T.; Shiraki, T.; Oyama, T.; Fujimoto, Y.; Maebara, K.; Kamiya, N.; Jingami, H.; Morikawa, K. Structural Insight into PPARγ Activation Through Covalent Modification with Endogenous Fatty Acids. *J. Mol. Biol.* **2009**, *385*, 188–199.

30. Johnson, B. A.; Wilson, E. M.; Li, Y.; Moller, D. E.; Smith, R. G.; Zhou, G. Ligand-induced stabilization of PPARγ monitored by NMR spectroscopy: implications for nuclear receptor activation. *J. Mol. Biol.* **2000**, *298*, 187–194.

31. Kelley, L. A.; Sutcliffe, M. J. OLDERADO: Online database of ensemble representatives and domains. *Protein Sci.* **1997**, *6*, 2628–2630.

32. Hartl, R. Berechnung der NMR-Struktur der PPARγ-LBD und Hochdruck-NMR-Messungen an HPr I14A, Ph.D. Thesis, University of Regensburg, Germany, 2008.

33. Riepl, H.; Hartl, R.; Bauer, M.; Nar, H.; Kauschke, S.; Kalbitzer, H.; Maurer, T. Sequential Backbone Assignment of Peroxisome Proliferator-Activated Receptor-γ Ligand Binding Domain. *J. Biomol. NMR* **2005**, *32*, 259.

34. Pettersson, I.; Ebdrup, S.; Havranek, M.; Pihera, P.; Kořínek, M.; Mogensen, J. P.; Jeppesen, C. B.; Johansson, E.; Sauerberg, P. Design of a partial PPARδ agonist. *Bioorg. Med. Chem. Lett.* **2007**, *17*, 4625–4629.

35. Xu, H. E.; Stanley, T. B.; Montana, V. G.; Lambert, M. H.; Shearer, B. G.; Cobb, J. E.; McKee, D. D.; Galardi, C. M.; Plunket, K. D.; Nolte, R. T.; Parks, D. J.; Moore, J. T.; Kliewer, S. A.; Willson, T. M.; Stimmel, J. B. Structural Basis for Antagonist-Mediated Recruitment of Nuclear Co-Repressors by PPARα. *Nature* **2002**, *415*, 813–817.

36. Kliewer, S. A.; Umesono, K.; Noonan, D. J.; Heyman, R. A.; Evans, R. M. Convergence of 9-cis retinoic acid and peroxisome proliferator signalling pathways through heterodimer formation of their receptors. *Nature* **1992**, *358*, 771–774.

37. Miyata, K. S.; McCaw, S. E.; Marcus, S. L.; Rachubinski, R. A.; Capone, J. P. The peroxisome proliferator-activated receptor interacts with the retinoid X receptor in vivo. *Gene* **1994**, *148*, 327–330.

38. Juge-Aubry, C.; Pernin, A.; Favez, T.; Burger, A. G.; Wahli, W.; Meier, C. A.; Desvergne, B. DNA Binding Properties Of Peroxisome Proliferator-activated Receptor Subtypes on Various Natural Peroxisome Proliferator Response Elements - Importance of the 5$\prime$-Flanking Region. *J. Biol. Chem.* **1997**, *272*, 25252–25259.

39. Zhang, H.; Xu, X.; Chen, L.; Chen, J.; Hu, L.; Jiang, H.; Shen, X. Molecular Determinants of Magnolol Targeting Both RXRα and PPARγ. *PLoS ONE* **2011**, *6*, e28253–e28259.

40. Venäläinen, T.; Molnár, F.; Oostenbrink, C.; Carlberg, C.; Peräkylä, M. Molecular mechanism of allosteric communication in the human PPARα-RXRα heterodimer. *Proteins: Struct., Funct., Bioinf.* **2010**, *78*, 873–887.

41. Chandra, V.; Huang, P.; Hamuro, Y.; Raghuram, S.; Wang, Y.; Burris, T. P.; Rastinejad, F. Structure of the intact PPAR-γ–RXR-α nuclear receptor complex on DNA. *Nature* **2008**, 350–356.

42. Lundell, K.; Thulin, P.; Hamsten, A.; Ehrenborg, E. Alternative splicing of human peroxisome proliferator-activated receptor delta (PPARdelta):effects on translation efficiency and trans-activation ability. *BMC Mol. Biol.* **2007**, *8*, 70–86.

43. Aprile, M.; Ambrosio, M. R.; D'Esposito, V.; Beguinot, F.; Formisano, P.; Costa, V.; Ciccodicola, A. PPARG in Human Adipogenesis: Differential Contribution of Canonical Transcripts and Dominant Negative Isoforms. *PPAR Res.* **2014**, *2014*, 1–11.

44. Hanselman, J. C.; Vartanian, M. V.; Koester, B. P.; Gray, S. A.; Essenburg, A. D.; Rea, T. J.; Bisgaier, C. L.; Pape, M. Expression of the mRNA encoding truncated PPARα does not correlate with hepatic insensitivity to peroxisome proliferators. *Mol. Cell. Biochem.* **2001**, *217*, 91–97.

45. Chen, Y.; Jimenez, A. R.; Medh, J. D. Identification and regulation of novel PPAR-γ splice variants in human THP-1 macrophages. *Biochim. Biophys. Acta, Gene Struct. Expression* **2006**, *1759*, 32–43.

46. Nakachi, Y.; Yagi, K.; Nikaido, I.; Bono, H.; Tonouchi, M.; Schönbach, C.; Okazaki, Y. Identification of novel PPARγ target genes by integrated analysis of ChIP-on-chip and microarray expression data during adipocyte differentiation. *Biochem. Biophys. Res. Commun.* **2008**, *372*, 362–366.

47. Abbott, B. D. Review of the expression of peroxisome proliferator-activated receptors alpha (PPARα), beta (PPARβ), and gamma (PPARγ) in rodent and human development. *Reprod. Toxicol.* **2009**, *27*, 246–257.

48. Kersten, S. Integrated physiology and systems biology of PPARα. *Mol. Metab.* **2014**, *3*, 354–371.

49. Bensinger, S. J.; Tontonoz, P. Integration of metabolism and inflammation by lipid-activated nuclear receptors. *Nature* **2008**, *454*, 470–477.

50. Westergaard, M.; Henningsen, J.; Rasmussen, S.; Kristiansen, K.; Johansen, C.; Svendsen, M. L.; Jensen, U. B.; Schrøder, H. D.; Staels, B.; Iversen, L.; Bolund, L.; Kragballe, K. Expression and Localization of Peroxisome Proliferator-Activated Receptors and Nuclear Factor κB in Normal and Lesional Psoriatic Skin. *J. Invest. Dermatol.* **2003**, *121*, 1104–1117.

51. Neels, J. G.; Grimaldi, P. A. Physiological Functions of Peroxisome Proliferator-Activated Receptor β. *Physiol. Rev.* **2014**, *94*, 795–858.

52. Chawla, A. Control of Macrophage Activation and Function by PPARs. *Circ. Res.* **2010**, *106*, 1559–1569.

53. Ahmadian, M.; Suh, J. M.; Hah, N.; Liddle, C.; Atkins, A. R.; Downes, M.; Evans, R. M. PPARγ signaling and metabolism: the good, the bad and the future. *Nat. Med.* **2013**, *99*, 557–566.

54. Wang, Y.-X. PPARs: diverse regulators in energy metabolism and metabolic diseases. *Cell Res.* **2010**, *20*, 124–137.

55. Willson, T. M.; Brown, P. J.; Sternbach, D. D.; Henke, B. R. The PPARs: From Orphan Receptors to Drug Discovery. *J. Med. Chem.* **2000**, *43*, 527–550.

56. Jüngling, E.; Kammermeier, H. A one-vial method for routine extraction and quantification of free fatty acids in blood and tissue by HPLC. *Anal. Biochem.* **1988**, *171*, 150–157.

57. Hughes, T. S.; Giri, P. K.; de Vera, I. M. S.; Marciano, D. P.; Kuruvilla, D. S.; Shin, Y.; Blayo, A.-L.; Kamenecka, T. M.; Burris, T. P.; Griffin, P. R.; Kojetin, D. J. An alternate binding site for PPARγ ligands. *Nat. Commun.* **2014**, *5*, 1–13.

58. Forman, B. M.; Tontonoz, P.; Chen, J.; Brun, R. P.; Spiegelman, B. M.; Evans, R. M. 15-Deoxy-$\Delta^{12,14}$-Prostaglandin J2 is a Ligand for the Adipocyte Determination Factor PPARγ. *Cell* **1995**, *83*, 803–812.

59. Forman, B. M.; Chen, J.; Evans, R. M. Hypolipidemic drugs, polyunsaturated fatty acids, and eicosanoids are ligands for peroxisome proliferator-activated receptors α and δ. *Proc. Natl. Acad. Sci. U.S.A.* **1997**, *94*, 4312–4317.

60. Hostetler, H. A.; Kier, A. B.; Schroeder, F. Very-Long-Chain and Branched-Chain Fatty Acyl-CoAs Are High Affinity Ligands for the Peroxisome Proliferator-Activated Receptor α (PPARα). *Biochemistry* **2006**, *45*, 7669–7681.

61. Popeijus, H. E.; van Otterdijk, S. D.; van der Krieken, S. E.; Konings, M.; Serbonij, K.; Plat, J.; Mensink, R. P. Fatty acid chain length and saturation influences PPARα transcriptional activation and repression in HepG2 cells. *Mol. Nutr. Food Res.* **2014**, *58*, 2342–2349.

62. Shureiqi, I.; Jiang, W.; Zuo, X.; Wu, Y.; Stimmel, J. B.; Leesnitzer, L. M.; Morris, J. S.; Fan, H.-Z.; Fischer, S. M.; Lippman, S. M. The 15-lipoxygenase-1 product 13-S-hydroxyoctadecadienoic acid down-regulates PPAR-δ to induce apoptosis in colorectal cancer cells. *Proc. Natl. Acad. Sci. U.S.A.* **2003**, *100*, 9968–9973.

63. Naruhn, S.; Meissner, W.; Adhikary, T.; Kaddatz, K.; Klein, T.; Watzer, B.; Müller-Brüsselbach, S.; Müller, R. 15-Hydroxyeicosatetraenoic Acid Is a Preferential Peroxisome Proliferator-Activated Receptor β/δ Agonist. *Mol. Pharmacol.* **2010**, *77*, 171–184.

64. Itoh, T.; Fairall, L.; Amin, K.; Inaba, Y.; Szanto, A.; Balint, B. L.; Nagy, L.; Yamamoto, K.; Schwabe, J. W. R. Structural basis for the activation of PPARγ by oxidized fatty acids. *Nat. Struct. Mol. Biol.* **2008**, *15*, 924–931.

65. Egawa, D.; Itoh, T.; Yamamoto, K. Characterization of Covalent Bond Formation between PPARγ and Oxo-Fatty Acids. *Bioconjugate Chem.* **2015**, *26*, 690–698.

66. Li, Y.; Zhang, J.; Schopfer, F. J.; Martynowski, D.; Garcia-Barrio, M. T.; Kovach, A.; Suino-Powell, K.; Baker, P. R. S.; Freeman, B. A.; Chen, Y. E.; Xu, H. E. Molecular recognition of nitrated fatty acids by PPARγ. *Nat. Struct. Mol. Biol.* **2008**, *15*, 865–867.

67. Schopfer, F. J.; Cole, M. P.; Groeger, A. L.; Chen, C.-S.; Khoo, N. K. H.; Woodcock, S. R.; Golin-Bisello, F.; Motanya, U. N.; Li, Y.; Zhang, J.; Garcia-Barrio, M. T.; Rudolph, T. K.; Rudolph, V.; Bonacci, G.; Baker, P. R. S.; Xu, H. E.; Batthyany, C. I.; Chen, Y. E.; Hallis, T. M.; Freeman, B. A. Covalent Peroxisome Proliferator-activated Receptor γ Adduction by Nitro-fatty Acids. *J. Biol. Chem.* **2010**, *285*, 12321–12333.

68. Malapaka, R. R. V.; Khoo, S.; Zhang, J.; Choi, J. H.; Zhou, X. E.; Xu, Y.; Gong, Y.; Li, J.; Yong, E.-L.; Chalmers, M. J.; Chang, L.; Resau, J. H.; Griffin, P. R.; Chen, Y. E.; Xu, H. E. Identification and Mechanism of 10-Carbon Fatty Acid as Modulating Ligand of Peroxisome Proliferator-activated Receptors. *J. Biol. Chem.* **2011**, *287*, 183–195.

69. Kornberg, R. D. The molecular basis of eukaryotic transcription. *Proc. Natl. Acad. Sci. U.S.A.* **2007**, *104*, 12955–12961.

70. Greer, E. L.; Shi, Y. Histone methylation: a dynamic mark in health, disease and inheritance. *Nat. Rev. Genet.* **2012**, *13*, 343–357.

71. Rossetto, D.; Avvakumov, N.; Côté, J. Histone phosphorylation: A chromatin modification involved in diverse nuclear events. *Epigenetics* **2012**, *7*, 1098–1108.

72. Cao, J.; Yan, Q. Histone Ubiquitination and Deubiquitination in Transcription, DNA Damage Response, and Cancer. *Front. Oncol.* **2012**, *2*, 1–9.

73. Verdone, L. Histone acetylation in gene regulation. *Brief. Funct. Genomic. Proteomic.* **2006**, *5*, 209–221.

74. Berrabah, W.; Aumercier, P.; Lefebvre, P.; Staels, B. Control of nuclear receptor activities in metabolism by post-translational modifications. *FEBS Lett.* **2011**, *585*, 1640–1650.

75. Privalsky, M. L. The Role of Corepressors in Transcriptional Regulation by Nuclear Hormone Receptors. *Annu. Rev. Physiol.* **2004**, *66*, 315–360.

76. Shi, Y.; Hon, M.; Evans, R. M. The peroxisome proliferator-activated receptor δ, an integrator of transcriptional repression and nuclear receptor signaling. *Proc. Natl. Acad. Sci. U.S.A.* **2002**, *99*, 2613–2618.

77. Perissi, V.; Staszewski, L. M.; McInerney, E. M.; Kurokawa, R.; Krones, A.; Rose, D. W.; Lambert, M. H.; Milburn, M. V.; Glass, C. K.; Rosenfeld, M. G. Molecular determinants of nuclear receptor–corepressor interaction. *Genes & development* **1999**, *13*, 3198–3208.

78. Glass, C. K.; Rosenfeld, M. G. The coregulator exchange in transcriptional functions of nuclear receptors. *Genes Dev.* **2000**, *14*, 121–141.

79. McKenna, N. J.; O'Malley, B. W. Combinatorial control of gene expression by nuclear receptors and coregulators. *Cell* **2002**, *108*, 465–474.

80. Ricote, M.; Glass, C. K. PPARs and molecular mechanisms of transrepression. *Biochim. Biophys. Acta, Mol. Cell. Biol. Lipids* **2007**, *1771*, 926–935.

81. Fernandes, I.; Bastien, Y.; Wai, T.; Nygard, K.; Lin, R.; Cormier, O.; Lee, H. S.; Eng, F.; Bertos, N. R.; Pelletier, N.; Mader, S.; Han, V. K.; Yang, X.-J.; White, J. H. Ligand-Dependent Nuclear Receptor Corepressor LCoR Functions by Histone Deacetylase-Dependent and -Independent Mechanisms. *Mol. Cell* **2003**, *11*, 139–150.

82. Cavaillès, V.; Dauvois, S.; L'Horset, F.; Lopez, G.; Hoare, S.; Kushner, P. J.; Parker, M. G. Nuclear factor RIP140 modulates transcriptional activation by the estrogen receptor. *EMBO J.* **1995**, *14*, 3741.

83. Treuter, E.; Albrektsen, T.; Johansson, L.; Leers, J.; Gustafsson, J.-Å. A regulatory role for RIP140 in nuclear receptor activation. *Mol. Endocrinol.* **1998**, *12*, 864–881.

84. Augereau, P.; Badia, E.; Balaguer, P.; Carascossa, S.; Castet, A.; Jalaguier, S.; Cavaillès, V. Negative regulation of hormone signaling by RIP140. *J. Steroid Biochem. Mol. Biol.* **2006**, *102*, 51–59.

85. Flores, A. M.; Gurevich, I.; Zhang, C.; Ramirez, V. P.; Devens, T. R.; Aneskievich, B. J. TNIP1 is a corepressor of agonist-bound PPARs. *Arch. Biochem. Biophys.* **2011**, *516*, 58–66.

86. Gurevich, I.; Flores, A. M.; Aneskievich, B. J. Corepressors of agonist-bound nuclear receptors. *Toxicol. Appl. Pharmacol.* **2007**, *223*, 288–298.

87. Bougarne, N.; Paumelle, R.; Caron, S.; Hennuyer, N.; Mansouri, R.; Gervois, P.; Staels, B.; Haegeman, G.; De Bosscher, K. PPARα blocks glucocorticoid receptor α-mediated transactivation but cooperates with the activated glucocorticoid receptor α for transrepression on NF-κB. *Proc. Natl. Acad. Sci. U.S.A.* **2009**, *106*, 7397–7402.

88. Choi, J. H.; Banks, A. S.; Estall, J. L.; Kajimura, S.; Boström, P.; Laznik, D.; Ruas, J. L.; Chalmers, M. J.; Kamenecka, T. M.; Blüher, M.; Griffin, P. R.; Spiegelman, B. M. Anti-diabetic drugs inhibit obesity-linked phosphorylation of PPARγ by Cdk5. *Nature* **2010**, *466*, 451–456.

89. Adhikary, T.; Brandt, D. T.; Kaddatz, K.; Stockert, J.; Naruhn, S.; Meissner, W.; Finkernagel, F.; Obert, J.; Lieber, S.; Scharfe, M.; Jarek, M.; Toth, P. M.; Scheer, F.; Diederich, W. E.; Reinartz, S.; Grosse, R.; Müller-Brüsselbach, S.; Müller, R. Inverse PPARβ/δ agonists suppress oncogenic signaling to the ANGPTL4 gene and inhibit cancer cell invasion. *Oncogene* **2013**, *32*, 5241–5252.

90. Marciano, D. P.; Kuruvilla, D. S.; Boregowda, S. V.; Asteian, A.; Hughes, T. S.; Garcia-Ordonez, R.; Corzo, C. A.; Khan, T. M.; Novick, S. J.; Park, H.; Kojetin, D. J.; Phinney, D. G.; Bruning, J. B.; Kamenecka, T. M.; Griffin, P. R. Pharmacological repression of PPARγ promotes osteogenesis. *Nat. Commun.* **2015**, *6*, 7443–7449.

91. Lipid lowering with fibric acid derivatives, URL: `http://www.uptodate.com/contents/lipid-lowering-with-fibric-acid-derivatives`, accessed October 30, 2015.

92. Qu, B.; Li, Q.-T.; Wong, K. P.; Tan, T. M. C.; Halliwell, B. Mechanism of clofibrate hepatotoxicity: mitochondrial damage and oxidative stress in hepatocytes. *Free Radic. Biol. Med.* **2001**, *31*, 659–669.

93. LiverTox - Drug Record - Clofibrate, URL: `http://livertox.nih.gov/Clofibrate.htm`, accessed October 29, 2015.

94. Oliver, M. F.; Heady, J. A.; Morris, J. N.; Cooper, J. WHO Cooperative Trial on Primary Prevention of Ischaemic Heart Disease with Clofibrate to Lower Serum Cholesterol: Final Mortality Follow-up: Report of the Committee of Principal Investigators. *Lancet* **1984**, *324*, Originally published as Volume 2, Issue 8403, 600–604.

95. Questions and answers on the review of medicines containing fibrates - EMA/643808/2010 Rev. 1, URL: `http://www.ema.europa.eu/ema/index.jsp?curl=pages/includes/document/document_detail.jsp?webContentId=WC500098373`, accessed October 30, 2015.

96. Staels, B.; Rubenstrunk, A.; Noel, B.; Rigou, G.; Delataille, P.; Millatt, L. J.; Baron, M.; Lucas, A.; Tailleux, A.; Hum, D. W., et al. Hepatoprotective effects of the dual peroxisome proliferator-activated receptor alpha/delta agonist, GFT505, in rodent models of nonalcoholic fatty liver disease/nonalcoholic steatohepatitis. *Hepatology* **2013**, *58*, 1941–1952.

97. Saltiel, A. R.; Olefsky, J. M. Thiazolidinediones in the Treatment of Insulin Resistance and Type II Diabetes. *Diabetes* **1996**, *45*, 1661–1669.

98. Phillips, L. S.; Grunberger, G.; Miller, E.; Patwardhan, R.; Rappaport, E. B.; Salzman, A. Once- and Twice-Daily Dosing With Rosiglitazone Improves Glycemic Control in Patients With Type 2 Diabetes. *Diabetes Care* **2001**, *24*, 308–315.

99. Pavo, I.; Jermendy, G.; Varkonyi, T. T.; Kerenyi, Z.; Gyimesi, A.; Shoustov, S.; Shestakova, M.; Herz, M.; Johns, D.; Schluchter, B. J.; Festa, A.; Tan, M. H. Effect of Pioglitazone Compared with Metformin on Glycemic Control and Indicators of Insulin Sensitivity in Recently Diagnosed Patients with Type 2 Diabetes. *J. Clin. Endocrinol. Metab.* **2003**, *88*, 1637–1645.

100. Gale, E. A. Lessons from the glitazones: a story of drug development. *Lancet* **2001**, *357*, 1870–1875.

101. LiverTox - Drug Record - Troglitazone, URL: `http://livertox.nih.gov/Troglitazone.htm`, accessed October 29, 2015.

102. Hirsch IB; Kelly J; Cooper S Pulmonary edema associated with troglitazone therapy. *Arch. Intern. Med.* **1999**, *159*, 1811–1817.

103. Cantello, B. C.; Cawthorne, M. A.; Haigh, D.; Hindley, R. M.; Smith, S. A.; Thurlby, P. L. The synthesis of BRL 49653 - a novel and potent antihyperglycaemic agent. *Bioorg. Med. Chem. Lett.* **1994**, *4*, 1181–1184.

104. Cantello, B. C.; Cawthorne, M. A.; Cottam, G. P.; Duff, P. T.; Haigh, D.; Hindley, R. M.; Lister, C. A.; Smith, S. A.; Thurlby, P. L. [[ω-(Heterocyclylamino) alkoxy]benzyl]-2, 4-thiazolidinediones as potent antihyperglycemic agents. *J. Med. Chem.* **1994**, *37*, 3977–3985.

105. FDA Application Number: 021071 - Approval Letter (Avandia), URL: `http://www.accessdata.fda.gov/drugsatfda_docs/nda/99/21071_Avandia_Approv.pdf`, accessed November 2, 2015.

106. FDA Drug Safety Communication: Updated Risk Evaluation and Mitigation Strategy (REMS) to Restrict Access to Rosiglitazone-containing Medicines including Avandia, Avandamet, and Avandaryl, URL: `http://www.fda.gov/Drugs/DrugSafety/ucm255005.htm`, accessed October 30, 2015.

107. Questions and answers on the suspension of rosiglitazone-containing medicines (Avandia, Avandamet and Avaglim) - EMA/CHMP/586211/2010, URL: `http://www.ema.europa.eu/ema/index.jsp?curl=pages/includes/document/document_detail.jsp?webContentId=WC500097003`, accessed October 30, 2015.

108. Letter dated 16.11.2010 regarding Prohibition of manufacture and sale of Rosiglitazone - F.no. 12-01/2010-DC(PT-18), URL: `http://cdsco.nic.in/writereaddata/prohibition_rosiglitazone.pdf`, accessed November 1, 2015.

109. Nissen, S. E.; Wolski, K. Effect of Rosiglitazone on the Risk of Myocardial Infarction and Death from Cardiovascular Causes. *N. Engl. J. Med.* **2007**, *356*, 2457–2471.

110. Home, P. D.; Pocock, S. J.; Beck-Nielsen, H.; Curtis, P. S.; Gomis, R.; Hanefeld, M.; Jones, N. P.; Komajda, M.; McMurray, J. J. Rosiglitazone evaluated for cardiovascular outcomes in oral agent combination therapy for type 2 diabetes (RECORD): a multicentre, randomised, open-label trial. *Lancet* **2009**, *373*, 2125–2135.

111. Komajda, M.; McMurray, J. J.; Beck-Nielsen, H.; Gomis, R.; Hanefeld, M.; Pocock, S. J.; Curtis, P. S.; Jones, N. P.; Home, P. D. Heart failure events with rosiglitazone in type 2 diabetes: data from the RECORD clinical trial. *Eur. Heart J.* **2010**, *31*, 824–831.

112. FDA Drug Safety Communication: FDA requires removal of some prescribing and dispensing restrictions for rosiglitazone-containing diabetes medicines, URL: `http://www.fda.gov/drugs/drugsafety/ucm376389.htm`, accessed October 30, 2015.

113. Nathan, D. M. Rosiglitazone and Cardiotoxicity — Weighing the Evidence. *N. Engl. J. Med.* **2007**, *357*, 64–66.

114. Nissen, S. E. The rise and fall of rosiglitazone. *Eur. Heart J.* **2010**, *31*, 773–776.

115. Slaoui, M. The rise and fall of rosiglitazone: reply. *Eur. Heart J.* **2010**, *31*, 1282–1284.

116. GlaxoSmithKline to Plead Guilty and Pay $3 Billion to Resolve Fraud Allegations and Failure to Report Safety Data | OPA |Department of Justice, URL: `http://www.justice.gov/opa/pr/glaxosmithkline-plead-guilty-and-pay-3-billion-resolve-fraud-allegations-and-failure-report`, accessed October 30, 2015.

117. Loke, Y. K.; Kwok, C. S.; Singh, S. Comparative cardiovascular effects of thiazolidinediones: systematic review and meta-analysis of observational studies. *BMJ* **2011**, *342*, d1309–d1317.

118. Ferwana, M.; Firwana, B.; Hasan, R.; Al-Mallah, M. H.; Kim, S.; Montori, V. M.; Murad, M. H. Pioglitazone and risk of bladder cancer: a meta-analysis of controlled studies. *Diabet. Med.* **2013**, *30*, 1026–1032.

119. Lewis JD; Habel LA; Quesenberry CP; et al Pioglitazone use and risk of bladder cancer and other common cancers in persons with diabetes. *JAMA* **2015**, *314*, 265–277.

120. Safety Alerts for Human Medical Products - Actos (pioglitazone): Ongoing Safety Review - Potential Increased Risk of Bladder Cancer, URL: `http://www.fda.gov/safety/medwatch/safetyinformation/safetyalerts-forhumanmedicalproducts/ucm226257.htm`, accessed October 30, 2015.

121. Public statement on Pioglitazone Krka: Withdrawal of the marketing authorisation in the European Union - EMEA/H/C/002453, URL: `http://www.ema.europa.eu/ema/index.jsp?curl=pages/includes/document/document_detail.jsp?webContentId=WC500180331`, accessed October 30, 2015.

122. Withdrawal assessment report for Pioglitazone Ratiopharm - EMA/394137/2012, URL: `http://www.ema.europa.eu/ema/index.jsp?curl=pages/includes/document/document_detail.jsp?webContentId=WC500129943`, accessed October 30, 2015.

123. Thiazolidinediones in the treatment of diabetes mellitus, URL: `http://www.uptodate.com/contents/thiazolidinediones{\penalty\z@}-in{\penalty\z@}-the{\penalty\z@}-treatment{\penalty\z@}-of-diabetes-mellitus`, accessed October 30, 2015.

124. Ehrenstein, V.; Hernandez, R. K.; Ulrichsen, S. P.; Rungby, J.; Lash, T. L.; Riis, A. H.; Li, L.; Sorensen, H. T.; Jick, S. S. Rosiglitazone use and post-discontinuation glycaemic control in two European countries, 2000-2010. *BMJ Open* **2013**, *3*, e003424–e003431.

125. Niyomnaitham, S.; Page, A.; La Caze, A.; Whitfield, K.; Smith, A. J. Utilisation trends of rosiglitazone and pioglitazone in Australia before and after safety warnings. *BMC Health Serv. Res.* **2014**, *14*, 151–157.

126. Iczkovitz, S.; Dhalla, D.; Terres, J. A. R. Rosiglitazone use and associated adverse event rates in Canada: an updated analysis. *BMC Res. Notes* **2015**, *8*, 505–509.

127. Cohen, D. Rosiglitazone: what went wrong? *BMJ* **2010**, *341*, c4848–c4861.

128. Montori, V. M.; Shah, N. D. What have we learnt from the rosiglitazone saga? *BMJ* **2011**, *342*, d1354–d1357.

129. Tenenbaum, A.; Motro, M.; Fisman, E. Dual and pan-peroxisome proliferator-activated receptors (PPAR) co-agonism: the bezafibrate lessons. *Cardiovasc. Diabetol.* **2005**, *4*, 14–18.

130. Feldman, P. L.; Lambert, M. H.; Henke, B. R. PPAR Modulators and PPAR Pan Agonists for Metabolic Diseases: The Next Generation of Drugs Targeting Peroxisome Proliferator-Activated Receptors? *Curr. Top. Med. Chem.* **2008**, *8*, 728–749.

131. Heald, M.; Cawthorne, M. In *Diabetes - Perspectives in Drug Therapy*, Schwanstecher, M., Ed.; Handbook of Experimental Pharmacology, Vol. 203; Springer Berlin Heidelberg: 2011, pp 35–51, DOI: `10.1007/978-3-642-17214-4_2`.

132. Updated List of FDC and New Drugs Approved For Marketing in India - Year 2013, URL: `http://www.cdsco.nic.in/writereaddata/list-Approved-apupdated-2013-list.pdf`, accessed November 1, 2015.

133. Nissen SE; Wolski K; Topol EJ Effect of muraglitazar on death and major adverse cardiovascular events in patients with type 2 diabetes mellitus. *JAMA* **2005**, *294*, 2581–2586.

134. Long, G. G.; Reynolds, V. L.; Dochterman, L. W.; Ryan, T. E. Neoplastic and Non-neoplastic Changes in F-344 Rats Treated with Naveglitazar, a γ-Dominant PPAR α/γ Agonist. *Toxicol. Pathol.* **2009**, *37*, 741–753.

135. Oleksiewicz, M. B.; Southgate, J.; Iversen, L.; Egerod, F. L. Rat Urinary Bladder Carcinogenesis by Dual-Acting PPAR Agonists. *PPAR Res.* **2008**, *2008*, 14–27.

136. Hellmold, H.; Zhang, H.; Andersson, U.; Blomgren, B.; Holland, T.; Berg, A.-L.; Elebring, M.; Sjögren, N.; Bamberg, K.; Dahl, B.; Westerberg, R.; Dillner, B.; Tugwood, J.; Tugwood, J.; Roberts, R.; Lundholm, E.; Camejo, G.; Skånberg, I.; Evans, J. Tesaglitazar, a PPARα/γ Agonist, Induces Interstitial Mesenchymal Cell DNA Synthesis and Fibrosarcomas in Subcutaneous Tissues in Rats. *Toxicol. Sci.* **2007**, *98*, 63–74.

137. Egerod, F. L.; Nielsen, H. S.; Iversen, L.; Thorup, I.; Storgaard, T.; Oleksiewicz, M. B. Biomarkers for early effects of carcinogenic dual-acting PPAR agonists in rat urinary bladder urothelium *in vivo*. *Biomarkers* **2005**, *10*, 295–309.

138. Sznaidman, M. L.; Haffner, C. D.; Maloney, P. R.; Fivush, A.; Chao, E.; Goreham, D.; Sierra, M. L.; LeGrumelec, C.; Xu, H.; Montana, V. G.; Lambert, M. H.; Willson, T. M.; Oliver Jr., W. R.; Sternbach, D. D. Novel selective small molecule agonists for peroxisome proliferator-activated receptor δ (PPARδ)—synthesis and biological activity. *Bioorg. Med. Chem. Lett.* **2003**, *13*, 1517–1521.

139. Bays, H. E.; Schwartz, S.; Littlejohn, T.; Kerzner, B.; Krauss, R. M.; Karpf, D. B.; Choi, Y.-J.; Wang, X.; Naim, S.; Roberts, B. K. MBX-8025, A Novel Peroxisome Proliferator Receptor-δ Agonist: Lipid and Other Metabolic Effects in Dyslipidemic Overweight Patients Treated with and without Atorvastatin. *J. Clin. Endocrinol. Metab.* **2011**, *96*, 2889–2897.

140. Choi, Y.-J.; Roberts, B. K.; Wang, X.; Geaney, J. C.; Naim, S.; Wojnoonski, K.; Karpf, D. B.; Krauss, R. M. Effects of the PPAR-δ agonist MBX-8025 on atherogenic dyslipidemia. *Atherosclerosis* **2012**, *220*, 470–476.

141. Olson, E. J.; Pearce, G. L.; Jones, N. P.; Sprecher, D. L. Lipid Effects of Peroxisome Proliferator-Activated Receptor-Δ Agonist GW501516 in Subjects With Low High-Density Lipoprotein Cholesterol: Characteristics of Metabolic Syndrome. *Arterioscler., Thromb., Vasc. Biol.* **2012**, *32*, 2289–2294.

142. Ooi, E. M. M.; Watts, G. F.; Sprecher, D. L.; Chan, D. C.; Barrett, P. H. R. Mechanism of Action of a Peroxisome Proliferator-Activated Receptor (PPAR)-δ Agonist on Lipoprotein Metabolism in Dyslipidemic Subjects with Central Obesity. *J. Clin. Endocrinol. Metab.* **2011**, *96*, E1568–E1576.

143. Targeting High Unmet Need and Orphan Diseases - MBX-8025 - Cymabay Therapeutics, URL: `http://www.cymabay.com/pipeline_mbx8025.html`, accessed November 3, 2015.

144. Geiger, L. E.; Dunsford, W. S.; Lewis, D. J.; Brennan, C.; Liu, K. C.; Newsholme, S. J. Rat Carcinogenicity Study with GW501516, a PPAR delta agonist. *The Toxicologist: Supplement to Toxicological Sciences,* 108 (1)*,* **2009**, Abstract no. 895.

145. Newsholme, S. J.; Dunsford, W. S.; Brodie, T.; Brennan, C.; Brown, M.; Geiger, L. E. Mouse Carcinogenicity Study with GW501516, a PPAR delta agonist. *The Toxicologist: Supplement to Toxicological Sciences,* 108 (1)*,* **2009**, Abstract no. 896.

146. Peters, J. M.; Shah, Y. M.; Gonzalez, F. J. The role of peroxisome proliferator-activated receptors in carcinogenesis and chemoprevention. *Nat. Rev. Cancer* **2012**, *12*, 181–195.

147. Peters, J. M.; Yao, P.-L.; Gonzalez, F. J. Targeting Peroxisome Proliferator-Activated Receptor-β/δ (PPARβ/δ) for Cancer Chemoprevention. *Curr. Pharmacol. Rep.* **2015**, *1*, 121–128.

148. Yin, Y.; Russell, R. G.; Dettin, L. E.; Bai, R.; Wei, Z.-L.; Kozikowski, A. P.; Kopelovich, L.; Glazer, R. I. Peroxisome Proliferator-Activated Receptor δ and γ Agonists Differentially Alter Tumor Differentiation and Progression during Mammary Carcinogenesis. *Cancer Res.* **2005**, *65*, 3950–3957.

149. Pollock, C. B.; Rodriguez, O.; Martin, P. L.; Albanese, C.; Li, X.; Kopelovich, L.; Glazer, R. I. Induction of Metastatic Gastric Cancer by Peroxisome Proliferator-Activated Receptor δ Activation. *PPAR Res.* **2010**, *2010*, 1–12.

150. Pollock, C. B.; Yin, Y.; Yuan, H.; Zeng, X.; King, S.; Li, X.; Kopelovich, L.; Albanese, C.; Glazer, R. I. PPARδ Activation Acts Cooperatively with 3-Phosphoinositide-Dependent Protein Kinase-1 to Enhance Mammary Tumorigenesis. *PLoS ONE* **2011**, *6*, e16215–e16226.

151. Wang, D.; Ning, W.; Xie, D.; Guo, L.; DuBois, R. N. Peroxisome proliferator-activated receptor δ confers resistance to peroxisome proliferator-activated receptor γ-induced apoptosis in colorectal cancer cells. *Oncogene* **2012**, *31*, 1013–1023.

152. Wang, Y.-X.; Zhang, C.-L.; Yu, R. T.; Cho, H. K.; Nelson, M. C.; Bayuga-Ocampo, C. R.; Ham, J.; Kang, H.; Evans, R. M. Regulation of Muscle Fiber Type and Running Endurance by PPARδ. *PLoS Biol.* **2004**, *2*, e294–e301.

153. Narkar, V. A.; Downes, M.; Yu, R. T.; Embler, E.; Wang, Y.-X.; Banayo, E.; Mihaylova, M. M.; Nelson, M. C.; Zou, Y.; Juguilon, H.; Kang, H.; Shaw, R. J.; Evans, R. M. AMPK and PPARδ Agonists Are Exercise Mimetics. *Cell* **2008**, *134*, 405–415.

154. WADA issues alert on GW501516 (March 21, 2013), URL: `http://www.wada-ama.org/en/media/news/2013-03/wada-issues-alert-on-gw501516`, accessed November 2, 2015.

155. Suggestions that more doping cases involving GW501516 have emerged, URL: `http://www.velonation.com/News/ID/14366/Suggestions-that-more-doping-cases-involving-GW501516-have-emerged.aspx`, accessed November 2, 2015.

156. Xu, H. E.; Lambert, M. H.; Montana, V. G.; Plunket, K. D.; Moore, L. B.; Collins, J. L.; Oplinger, J. A.; Kliewer, S. A.; Gampe, R. T.; McKee, D. D.; Moore, J. T.; Willson, T. M. Structural determinants of ligand binding selectivity between the peroxisome proliferator-activated receptors. *Proc. Natl. Acad. Sci. U.S.A.* **2001**, *98*, 13919–13924.

157. Gampe, R. T.; Montana, V. G.; Lambert, M. H.; Miller, A. B.; Bledsoe, R. K.; Milburn, M. V.; Kliewer, S. A.; Willson, T. M.; Xu, H. Asymmetry in the PPARγ/RXRα Crystal Structure Reveals the Molecular Basis of Heterodimerization among Nuclear Receptors. *Mol. Cell* **2000**, *5*, 545–555.

158. Huang, P.; Chandra, V.; Rastinejad, F. Structural Overview of the Nuclear Receptor Superfamily: Insights into Physiology and Therapeutics. *Annu. Rev. Physiol.* **2010**, *72*, 247–272.

159. Wang, L.; Waltenberger, B.; Pferschy-Wenzig, E.-M.; Blunder, M.; Liu, X.; Malainer, C.; Blazevic, T.; Schwaiger, S.; Rollinger, J. M.; Heiss, E. H.; Schuster, D.; Kopp, B.; Bauer, R.; Stuppner, H.; Dirsch, V. M.; Atanasov, A. G. Natural product agonists of peroxisome proliferator-activated receptor gamma (PPARγ): a review. *Biochem. Pharmacol.* **2014**, *92*, 73–89.

160. Kroker, A. J.; Bruning, J. B. Review of the Structural and Dynamic Mechanisms of PPARγ Partial Agonism. *PPAR Res.* **2015**, *2015*, 15–29.

161. Amato, A. A.; Rajagopalan, S.; Lin, J. Z.; Carvalho, B. M.; Figueira, A. C. M.; Lu, J.; Ayers, S. D.; Mottin, M.; Silveira, R. L.; Souza, P. C. T.; Mourao, R. H. V.; Saad, M. J. A.; Togashi, M.; Simeoni, L. A.; Abdalla, D. S. P.; Skaf, M. S.; Polikparpov, I.; Lima, M. C. A.; Galdino, S. L.; Brennan, R. G.; Baxter, J. D.; Pitta, I. R.; Webb, P.; Phillips, K. J.; Neves, F. A. R. GQ-16, a Novel Peroxisome Proliferator-activated Receptor (PPAR) Ligand, Promotes Insulin Sensitization without Weight Gain. *J. Biol. Chem.* **2012**, *287*, 28169–28179.

162. Kojetin, D. J.; Burris, T. P. Small Molecule Modulation of Nuclear Receptor Conformational Dynamics: Implications for Function and Drug Discovery. *Mol. Pharmacol.* **2012**, *83*, 1–8.

163. Hughes, T.; Chalmers, M.; Novick, S.; Kuruvilla, D.; Chang, M.; Kamenecka, T.; Rance, M.; Johnson, B.; Burris, T.; Griffin, P.; Kojetin, D. Ligand and Receptor Dynamics Contribute to the Mechanism of Graded PPARγ Agonism. *Structure* **2012**, *20*, 139–150.

164. Bruning, J. B.; Chalmers, M. J.; Prasad, S.; Busby, S. A.; Kamenecka, T. M.; He, Y.; Nettles, K. W.; Griffin, P. R. Partial Agonists Activate PPARγ Using a Helix 12 Independent Mechanism. *Structure* **2007**, *15*, 1258–1271.

165. Hamuro, Y.; Coales, S. J.; Morrow, J. A.; Molnar, K. S.; Tuske, S. J.; Southern, M. R.; Griffin, P. R. Hydrogen/deuterium-exchange (H/D-Ex) of PPARγ LBD in the presence of various modulators. *Protein Sci.* **2006**, *15*, 1883–1892.

166. Rangwala, S. M.; Lazar, M. A. The dawn of the SPPARMs? *Science Signaling* **2002**, *2002*, pe9–pe11.

167. Berger, J. P.; Petro, A. E.; Macnaul, K. L.; Kelly, L. J.; Zhang, B. B.; Richards, K.; Elbrecht, A.; Johnson, B. A.; Zhou, G.; Doebber, T. W.; Biswas, C.; Parikh, M.; Sharma, N.; Tanen, M. R.; Thompson, G. M.; Ventre, J.; Adams, A. D.; Mosley, R.; Surwit, R. S.; Moller, D. E. Distinct Properties and Advantages of a Novel Peroxisome Proliferator-Activated Protein γ Selective Modulator. *Mol. Endocrinol.* **2003**, *17*, 662–676.

168. Puhl, A. C.; Milton, F. A.; Cvoro, A.; Sieglaff, D. H.; Campos, J. C.; Bernardes, A.; Filgueira, C. S.; Lindemann, J. L.; Deng, T.; Neves, F. A.; Polikarpov, I.; Webb, P. Mechanisms of peroxisome proliferator activated receptor γ regulation by non-steroidal anti-inflammatory drugs. *Nuc. Receptor Signal.* **2015**, *13*, e004–e020.

169. Laghezza, A.; Pochetti, G.; Lavecchia, A.; Fracchiolla, G.; Faliti, S.; Piemontese, L.; Di Giovanni, C.; Iacobazzi, V.; Infantino, V.; Montanari, R.; Capelli, D.; Tortorella, P.; Loiodice, F. New 2-(Aryloxy)-3-phenylpropanoic Acids as Peroxisome Proliferator-Activated Receptor α/γ Dual Agonists Able To Upregulate Mitochondrial Carnitine Shuttle System Gene Expression. *J. Med. Chem.* **2013**, *56*, 60–72.

170. Hopkins, C. R.; O'Neil, S. V.; Laufersweiler, M. C.; Wang, Y.; Pokross, M.; Mekel, M.; Evdokimov, A.; Walter, R.; Kontoyianni, M.; Petrey, M. E.; Sabatakos, G.; Roesgen, J. T.; Richardson, E.; Demuth, T. P. Design and synthesis of novel N-sulfonyl-2-indole carboxamides as potent PPAR-γ binding agents with potential application to the treatment of osteoporosis. *Bioorg. Med. Chem. Lett.* **2006**, *16*, 5659–5663.

171. Sheu, S.-H.; Kaya, T.; Waxman, D. J.; Vajda, S. Exploring the Binding Site Structure of the PPARγ Ligand-Binding Domain by Computational Solvent Mapping. *Biochemistry* **2004**, *44*, 1193–1209.

172. Puhl, A. C.; Bernardes, A.; Silveira, R. L.; Yuan, J.; Campos, J. L. O.; Saidemberg, D. M.; Palma, M. S.; Cvoro, A.; Ayers, S. D.; Webb, P.; Reinach, P. S.; Skaf, M. S.; Polikarpov, I. Mode of Peroxisome Proliferator-Activated Receptor Activation by Luteolin. *Mol. Pharmacol.* **2012**, *81*, 788–799.

173. Li, Y.; Wang, Z.; Furukawa, N.; Escaron, P.; Weiszmann, J.; Lee, G.; Lindstrom, M.; Liu, J.; Liu, X.; Xu, H.; Plotnikova, O.; Prasad, V.; Walker, N.; Learned, R. M.; Chen, J.-L. T2384, a Novel Antidiabetic Agent with Unique Peroxisome Proliferator-activated Receptor Binding Properties. *J. Biol. Chem.* **2008**, *283*, 9168–9176.

174. De Groot, J. C.; Weidner, C.; Krausze, J.; Kawamoto, K.; Schroeder, F. C.; Sauer, S.; Büssow, K. Structural Characterization of Amorfrutins Bound to the Peroxisome Proliferator-Activated Receptor γ. *J. Med. Chem.* **2013**, *56*, 1535–1543.

175. Zheng, W.; Feng, X.; Qiu, L.; Pan, Z.; Wang, R.; Lin, S.; Hou, D.; Jin, L.; Li, Y. Identification of the antibiotic ionomycin as an unexpected peroxisome proliferator-activated receptor γ (PPARγ) ligand with a unique binding mode and effective glucose-lowering activity in a mouse model of diabetes. *Diabetologia* **2012**, *56*, 401–411.

176. Zheng, W.; Qiu, L.; Wang, R.; Feng, X.; Han, Y.; Zhu, Y.; Chen, D.; Liu, Y.; Jin, L.; Li, Y. Selective targeting of PPARγ by the natural product chelerythrine with a unique binding mode and improved antidiabetic potency. *Sci. Rep.* **2015**, *5*, 12222–12233.

177. Wu, G.; Yi, J.; Liu, L.; Wang, P.; Zhang, Z.; Li, Z. Pseudoginsenoside F11, a Novel Partial PPARγ Agonist, Promotes Adiponectin Oligomerization and Secretion in 3T3-L1 Adipocytes. *PPAR Res.* **2013**, *2013*, 8–15.

178. Zhang, Y.; Yu, L.; Cai, W.; Fan, S.; Feng, L.; Ji, G.; Huang, C. Protopanaxatriol, a novel PPARγ antagonist from Panax ginseng, alleviates steatosis in mice. *Sci. Rep.* **2014**, *4*, 7375–7386.

179. Kolli, V.; Stechschulte, L. A.; Dowling, A. R.; Rahman, S.; Czernik, P. J.; Lecka-Czernik, B. Partial Agonist, Telmisartan, Maintains PPARγ Serine 112 Phosphorylation, and Does Not Affect Osteoblast Differentiation and Bone Mass. *PLoS ONE* **2014**, *9*, e96323–e96335.

180. Liu, C.; Feng, T.; Zhu, N.; Liu, P.; Han, X.; Chen, M.; Wang, X.; Li, N.; Li, Y.; Xu, Y.; Si, S. Identification of a novel selective agonist of PPARγ with no promotion of adipogenesis and less inhibition of osteoblastogenesis. *Sci. Rep.* **2015**, *5*, 9530–9541.

181. Choi, J. H.; Choi, S.-S.; Kim, E. S.; Jedrychowski, M. P.; Yang, Y. R.; Jang, H.-J.; Suh, P.-G.; Banks, A. S.; Gygi, S. P.; Spiegelman, B. M. Thrap3 docks on phosphoserine 273 of PPARγ and controls diabetic gene programming. *Genes Dev.* **2014**, *28*, 2361–2369.

182. Zhou, G.; Cummings, R.; Li, Y.; Mitra, S.; Wilkinson, H. A.; Elbrecht, A.; Hermes, J. D.; Schaeffer, J. M.; Smith, R. G.; Moller, D. E. Nuclear Receptors Have Distinct Affinities for Coactivators: Characterization by Fluorescence Resonance Energy Transfer. *Mol. Endocrinol.* **1998**, *12*, 1594–1604.

183. Walkey, C. J.; Spiegelman, B. M. A Functional Peroxisome Proliferator-activated Receptor-γ Ligand-binding Domain Is Not Required for Adipogenesis. *J. Biol. Chem.* **2008**, *283*, 24290–24294.

184. Burgermeister, E.; Schnoebelen, A.; Flament, A.; Benz, J.; Stihle, M.; Gsell, B.; Rufer, A.; Ruf, A.; Kuhn, B.; Märki, H. P.; Mizrahi, J.; Sebokova, E.; Niesor, E.; Meyer, M. A Novel Partial Agonist of Peroxisome Proliferator-Activated Receptor-γ (PPARγ) Recruits PPARγ-Coactivator-1α, Prevents Triglyceride Accumulation, and Potentiates Insulin Signaling *in Vitro*. *Mol. Endocrinol.* **2006**, *20*, 809–830.

185. Lu, I.-L.; Huang, C.-F.; Peng, Y.-H.; Lin, Y.-T.; Hsieh, H.-P.; Chen, C.-T.; Lien, T.-W.; Lee, H.-J.; Mahindroo, N.; Prakash, E.; Yueh, A.; Chen, H.-Y.; Goparaju, C. M. V.; Chen, X.; Liao, C.-C.; Chao, Y.-S.; Hsu, J. T.-A.; Wu, S.-Y. Structure-Based Drug Design of a Novel Family of PPARγ Partial Agonists: Virtual Screening, X-ray Crystallography, and in Vitro/in Vivo Biological Activities. *J. Med. Chem.* **2006**, *49*, 2703–2712.

186. Wu, Y.; Chin, W. W.; Wang, Y.; Burris, T. P. Ligand and Coactivator Identity Determines the Requirement of the Charge Clamp for Coactivation of the Peroxisome Proliferator-activated Receptor γ. *J. Biol. Chem.* **2003**, *278*, 8637–8644.

187. Lemkul, J. A.; Lewis, S. N.; Bassaganya-Riera, J.; Bevan, D. R. Phosphorylation of PPARγ Affects the Collective Motions of the PPARγ-RXRα-DNA Complex. *PLoS ONE* **2015**, *10*, e0123984–e0124004.

188. Li, Y.; Wang, Z.; Motani, A.; Mcgee, L. R.; Learned, M.; Timmermans, P. B.; Chen, J.-L. In *Proceedings of the 64th Annual Scientific Sessions of the American Diabetes Association (ADA '04), Orlando, FL, USA*; June 2004, Abstract 659-P, 2004.

189. Motani, A.; Wang, Z.; Weiszmann, J.; McGee, L. R.; Lee, G.; Liu, Q.; Staunton, J.; Fang, Z.; Fuentes, H.; Lindstrom, M.; Liu, J.; Biermann, D. H.; Jaen, J.; Walker, N. P.; Learned, R. M.; Chen, J.-L.; Li, Y. INT131: A Selective Modulator of PPARγ. *J. Mol. Biol.* **2009**, *386*, 1301–1311.

190. Taygerly, J. P.; McGee, L. R.; Rubenstein, S. M.; Houze, J. B.; Cushing, T. D.; Li, Y.; Motani, A.; Chen, J.-L.; Frankmoelle, W.; Ye, G.; Learned, M. R.; Jaen, J.; Miao, S.; Timmermans, P. B.; Thoolen, M.; Kearney, P.; Flygare, J.; Beckmann, H.; Weiszmann, J.; Lindstrom, M.; Walker, N.; Liu, J.; Biermann, D.; Wang, Z.; Hagiwara, A.; Iida, T.; Aramaki, H.; Kitao, Y.; Shinkai, H.; Furukawa, N.; Nishiu, J.; Nakamura, M. Discovery of INT131: A selective PPARγ modulator that enhances insulin sensitivity. *Bioorg. Med. Chem.* **2013**, *21*, 979–992.

191. McGee, L. R.; Rubenstein, S. M.; Houze, J. B.; Ye, G.; Li, Y.; Learned, R. M.; Chen, J.-L.; Wang, Z.; Motani, A.; Timmermans, P. B.; Shinkai, H.; Hagiwara, A.; Furukawa, N.; Nishiu, J.; Nakamura, M. In *Proceedings of the 231st American Chemical Society National Meeting, Atlanta, GA, USA*; March 2006, Abstract MEDI 20, 2006.

192. Higgins, L. S.; Mantzoros, C. S. The Development of INT131 as a Selective PPARγ Modulator: Approach to a Safer Insulin Sensitizer. *PPAR Res.* **2008**, *2008*, 1–9.

193. Dunn, F. L.; Higgins, L. S.; Fredrickson, J.; DePaoli, A. M. Selective modulation of PPARγ activity can lower plasma glucose without typical thiazolidinedione side-effects in patients with Type 2 diabetes. *J. Diabetes Complications* **2011**, *25*, 151–158.

194. DePaoli, A. M.; Higgins, L. S.; Henry, R. R.; Mantzoros, C.; Dunn, F. L. Can a Selective PPARγ Modulator Improve Glycemic Control in Patients With Type 2 Diabetes With Fewer Side Effects Compared With Pioglitazone? *Diabetes Care* **2014**, *37*, 1918–1923.

195. Lee, D. H.; Huang, H.; Choi, K.; Mantzoros, C.; Kim, Y.-B. Selective PPAR modulator INT131 normalizes insulin signaling defects and improves bone mass in diet-induced obese mice. *Am. J. Physiol. Endocrinol. Metab.* **2012**, *302*, E552–E560.

196. Weinstein, D. PPARγ Agonists For Treatment Of Multiple Sclerosis, WO2014120538A1, 2014.

197. A PPARγ Modulator for MS - Drug Repurposing Patents for August 2014, URL: `http://hmpharmacon.blogspot.no/2014/09/drug-repurposing-patents-for-august-2014.html`, accessed January 7, 2016.

198. Szalardy, L.; Zadori, D.; Tanczos, E.; Simu, M.; Bencsik, K.; Vecsei, L.; Klivenyi, P. Elevated levels of PPAR-gamma in the cerebrospinal fluid of patients with multiple sclerosis. *Neurosci. Lett.* **2013**, *554*, 131–134.

199. Hanafy, K. A.; Sloane, J. A. Regulation of remyelination in multiple sclerosis. *FEBS Lett.* **2011**, *585*, 3821–3828.

200. Mandrekar-Colucci, S.; Sauerbeck, A.; Popovich, P. G.; McTigue, D. M. PPAR agonists as therapeutics for CNS trauma and neurological diseases. *ASN Neuro* **2013**, *5*, 347–362.

201. Santilli, A. A.; Scotese, A. C.; Tomarelli, R. M. A potent antihypercholesterolemic agent:[4-chloro-6-(2, 3-xylidino)-2-pyrimidinylthio] acetic acid (Wy-14643). *Cell. Mol. Life Sci.* **1974**, *30*, 1110–1111.

202. Blanquart, C.; Mansouri, R.; Paumelle, R.; Fruchart, J.-C.; Staels, B.; Glineur, C. The Protein Kinase C Signaling Pathway Regulates a Molecular Switch between Transactivation and Transrepression Activity of the Peroxisome Proliferator-Activated Receptor α. *Mol. Endocrinol.* **2004**, *18*, 1906–1918.

203. Endo, A. Monacolin K, a new hypocholesterolemic agent produced by a Monascus species. *J. Antibiot.* **1979**, *32*, 852–854.

204. Tobert, J. A. Case history: Lovastatin and beyond: the history of the HMG-CoA reductase inhibitors. *Nat. Rev. Drug Discovery* **2003**, *2*, 517–526.

205. Paumelle, R. Acute Antiinflammatory Properties of Statins Involve Peroxisome Proliferator-Activated Receptor-via Inhibition of the Protein Kinase C Signaling Pathway. *Circ. Res.* **2006**, *98*, 361–369.

206. Delerive, P.; Fruchart, J.-C.; Staels, B. Peroxisome proliferator-activated receptors in inflammation control. *J. Endocrinol.* **2001**, *169*, 453–459.

207. Bernardes, A.; Souza, P. C.; Muniz, J. R.; Ricci, C. G.; Ayers, S. D.; Parekh, N. M.; Godoy, A. S.; Trivella, D. B.; Reinach, P.; Webb, P.; Skaf, M. S.; Polikarpov, I. Molecular Mechanism of Peroxisome Proliferator-Activated Receptor α Activation by WY14643: a New Mode of Ligand Recognition and Receptor Stabilization. *J. Mol. Biol.* **2013**, *425*, 2878–2893.

208. Diradourian, C.; Girard, J.; Pégorier, J.-P. Phosphorylation of PPARs: from molecular characterization to physiological relevance. *Biochimie* **2005**, *87*, 33–38.

209. Keil, S.; Matter, H.; Schönafinger, K.; Glien, M.; Mathieu, M.; Marquette, J.-P.; Michot, N.; Haag-Diergarten, S.; Urmann, M.; Wendler, W. Sulfonylthiadiazoles with an Unusual Binding Mode as Partial Dual Peroxisome Proliferator-Activated Receptor (PPAR) γ/δ Agonists with High Potency and in vivo Efficacy. *Chemmedchem* **2011**, *6*, 633–653.

210. Shearer, B. G.; Patel, H. S.; Billin, A. N.; Way, J. M.; Winegar, D. A.; Lambert, M. H.; Xu, R. X.; Leesnitzer, L. M.; Merrihew, R. V.; Huet, S.; Willson, T. M. Discovery of a novel class of PPARδ partial agonists. *Bioorg. Med. Chem. Lett.* **2008**, *18*, 5018–5022.

211. Adhikary, T.; Kaddatz, K.; Finkernagel, F.; Schönbauer, A.; Meissner, W.; Scharfe, M.; Jarek, M.; Blöcker, H.; Müller-Brüsselbach, S.; Müller, R. Genomewide Analyses Define Different Modes of Transcriptional Regulation by Peroxisome Proliferator-Activated Receptor-β/δ (PPARβ/δ). *PLoS ONE* **2011**, *6*, e16344–e16354.

212. Hashimoto, Y.; Miyachi, H. Nuclear receptor antagonists designed based on the helix-folding inhibition hypothesis. *Bioorg. Med. Chem.* **2005**, *13*, 5080–5093.

213. Ohashi, M.; Gamo, K.; Tanaka, Y.; Waki, M.; Beniyama, Y.; Matsuno, K.; Wada, J.; Tenta, M.; Eguchi, J.; Makishima, M.; Matsuura, N.; Oyama, T.; Miyachi, H. Structural design and synthesis of arylalkynyl amide-type peroxisome proliferator-activated receptor γ (PPARγ)-selective antagonists based on the helix12-folding inhibition hypothesis. *Eur. J. Med. Chem.* **2015**, *90*, 53–67.

214. Ammazzalorso, A.; D'Angelo, A.; Giancristofaro, A.; De Filippis, B.; Di Matteo, M.; Fantacuzzi, M.; Giampietro, L.; Linciano, P.; Maccallini, C.; Amoroso, R. Fibrate-derived N-(methylsulfonyl)amides with antagonistic properties on PPARα. *Eur. J. Med. Chem.* **2012**, *58*, 317–322.

215. Ammazzalorso, A.; Giancristofaro, A.; D'Angelo, A.; Filippis, B. D.; Fantacuzzi, M.; Giampietro, L.; Maccallini, C.; Amoroso, R. Benzothiazole-based N-(phenylsulfonyl)amides as a novel family of PPARα antagonists. *Bioorg. Med. Chem. Lett.* **2011**, *21*, 4869–4872.

216. Kasuga, J.-i.; Ishida, S.; Yamasaki, D.; Makishima, M.; Doi, T.; Hashimoto, Y.; Miyachi, H. Novel biphenylcarboxylic acid peroxisome proliferator-activated receptor (PPAR) δ selective antagonists. *Bioorg. Med. Chem. Lett.* **2009**, *19*, 6595–6599.

217. Trump, R. P.; Cobb, J. E.; Shearer, B. G.; Lambert, M. H.; Nolte, R. T.; Willson, T. M.; Buckholz, R. G.; Zhao, S. M.; Leesnitzer, L. M.; Iannone, M. A.; Pearce, K. H.; Billin, A. N.; Hoekstra, W. J. Co-crystal structure guided array synthesis of PPARγ inverse agonists. *Bioorg. Med. Chem. Lett.* **2007**, *17*, 3916–3920.

218. Puigserver, P.; Wu, Z.; Park, C. W.; Graves, R.; Wright, M.; Spiegelman, B. M. A cold-inducible coactivator of nuclear receptors linked to adaptive thermogenesis. *Cell* **1998**, *92*, 829–839.

219. Li, Y.; Kovach, A.; Suino-Powell, K.; Martynowski, D.; Xu, H. E. Structural and Biochemical Basis for the Binding Selectivity of Peroxisome Proliferator-activated Receptor to PGC-1. *J. Biol. Chem.* **2008**, *283*, 19132–19139.

220. Guan, H.-P. Corepressors selectively control the transcriptional activity of PPAR in adipocytes. *Genes Dev.* **2005**, *19*, 453–461.

221. Leesnitzer, L. M.; Parks, D. J.; Bledsoe, R. K.; Cobb, J. E.; Collins, J. L.; Consler, T. G.; Davis, R. G.; Hull-Ryde, E. A.; Lenhard, J. M.; Patel, L.; Plunket, K. D.; Shenk, J. L.; Stimmel, J. B.; Therapontos, C.; Willson, T. M.; Blanchard, S. G. Functional Consequences of Cysteine Modification in the Ligand Binding Sites of Peroxisome Proliferator Activated Receptors by GW9662. *Biochemistry* **2002**, *41*, 6640–6650.

222. Shiraki, T.; Kamiya, N.; Shiki, S.; Kodama, T. S.; Kakizuka, A.; Jingami, H. α,β-Unsaturated Ketone Is a Core Moiety of Natural Ligands for Covalent Binding to Peroxisome Proliferator-activated Receptor γ. *J. Biol. Chem.* **2005**, *280*, 14145–14153.

223. Waku, T.; Shiraki, T.; Oyama, T.; Morikawa, K. Atomic structure of mutant PPARγ LBD complexed with 15d-PGJ2: Novel modulation mechanism of PPARγ/RXRα function by covalently bound ligands. *FEBS Lett.* **2009**, *583*, 320–324.

224. Elbrecht, A.; Chen, Y.; Adams, A.; Berger, J.; Griffin, P.; Klatt, T.; Zhang, B.; Menke, J.; Zhou, G.; Smith, R. G.; Moller, D. E. L-764406 Is a Partial Agonist of Human Peroxisome Proliferator-activated Receptor γ. *J. Biol. Chem.* **1999**, *274*, 7913–7922.

225. Ohtera, A.; Miyamae, Y.; Yoshida, K.; Maejima, K.; Akita, T.; Kakizuka, A.; Irie, K.; Masuda, S.; Kambe, T.; Nagao, M. Identification of a New Type of Covalent PPARγ Agonist using a Ligand-Linking Strategy. *ACS Chem. Biol.* **2015**, *10*, 2794–2804.

226. Lee, G. T0070907, a Selective Ligand for Peroxisome Proliferator-activated Receptor γ, Functions as an Antagonist of Biochemical and Cellular Activities. *J. Biol. Chem.* **2002**, *277*, 19649–19657.

227. Brown, P. J.; Smith-Oliver, T. A.; Charifson, P. S.; Tomkinson, N. C.; Fivush, A. M.; Sternbach, D. D.; Wade, L. E.; Orband-Miller, L.; Parks, D. J.; Blanchard, S. G.; Kliewer, S. A.; Lehmann, J. M.; Willson, T. M. Identification of peroxisome proliferator-activated receptor ligands from a biased chemical library. *Chem. Biol.* **1997**, *4*, 909–918.

228. Shearer, B. G.; Wiethe, R. W.; Ashe, A.; Billin, A. N.; Way, J. M.; Stanley, T. B.; Wagner, C. D.; Xu, R. X.; Leesnitzer, L. M.; Merrihew, R. V.; Shearer, T. W.; Jeune, M. R.; Ulrich, J. C.; Willson, T. M. Identification and Characterization of 4-Chloro-N-(2-{[5-trifluoromethyl)-2-pyridyl]sulfonyl}ethyl)benzamide (GSK3787), a Selective and Irreversible Peroxisome Proliferator-Activated Receptor δ (PPARδ) Antagonist. *J. Med. Chem.* **2010**, *53*, 1857–1861.

229. Palkar, P. S.; Borland, M. G.; Naruhn, S.; Ferry, C. H.; Lee, C.; Sk, U. H.; Sharma, A. K.; Amin, S.; Murray, I. A.; Anderson, C. R.; Perdew, G. H.; Gonzalez, F. J.; Müller, R.; Peters, J. M. Cellular and Pharmacological Selectivity of the Peroxisome Proliferator-Activated Receptor-β/δ Antagonist GSK3787. *Mol. Pharmacol.* **2010**, *78*, 419–430.

230. Romanowska, M.; Al Yacoub, N.; Seidel, H.; Donandt, S.; Gerken, H.; Phillip, S.; Haritonova, N.; Artuc, M.; Schweiger, S.; Sterry, W., et al. PPARδ enhances keratinocyte proliferation in psoriasis and induces heparin-binding EGF-like growth factor. *J. Invest. Dermatol.* **2008**, *128*, 110–124.

231. Hack, K.; Reilly, L.; Palmer, C.; Read, K. D.; Norval, S.; Kime, R.; Booth, K.; Foerster, J. Skin-Targeted Inhibition of PPAR β/δ by Selective Antagonists to Treat PPAR β/δ – Mediated Psoriasis-Like Skin Disease In Vivo. *PLoS ONE* **2012**, *7*, e37097–e37107.

232. Schumann, T.; Adhikary, T.; Wortmann, A.; Finkernagel, F.; Lieber, S.; Schnitzer, E.; Legrand, N.; Schober, Y.; Nockher, W. A.; Toth, P. M., et al. Deregulation of PPARβ/δ target genes in tumor-associated macrophages by fatty acid ligands in the ovarian cancer microenvironment. *Oncotarget* **2015**, *6*, 13416–13433.

233. Bakan, A.; Bahar, I. Computational Generation inhibitor-Bound Conformers of P38 Map Kinase and Comparison with Experiments. *Pac. Symp. Biocomput.* **2011**, *16*, 181–192.

234. Bakan, A.; Bahar, I. The intrinsic dynamics of enzymes plays a dominant role in determining the structural changes induced upon inhibitor binding. *Proc. Natl. Acad. Sci. U.S.A.* **2009**, *106*, 14349–14354.

235. Yang, L.; Song, G.; Carriquiry, A.; Jernigan, R. L. Close Correspondence between the Motions from Principal Component Analysis of Multiple HIV-1 Protease Structures and Elastic Network Modes. *Structure* **2008**, *16*, 321–330.

236. Evans, D. A. History of the Harvard ChemDraw Project. *Angew. Chem. Int. Ed. Engl.* **2014**, *53*, 11140–11145.

237. Ciocoiu, C. C. Synthesis and biological evaluation of regulators of peroxisome proliferator-activated receptors, Ph.D. Thesis, University of Oslo, Norway, 2010.

238. Ciocoiu, C. C.; Ravna, A. W.; Sylte, I.; Rustan, A. C.; Hansen, T. V. Synthesis, molecular modeling studies and biological evaluation of fluorine substituted analogs of GW 501516. *Bioorg. Med. Chem.* **2011**, *19*, 6982–6988.

239. Connors, R. V.; Wang, Z.; Harrison, M.; Zhang, A.; Wanska, M.; Hiscock, S.; Fox, B.; Dore, M.; Labelle, M.; Sudom, A.; Johnstone, S.; Liu, J.; Walker, N. P.; Chai, A.; Siegler, K.; Li, Y.; Coward, P. Identification of a PPARδ agonist with partial agonistic activity on PPARγ. *Bioorg. Med. Chem. Lett.* **2009**, *19*, 3550–3554.

240. Wensaas, A. J.; Rustan, A. C.; Lovstedt, K.; Kull, B.; Wikstrom, S.; Drevon, C. A.; Hallen, S. Cell-based multiwell assays for the detection of substrate accumulation and oxidation. *J. Lipid Res.* **2007**, *48*, 961–967.

241. Ehrenborg, E.; Krook, A. Regulation of Skeletal Muscle Physiology and Metabolism by Peroxisome Proliferator-Activated Receptor δ. *Pharmacol. Rev.* **2009**, *61*, 373–393.

242. Staiger, H.; Haas, C.; Machann, J.; Werner, R.; Weisser, M.; Schick, F.; Machicao, F.; Stefan, N.; Fritsche, A.; Haring, H.-U. Muscle-Derived Angiopoietin-Like Protein 4 Is Induced by Fatty Acids via Peroxisome Proliferator-Activated Receptor (PPAR)-δ and Is of Metabolic Relevance in Humans. *Diabetes* **2009**, *58*, 579–589.

243. Feng, Y. Z.; Nikolić, N.; Bakke, S. S.; Boekschoten, M. V.; Kersten, S.; Kase, E. T.; Rustan, A. C.; Thoresen, G. H. PPARδ activation in human myotubes increases mitochondrial fatty acid oxidative capacity and reduces glucose utilization by a switch in substrate preference. *Arch. Physiol. Biochem.* **2014**, *120*, 12–21.

244. Ciocoiu, C. C.; Nikolić, N.; Nguyen, H. H.; Thoresen, G. H.; Aasen, A. J.; Hansen, T. V. Synthesis and dual PPARα/δ agonist effects of 1,4-disubstituted 1,2,3-triazole analogues of GW 501516. *Eur. J. Med. Chem.* **2010**, *45*, 3047–3055.

245. Ciocoiu, C. C.; Ravna, A. W.; Sylte, I.; Hansen, T. V. Synthesis, Biological Evaluation and Molecular Modeling of GW 501516 Analogues. *Arch. Pharm. Chem. Life Sci.* **2010**, *343*, 612–624.

246. Vo, C. Synthesis of putative peroxisome proliferator-activated receptor δ antagonists, URL: `http://urn.nb.no/URN:NBN:no-31629`, M.Sc. Thesis, University of Oslo, **2012**.

247. Amundsen, M. Synthesis of analogues of GSK3787 as putative PPARδ antagonists, URL: `http://urn.nb.no/URN:NBN:no-35414`, M.Sc. Thesis, University of Oslo, **2013**.

248. Mikhlina, E. E.; Yanina, A. D.; Yakhontov, L. N. Some properties and transformations of γ-acetopropyl alcohol. *Pharm. Chem. J.* **1970**, *4*, 328–329.

249. Rymoreva, I. N.; Biryukova, V. S.; Shaps, I. A.; Letunova, A. B. Formation of γ-chloro-γ-acetopropyl alcohol from α-chloro-α-aceto-γ-butyrolactone by GLC. *Pharm. Chem. J.* **1982**, *16*, 692–696.

250. Tada, M.; Hiratsuka, M.; Goto, H. Photolyses of (3-naphthoxypropyl)-, (4-naphthylbutyl)-, and (4-naphthyl-4-oxobutyl)cobaloxime. *J. Org. Chem.* **1990**, *55*, 4364–4370.

251. Lakowicz, J. R., Principles of fluorescence spectroscopy, 3rd ed; Springer: New York, 2006.

252. Stafslien, D. K.; Vedvik, K. L.; De Rosier, T.; Ozers, M. S. Analysis of ligand-dependent recruitment of coactivator peptides to RXRβ in a time-resolved fluorescence resonance energy transfer assay. *Mol. Cell. Endocrinol.* **2007**, *264*, 82–89.

253. LanthaScreen™ TR-FRET PPAR Delta Competitive Binding Assay Kit Manual, URL: `https://tools.lifetechnologies.com/content/sfs/manuals/lanthascreen_PPARdelta_competitivebinding_man.pdf`, accessed February 16, 2016.

254. Zhang, J.-H. A Simple Statistical Parameter for Use in Evaluation and Validation of High Throughput Screening Assays. *J. Biomol. Screen.* **1999**, *4*, 67–73.

255. Lieber, S.; Scheer, F.; Meissner, W.; Naruhn, S.; Adhikary, T.; Müller-Brüsselbach, S.; Diederich, W. E.; Müller, R. (*Z*)-2-(2-Bromophenyl)-3-{[4-(1-methyl-piperazine)amino]phenyl}acrylonitrile (DG172): An Orally Bioavailable PPARβ/δ-Selective Ligand with Inverse Agonistic Properties. *J. Med. Chem.* **2012**, *55*, 2858–2868.

256. LanthaScreen™ TR-FRET PPAR Gamma Competitive Binding Assay Kit Manual, URL: `https://tools.thermofisher.com/content/sfs/manuals/lanthascreen_PPARgamma_competitivebinding_man.pdf`, accessed February 16, 2016.

257. Dreyer, C.; Krey, G.; Keller, H.; Givel, F.; Helftenbein, G.; Wahli, W. Control of the peroxisomal β-oxidation pathway by a novel family of nuclear hormone receptors. *Cell* **1992**, *68*, 879–887.

258. Schmidt, A.; Endo, N.; Rutledge, S. J.; Vogel, R.; Shinar, D.; Rodan, G. A. Identification of a new member of the steroid hormone receptor superfamily that is activated by a peroxisome proliferator and fatty acids. *Mol. Endocrinol.* **1992**, *6*, 1634–1641.

259. He, T.-C.; Chan, T. A.; Vogelstein, B.; Kinzler, K. W. PPARδ is an APC-regulated target of nonsteroidal anti-inflammatory drugs. *Cell* **1999**, *99*, 335–345.

260. Bartmann, W.; Beck, G. Prostacyclin and Synthetic Analogues. *Angew. Chem. Int. Ed. Engl.* **1982**, *21*, 751–764.

261. Jarvis, M. C.; Gray, T. J. B.; Palmer, C. N. A. Both PPARγ and PPARδ influence sulindac sulfide-mediated p21WAF1//CIP1 upregulation in a human prostate epithelial cell line. *Oncogene* **2005**, *24*, 8211–8215.

262. Handeli, S.; Simon, J. A. A small-molecule inhibitor of Tcf/β-catenin signaling down-regulates PPARγ and PPARδ activities. *Mol. Cancer Ther.* **2008**, *7*, 521–529.

263. Li, C.-W.; Pati, K.; Lin, G.-Y.; Sohel, S. M. A.; Hung, H.-H.; Liu, R.-S. Gold-Catalyzed Oxidative Ring Expansions and Ring Cleavages of Alkynylcyclopropanes by Intermolecular Reactions Oxidized by Diphenylsulfoxide. *Angew. Chem. Int. Ed.* **2010**, *49*, 9891–9894.

264. Toscano, J.; Brookfield, F. A.; Cohen, A. D.; Courtney, S. M.; Frost, L. M.; Kalish, V. J. *N*-hydroxysulfonamide derivatives as new physiologically useful nitroxyl donors, WO2009042970A1, 2009.

265. Levitt, G. Alkyl sulfones, US4645531A, 1987.

266. Shearer, B. G.; Steger, D. J.; Way, J. M.; Stanley, T. B.; Lobe, D. C.; Grillot, D. A.; Iannone, M. A.; Lazar, M. A.; Willson, T. M.; Billin, A. N. Identification and Characterization of a Selective Peroxisome Proliferator-Activated Receptor β/δ (NR1C2) Antagonist. *Mol. Endocrinol.* **2008**, *22*, 523–529.

267. Naruhn, S.; Toth, P. M.; Adhikary, T.; Kaddatz, K.; Pape, V.; Dörr, S.; Klebe, G.; Müller-Brüsselbach, S.; Diederich, W. E.; Müller, R. High-Affinity Peroxisome Proliferator-Activated Receptor β/δ-Specific Ligands with Pure Antagonistic or Inverse Agonistic Properties. *Mol. Pharmacol.* **2011**, *80*, 828–838.

268. Toth, P. M.; Naruhn, S.; Pape, V. F. S.; Dörr, S. M. A.; Klebe, G.; Müller, R.; Diederich, W. E. Development of Improved PPARβ/δ Inhibitors. *ChemMedChem* **2012**, *7*, 159–170.

269. Adhikary, T.; Wortmann, A.; Schumann, T.; Finkernagel, F.; Lieber, S.; Roth, K.; Toth, P. M.; Diederich, W. E.; Nist, A.; Stiewe, T.; Kleinesudeik, L.; Reinartz, S.; Muller-Brusselbach, S.; Muller, R. The transcriptional PPAR β/δ network in human macrophages defines a unique agonist-induced activation state. *Nucleic Acids Res.* **2015**, *43*, 5033–5051.

270. Moretto, A.; Kirincich, S.; Xu, W.; Smith, M.; Wan, Z.-K.; Wilson, D.; Follows, B.; Binnun, E.; Joseph-McCarthy, D.; Foreman, K.; Erbe, D.; Zhang, Y.; Tam, S.; Tam, S.; Lee, J. Bicyclic and tricyclic thiophenes as protein tyrosine phosphatase 1B inhibitors. *Bioorg. Med. Chem.* **2006**, *14*, 2162–2177.

271. Lô, C.; Aaron, J.-J.; Kozmík, V.; Svoboda, J.; Brochon, J.-C.; Na, L. Synthesis, Electrochemical, and Optical Properties of New Fluorescent, Substituted Thieno[3,2-b][1]Benzothiophenes. *J. Fluoresc.* **2010**, *20*, 1037–1047.

272. Corral, C.; Lasso, A.; Lissavetzky, J.; Valdeolmillos, A. M. Synthesis of 10-(4-methyl-1-piperazinyl)thieno [3,2-b][1,5]benzothiazepines. *J. Heterocycl. Chem.* **1985**, *22*, 1345–1348.

273. Montforts, F.-P.; Osmers, M. In *Amines and Ammonium Salts; Enders, D.; Schaumann, E., Eds.; Science of Synthesis*; Georg Thieme Verlag: Stuttgart, 2008; Vol. 40a, pp 233–239.

274. Cardullo, F.; Donati, D.; Merlo, G.; Paio, A.; Salaris, M.; Taddei, M. Deprotection of *o*-Nitrobenzensulfonyl (Nosyl) Derivatives of Amines Mediated by a Solid-Supported Thiol. *Synlett* **2005**, *2005*, 2996–2998.

275. Kay, C. Development of amine releasing linkers and novel technologies for solid phase organic chemistry, Ph.D. Thesis, University of Cambridge, United Kingdom, 2000.

276. Maligres, P. E.; See, M. M.; Askin, D.; Reider, P. J. Nosylaziridines: Activated Aziridine Electrophiles. *Tetrahedron Lett.* **1997**, *38*, 5253–5256.

277. Fukuyama, T.; Jow, C.-K.; Cheung, M. 2- and 4-Nitrobenzenesulfonamides: Exceptionally versatile means for preparation of secondary amines and protection of amines. *Tetrahedron Lett.* **1995**, *36*, 6373–6374.

278. Markt, P.; Petersen, R. K.; Flindt, E. N.; Kristiansen, K.; Kirchmair, J.; Spitzer, G.; Distinto, S.; Schuster, D.; Wolber, G.; Laggner, C.; Langer, T. Discovery of Novel PPAR Ligands by a Virtual Screening Approach Based on Pharmacophore Modeling, 3D Shape, and Electrostatic Similarity Screening. *J. Med. Chem.* **2008**, *51*, 6303–6317.

279. Zaveri, N. T.; Sato, B. G.; Jiang, F.; Calaoagan, J.; Laderoute, K.; Murphy, B. J. A novel peroxisome proliferator-activated receptor delta antagonist, SR13904, has anti-proliferative activity in human cancer cells. *Cancer Biol. Ther.* **2009**, *8*, 1252–1261.

280. Kasuga, J.-i.; Nakagome, I.; Aoyama, A.; Sako, K.; Ishizawa, M.; Ogura, M.; Makishima, M.; Hirono, S.; Hashimoto, Y.; Miyachi, H. Design, synthesis, and evaluation of potent, structurally novel peroxisome proliferator-activated receptor (PPAR) δ-selective agonists. *Bioorg. Med. Chem.* **2007**, *15*, 5177–5190.

281. Fedi, V.; Altamura, M.; Catalioto, R.-M.; Giannotti, D.; Giolitti, A.; Giuliani, S.; Guidi, A.; Harmat, N. J. S.; Lecci, A.; Meini, S.; Nannicini, R.; Pasqui, F.; Tramontana, M.; Triolo, A.; Maggi, C. A. Discovery of a New Series of Potent and Selective Linear Tachykinin NK_2 Receptor Antagonists. *J. Med. Chem.* **2007**, *50*, 4793–4807.

282. Jorgensen, W. L.; Trofimov, A.; Du, X.; Hare, A. A.; Leng, L.; Bucala, R. Benzisothiazolones as modulators of macrophage migration inhibitory factor. *Bioorg. Med. Chem. Lett.* **2011**, *21*, 4545–4549.

283. Wendt, M. D.; Kunzer, A. R. Ortho-selectivity in S_NAr substitutions of 2,4-dihaloaromatic compounds. Reactions with anionic nucleophiles. *Tetrahedron Lett.* **2010**, *51*, 3041–3044.

284. Oyama, T.; Toyota, K.; Waku, T.; Hirakawa, Y.; Nagasawa, N.; Kasuga, J.-i.; Hashimoto, Y.; Miyachi, H.; Morikawa, K. Adaptability and selectivity of human peroxisome proliferator-activated receptor (PPAR) pan agonists revealed from crystal structures. *Acta Crystallogr., Sect. D: Biol. Crystallogr.* **2009**, *65*, 786–795.

285. Kaupang, Å.; Paulsen, S. M.; Steindal, C. C.; Ravna, A. W.; Sylte, I.; Halvorsen, T. G.; Thoresen, G. H.; Hansen, T. V. Synthesis, biological evaluation and molecular modeling studies of the PPARβ/δ antagonist CC618. *Eur. J. Med. Chem.* **2015**, *94*, 229–236.

286. Furukawa, N.; Ogawa, S.; Kawai, T.; Oae, S. Selective *ipso*-substitution in pyridine ring and its application for the synthesis of macrocycles containing both oxa- and thia-bridges. *Tetrahedron Lett.* **1983**, *24*, 3243–3246.

287. Oae, S.; Furukawa, N. Heteroaromatic Sulfoxides and Sulfones: Ligand Exchange and Coupling in Sulfuranes and Ipso-Substitutions. *Adv. Heterocycl. Chem.* **1990**, *48*, 1–63.

288. Krishnan, S.; Miller, R. M.; Tian, B.; Mullins, R. D.; Jacobson, M. P.; Taunton, J. Design of Reversible, Cysteine-Targeted Michael Acceptors Guided by Kinetic and Computational Analysis. *J. Am. Chem. Soc.* **2014**, *136*, 12624–12630.

289. Miller, R. M.; Paavilainen, V. O.; Krishnan, S.; Serafimova, I. M.; Taunton, J. Electrophilic Fragment-Based Design of Reversible Covalent Kinase Inhibitors. *J. Am. Chem. Soc.* **2013**, *135*, 5298–5301.

290. Serafimova, I. M.; Pufall, M. A.; Krishnan, S.; Duda, K.; Cohen, M. S.; Maglathlin, R. L.; McFarland, J. M.; Miller, R. M.; Frödin, M.; Taunton, J. Reversible targeting of noncatalytic cysteines with chemically tuned electrophiles. *Nat. Chem. Biol.* **2012**, *8*, 471–476.

291. Pritchard, R. B.; Lough, C. E.; Currie, D. J.; Holmes, H. L. Equilibrium reactions of *n*-butanethiol with some conjugated heteroenoid compounds. *Can. J. Chem.* **1968**, *46*, 775–781.

292. Allen, C. F. H.; Humphlett, W. J. The Thermal Reversibility of the Michael Reaction: V. the Effect of the Structure of Certain Thiol Adducts on Cleavage. *Can. J. Chem.* **1966**, *44*, 2315–2321.

293. Allen, C. F. H.; Fournier, J. O.; Humphlett, W. J. The Thermal Reversibility of the Michael Reaction: IV. Thiol Adducts. *Can. J. Chem.* **1964**, *42*, 2616–2620.

294. Hildonen, S.; Halvorsen, T. G.; Reubsaet, L. Why less is more when generating tryptic peptides in bottom-up proteomics. *Proteomics* **2014**, *14*, 2031–2041.

295. Seksek, O.; Bolard, J. Nuclear pH gradient in mammalian cells revealed by laser microspectrofluorimetry. *J. Cell Sci.* **1996**, *109*, 257–262.

296. Zhu, K.; Borrelli, K. W.; Greenwood, J. R.; Day, T.; Abel, R.; Farid, R. S.; Harder, E. Docking Covalent Inhibitors: A Parameter Free Approach To Pose Prediction and Scoring. *J. Chem. Inf. Model.* **2014**, *54*, 1932–1940.

297. Schrödinger - Product Suites - List of All Products, URL: `http://www.schrodinger.com/products/`, accessed February 17, 2016.

298. Niesen, F. H.; Berglund, H.; Vedadi, M. The use of differential scanning fluorimetry to detect ligand interactions that promote protein stability. *Nat. Protocols* **2007**, *2*, 2212–2221.

299. Catalán, J.; Díaz, C.; García-Blanco, F. Characterization of Binary Solvent Mixtures of DMSO with Water and Other Cosolvents. *J. Org. Chem.* **2001**, *66*, 5846–5852.

300. O'Hare, T.; Eide, C. A.; Agarwal, A.; Adrian, L. T.; Zabriskie, M. S.; MacKenzie, R. J.; LaTocha, D. H.; Johnson, K. J.; You, H.; Luo, J.; Riddle, S. M.; Marks, B. D.; Vogel, K. W.; Koop, D. R.; Apgar, J.; Tyner, J. W.; Deininger, M. W.; Druker, B. J. Threshold Levels of ABL Tyrosine Kinase Inhibitors Retained in Chronic Myeloid Leukemia Cells Determine Their Commitment to Apoptosis. *Cancer Res.* **2013**, *73*, 3356–3370.

301. Application Note O-091090 - Simple Off-rate Measurements, URL: `https://tools.lifetechnologies.com/content/sfs/brochures/O-091090_KBA_AppNote_OffRates_Final.pdf`, accessed February 10, 2016.

302. Determination of Drug-Kinase Residence Time in a Homogenous, Low-Volume Format, URL: `http://tools.lifetechnologies.com/content/sfs/posters/Determination_of_Drug-Kinase_Residence_Time_in_a_Homogenous,_Low-Volume_Format_v2.pdf`, accessed February 10, 2016.

303. Nakasako, M. Water-protein interactions from high-resolution protein crystallography. *Phil. Trans. R. Soc. B* **2004**, *359*, 1191–1206.

304. Ma, P.; Xue, Y.; Coquelle, N.; Haller, J. D.; Yuwen, T.; Ayala, I.; Mikhailovskii, O.; Willbold, D.; Colletier, J.-P.; Skrynnikov, N. R.; Schanda, P. Observing the overall rocking motion of a protein in a crystal. *Nat. Commun.* **2015**, *6*, 8361–8370.

305. Hinsen, K. Structural flexibility in proteins: impact of the crystal environment. *Bioinformatics* **2008**, *24*, 521–528.

306. Jolliffe, I. T. In *Principal Component Analysis*; Springer Series in Statistics; Springer New York: 2002, pp 1–9, DOI: `10.1007/0-387-22440-8_1`.

307. Altis, A.; Nguyen, P. H.; Hegger, R.; Stock, G. Dihedral angle principal component analysis of molecular dynamics simulations. *J. Chem. Phys.* **2007**, *126*, 244111–244120.

308. Mu, Y.; Nguyen, P. H.; Stock, G. Energy landscape of a small peptide revealed by dihedral angle principal component analysis. *Proteins: Struct., Funct., Bioinf.* **2005**, *58*, 45–52.

309. Altis, A.; Otten, M.; Nguyen, P. H.; Hegger, R.; Stock, G. Construction of the free energy landscape of biomolecules via dihedral angle principal component analysis. *J. Chem. Phys.* **2008**, *128*, 245102–245112.

310. Joosten, R. P.; Long, F.; Murshudov, G. N.; Perrakis, A. The *PDB_REDO* server for macromolecular structure model optimization. *IUCrJ* **2014**, *1*, 213–220.

311. Joosten, R. P.; Salzemann, J.; Bloch, V.; Stockinger, H.; Berglund, A.-C.; Blanchet, C.; Bongcam-Rudloff, E.; Combet, C.; Da Costa, A. L.; Deleage, G.; Diarena, M.; Fabbretti, R.; Fettahi, G.; Flegel, V.; Gisel, A.; Kasam, V.; Kervinen, T.; Korpelainen, E.; Mattila, K.; Pagni, M.; Reichstadt, M.; Breton, V.; Tickle, I. J.; Vriend, G. PDB_REDO: automated re-refinement of X-ray structure models in the PDB. *J. Appl. Crystallogr.* **2009**, *42*, 376–384.

312. Bakan, A.; Meireles, L. M.; Bahar, I. ProDy: Protein Dynamics Inferred from Theory and Experiments. *Bioinformatics* **2011**, *27*, 1575–1577.

313. Humphrey, W.; Dalke, A.; Schulten, K. VMD – Visual Molecular Dynamics. *J. Mol. Graph.* **1996**, *14*, 33–38.

314. Best, R. B.; Zhu, X.; Shim, J.; Lopes, P. E. M.; Mittal, J.; Feig, M.; MacKerell, A. D. Optimization of the Additive CHARMM All-Atom Protein Force Field Targeting Improved Sampling of the Backbone ϕ, ψ and Side-Chain χ1 and χ2 Dihedral Angles. *J. Chem. Theory Comput.* **2012**, *8*, 3257–3273.

315. Glykos, N. M. Software news and updates carma: A molecular dynamics analysis program. *J. Comput. Chem.* **2006**, *27*, 1765–1768.

316. Python Reference Manual, URL: `https://docs.python.org/2.7/`, accessed February 23, 2016.

317. Lori, C.; Pasquo, A.; Montanari, R.; Capelli, D.; Consalvi, V.; Chiaraluce, R.; Cervoni, L.; Loiodice, F.; Laghezza, A.; Aschi, M.; Giorgi, A.; Pochetti, G. Structural basis of the transactivation deficiency of the human PPARγ F360L mutant associated with familial partial lipodystrophy. *Acta Crystallogr., Sect. D: Biol. Crystallogr.* **2014**, *70*, 1965–1976.

318. Choi, J. H.; Banks, A. S.; Kamenecka, T. M.; Busby, S. A.; Chalmers, M. J.; Kumar, N.; Kuruvilla, D. S.; Shin, Y.; He, Y.; Bruning, J. B.; Marciano, D. P.; Cameron, M. D.; Laznik, D.; Jurczak, M. J.; Schürer, S. C.; Vidović, D.; Shulman, G. I.; Spiegelman, B. M.; Griffin, P. R. Antidiabetic actions of a non-agonist PPARγ ligand blocking Cdk5-mediated phosphorylation. *Nature* **2011**, *477*, 477–481.

319. Weidner, C.; de Groot, J. C.; Prasad, A.; Freiwald, A.; Quedenau, C.; Kliem, M.; Witzke, A.; Kodelja, V.; Han, C.-T.; Giegold, S. Amorfrutins are potent antidiabetic dietary natural products. *Proc. Natl. Acad. Sci. U.S.A.* **2012**, *109*, 7257–7262.

Appendix A

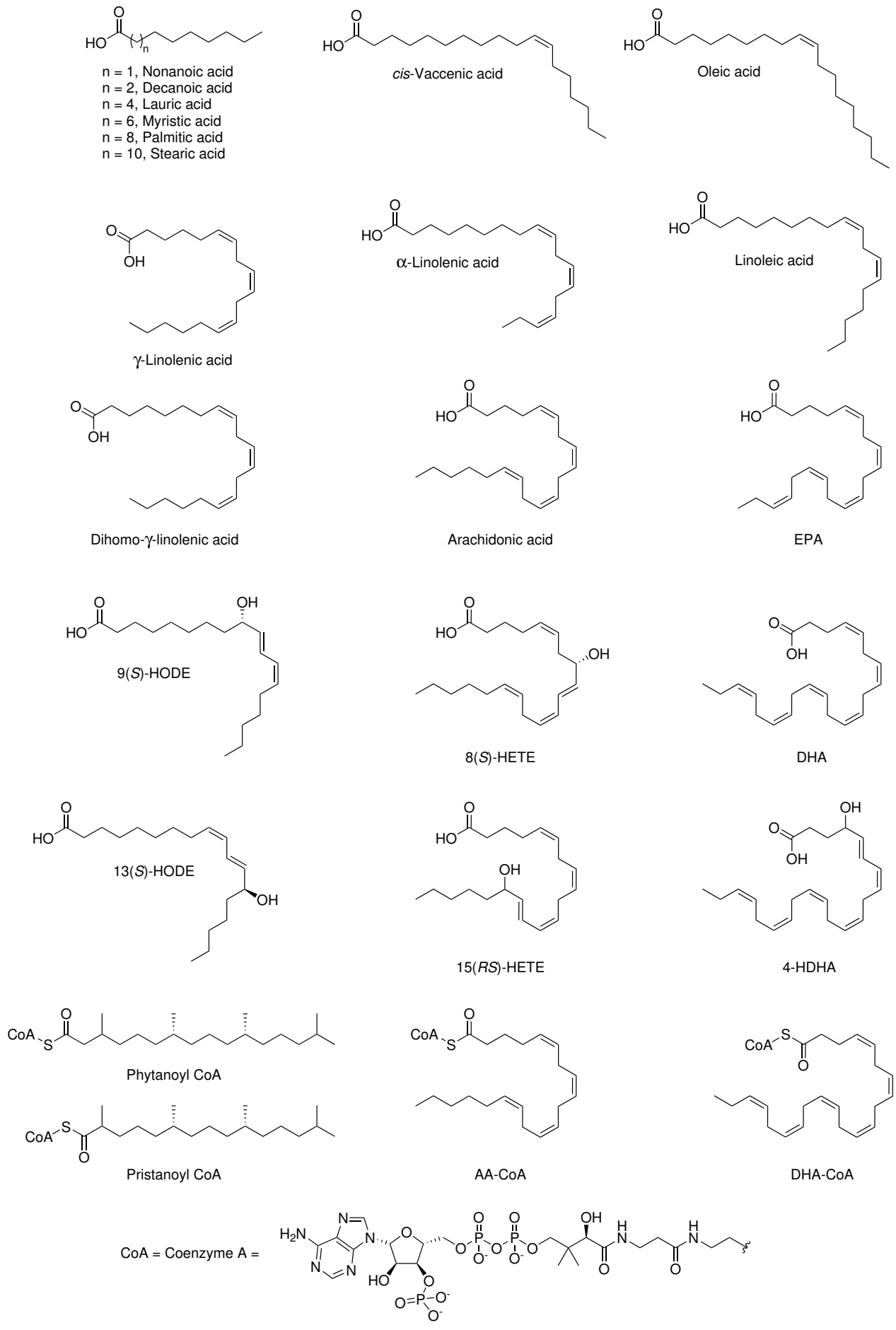

Figure 9.1. Endogenous PPAR ligands listed in Table 3.1 in Chapter 3. Page 1 of 2.

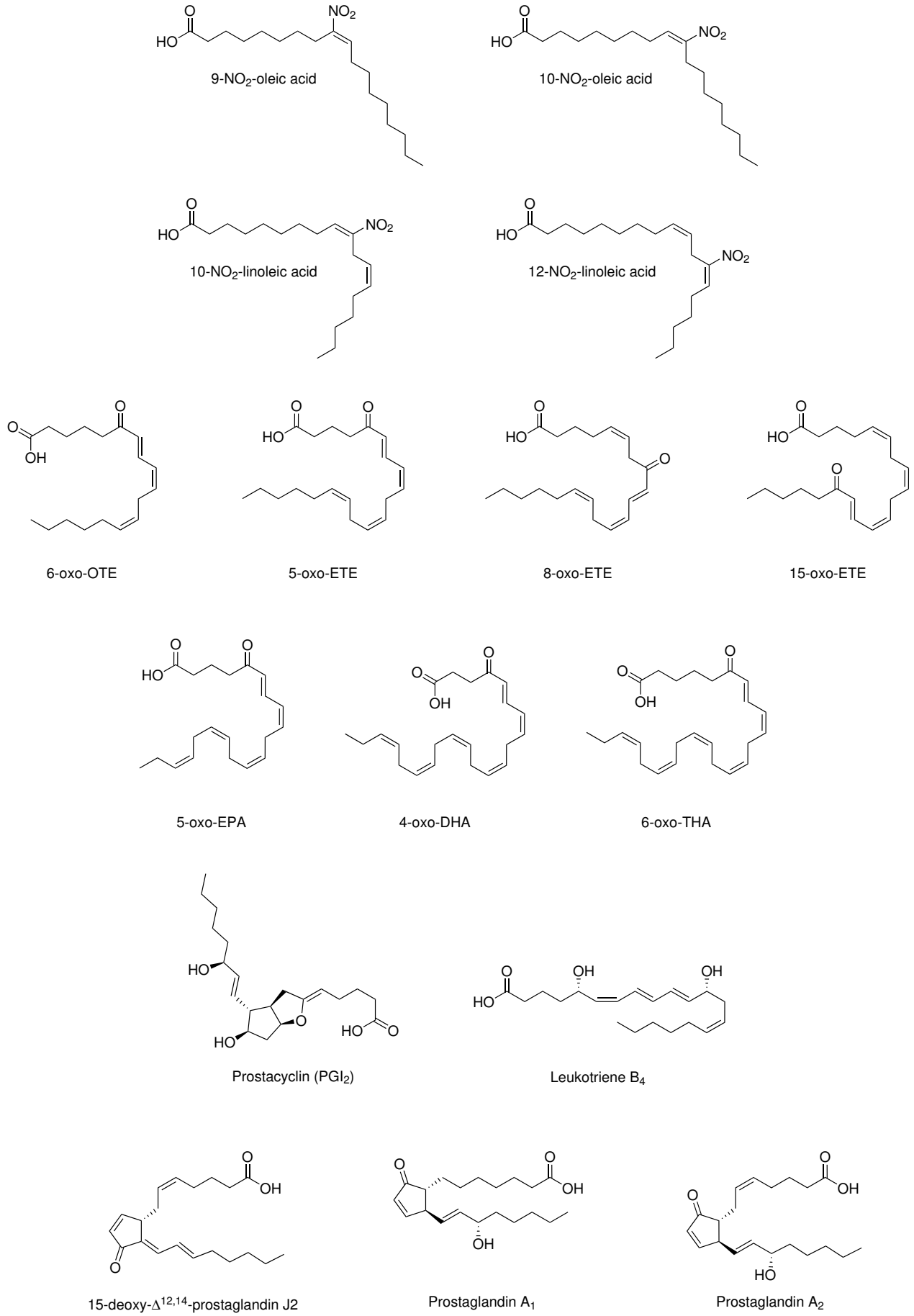

Figure 9.2. Endogenous PPAR ligands listed in Table 3.1 in Chapter 3. Page 2 of 2.

Appendix B